ISBN 978-81-934762-0-8
9 788193 476208

Ramakrishna Mission Vidyamandira

Belur Math, Howrah – 711202

(on the occasion of Platinum Jubilee of the College)

UGC-sponsored National Level Seminar on

"Recent Developments in Mathematics and its Applications"

on

26 & 27 September 2016

organized by

Department of Mathematics
Ramakrishna Mission Vidyamandira

in collaboration with

Theoretical Statistics and Mathematics Unit
Indian Statistical Institute, Kolkata

UGC-sponsored National level Seminar on

"Recent Developments in Mathematics and its Applications"

Organized by

Department of Mathematics

Ramakrishna Mission Vidyamandira

Belur Math, Howrah–711202

in collaboration with

Theoretical Statistics and Mathematics Unit,

Indian Statistical Institute, Kolkata

Published by:
Swami Shastrajnananda
Principal
Ramakrishna Mission Vidyamandira
P.O. : Belur Math, Dist. : Howrah – 711 202
Phone : 2654-9181 / 9632
e-mail : vidyamandira@gmail.com

ISBN: 978-81-934762-0-8

December 2016

Coverpage Design & Type setting by :
Niladri Shekhar Chakrabortty

Printed at :
Soumen Traders Syndicate
9/3, K.P. Coomar Street
Bally, Howrah – 711 201
Phone : 2654-3536

Index

Publisher's Note

As we all know, Ramakrishna Mission Vidyamandira is celebrating the Platinum Jubilee this year. As an integral part of the celebration, each department is organizing a National / International level seminar. I am happy to note that teachers and students of the Dept. of Mathematics worked hard to make the departmental seminar, a UGC-sponsored one, a grand success and that now the proceedings of the seminar are being published in the form of a booklet. I congratulate each and every member of the faculty, honorable guest-speakers, the young research scholars who presented papers and all the members of the non-teaching staff who assisted in every possible way in bringing out this volume.

Swami Shastrajnananda

Introductory Words

Kartick Chandra Pal
Head, Department of Mathematics
Ramakrishna Mission Vidyamandira

"The Mathematics are distinguished by a particular privilege, that is, in the course of ages, they may always advance and can never recede.[1] " said Edward Gibbon in his celebrated magnum opus 'The History of the Decline and Fall of the Roman Empire'. And never was this advancement more rapid and spectacular than in our age of high-speed computers. Today, an ardent student of Mathematics can afford to remain oblivious of these advancements only at the grave risk of stagnation. Indeed, in a bid to surveying the current developments in certain areas of Mathematics, Ramakrishna Mission Vidyamandira, in collaboration with ISI, Kolkata, hosted a two-day national seminar (UGC-Sponsored) on 'Recent Developments in Mathematics and its Applications'.

The participants in this seminar were prominent specialists in their fields. Their respective presentations were eminently thought- provoking. Mention may be made of some of these topics such as 'Syzygies and Betti numbers of curves' by Prof. B.N. Mondal, 'Young's old theorem revisited' by Prof. Alok Goswami, 'Applications of Gothendick Inequality in Operator Theory by Prof. Gadadhar Misra etc. In essence, the strength of these illuminating lectures lay in their kindling in students and teachers alike the spirit to explore newer vistas of Mathematics.

Ramakrishna Mission Vidyamandira is pleased to bring out this volume containing the proceedings of the seminar. We hope the perceptive readers would find this collection enriching.

[1] The History of the Decline and Fall of the Roman Empire - Vol V, page 269

CONTINUITY OF A REAL VALUED FUNCTION : AN INSIGHT

KALLOL PAUL
DEPARTMENT OF MATHEMATICS
JADAVPUR UNIVERSITY

Abstract. Given a subset $A \subset \mathbb{R}$ can we construct a function $f : \mathbb{R} \longrightarrow \mathbb{R}$ such that f is continuous exactly on A? We illustrate with examples to see how does A look like. The main theme of this lecture is to completely characterize the continuity set A.

1. Preliminary notions

Let $\mathbb{R}$ denote the set of real numbers, $A \subset \mathbb{R}$ and $f : A \longrightarrow \mathbb{R}$ is a given function. Consider

$$S = \{x \in A : f \text{ is continuous at } x\} \text{ and } D = \{x \in A : f \text{ is discontinuous at } x\}.$$

Then our aim is to study the nature of D and S i.e. the set of points of discontinuity and continuity. If we consider the polynomial functions, exponential functions, trigonometric functions sine, cosine then we know that the set of continuity is the domain of the function, which may be whole of $\mathbb{R}$, accordingly the set of discontinuity is the empty set. We have seen examples of functions which are discontinuous at one or more points like the step functions. We also have the example of Thomae function $f : \mathbb{R} \longrightarrow \mathbb{R}$

$$\begin{aligned} f(x) &= 0, \ x \text{ is irrational} \\ &= 1, \ x = 0 \\ &= 1/n, \ x = \frac{\pm m}{n}, m, n \in \mathbb{N}, \text{ with } gcd(m, n) = 1 \end{aligned}$$

where f is continuous only at the irrationals.
Surprisingly enough we have never come across a real valued function which is continuous only at the rationals! Now student may think in two ways, either this is going to be a very complicated function or such a function does not exist. By the end of this lecture we will come to know the answer.
The question that we raise is that suppose we are given a subset S of $\mathbb{R}$, then can we find a function $f : \mathbb{R} \longrightarrow \mathbb{R}$ such that f is continuous only on S.
We first look at some examples to see how does S or D look like?

Example 1. *Let $f : \mathbb{R} \longrightarrow \mathbb{R}$ be defined by*

$$\begin{aligned} f(x) &= x sin\frac{1}{x}, \ x \neq 0 \\ &= 0 \end{aligned}$$

Then $D = \phi$ and $S = \mathbb{R}$.

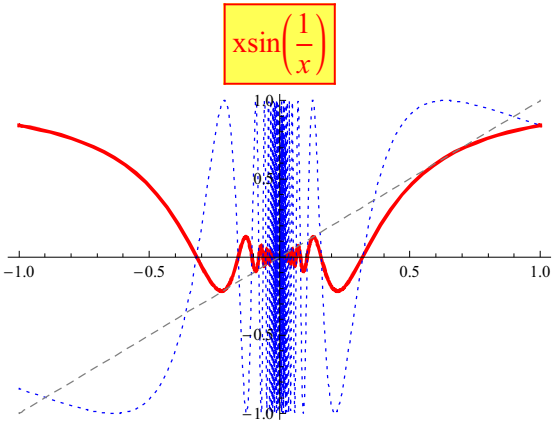

Example 2. *Let* $f : \mathbb{R} \longrightarrow \mathbb{R}$ *be defined by*

$$\begin{aligned} f(x) &= -1,\ x \leq 0 \\ &= 1,\ x > 0 \end{aligned}$$

Then $D = \{0\}$ *and* $S = \mathbb{R} - \{0\}$.

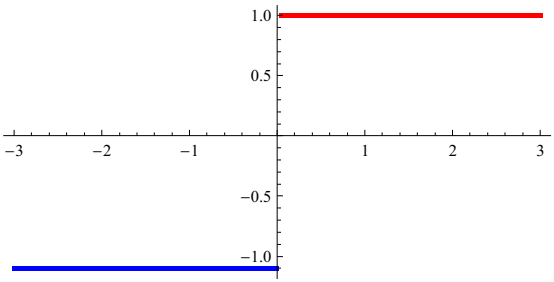

Example 3. *Let* $f : \mathbb{R} \longrightarrow \mathbb{R}$ *be defined by*

$$\begin{aligned} f(x) &= 0,\ x \leq 1 \\ &= 1,\ 1 < x \leq 2 \\ &= 2,\ x > 2 \end{aligned}$$

Then $D = \{1, 2\}$ *and* $S = \mathbb{R} - \{1, 2\}$.

Example 4. *Let* $f : \mathbb{R} \longrightarrow \mathbb{R}$ *be defined by*

$$\begin{aligned} f(x) &= 0,\ x \leq 1 \\ &= 1,\ 1 < x \leq 2 \\ &= 2,\ 2 < x \leq 3 \\ &\dots \\ &= k-1,\ k-1 < x \leq k \\ &= k,\ x > k \end{aligned}$$

Then $D = \{1, 2, \dots k\}$ *and* $S = \mathbb{R} - \{1, 2, \dots, k\}$.

Example 5. *Let* $f : \mathbb{R} \longrightarrow \mathbb{R}$ *be defined by*

$$\begin{aligned} f(x) &= 0,\ x < 1 \\ &= n,\ n \leq x < n+1,\ n \in \mathbb{N} \end{aligned}$$

Then $D = \mathbb{N}$ *and* $S = \mathbb{R} - \mathbb{N}$.

Example 6. *Let* $f : \mathbb{R} \longrightarrow \mathbb{R}$ *be defined by*

$$f(x) = n,\ n \leq x < n+1,\ n \in \mathbb{Z}$$

Then $D = \mathbb{Z}$ *and* $S = \mathbb{R} - \mathbb{Z}$.

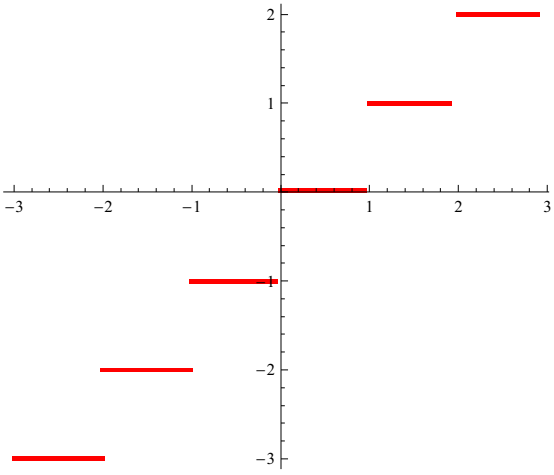

Example 7 (Thomae function)**.** *Let* $f : \mathbb{R} \longrightarrow \mathbb{R}$ *be defined by*

$$\begin{aligned} f(x) &= 0,\ x \ \text{ is irrational} \\ &= 1,\ x = 0 \\ &= 1/n,\ x = \frac{\pm m}{n}, m, n \in \mathbb{N},\ \text{with } gcd(m, n) = 1 \end{aligned}$$

Then $D = \mathbb{Q}$ *and* $S = \mathbb{Q}^c$.

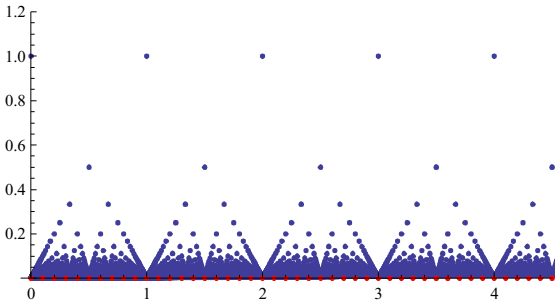

Example 8. *Let* $f : \mathbb{R} \longrightarrow \mathbb{R}$ *be defined by*

$$\begin{aligned} f(x) &= \sin x,\ x \ \text{ is rational} \\ &= \cos x,\ x \ \text{ is irrational} \end{aligned}$$

Then $S = \{\frac{1}{4}(4n + 1)\pi,\ n \in \mathbb{Z}\}$. *Thus* S *is a countable discrete subset of* $\mathbb{R}$ *so that the set of*

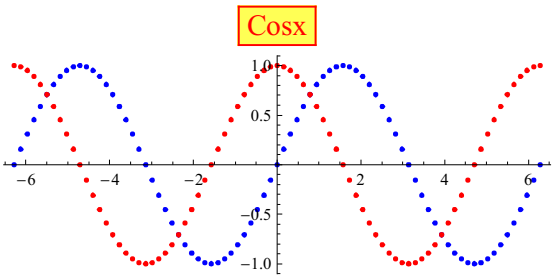

discontinuity D *is an uncountable dense subset of* $\mathbb{R}$.

Example 9. *Let* $B = \{x : -k < x < k\}$ *and consider* $f : \mathbb{R} \longrightarrow \mathbb{R}$ *be defined by*

$$\begin{aligned} f(x) &= \sin x,\ x \in \mathbb{Q} \cap B \\ &= \cos x,\ x \in \mathbb{Q}^c \cap B \\ &= 1,\ x \in \mathbb{Q} \cap B^c \\ &= -1,\ x \in \mathbb{Q}^c \cap B^c \end{aligned}$$

Then f *is continuous at finitely many points of the form* $x = \frac{1}{4}(4n+1)\pi \in B$. *Thus* S *is a finite*

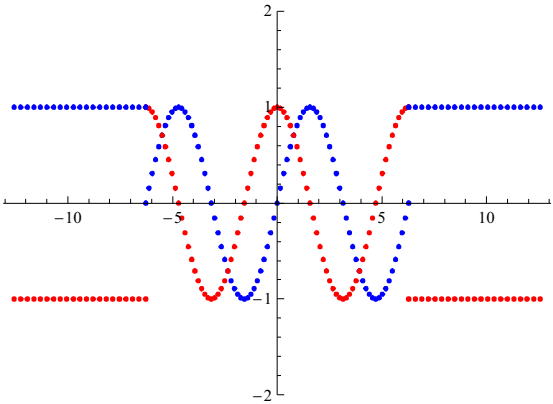

subset of $\mathbb{R}$ *so that the set of discontinuity* D *is the whole* $\mathbb{R}$ *except finitely many points.*

Example 10. *Let* $f : \mathbb{R} \longrightarrow \mathbb{R}$ *be defined by*

$$\begin{aligned} f(x) &= x,\ x \in \mathbb{Q} \\ &= -x,\ x \in \mathbb{Q}^c \end{aligned}$$

Then $D = \mathbb{R} - \{0\}$ *and* $S = \{0\}$.

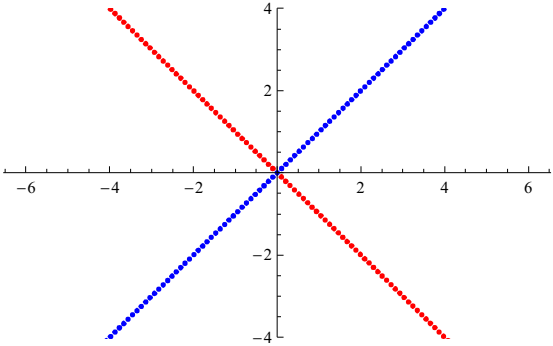

Example 11. *Let* $f : \mathbb{R} \longrightarrow \mathbb{R}$ *be defined by*

$$\begin{aligned} f(x) &= 1,\ x \in \mathbb{Q} \\ &= -1,\ x \in \mathbb{Q}^c \end{aligned}$$

Then $D = \mathbb{R}$ *and* $S = \phi$.

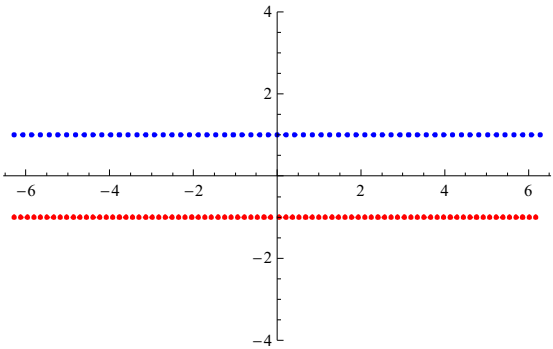

From the above examples it follows that the set of points of discontinuity may be finite, countably infinite, whole of $\mathbb{Q}$, whole of $\mathbb{R}$. Looking at example 6 we see that there exists a function continuous on irrationals but we did not give an example of a function which is continuous exactly on the rationals. The question is whether there exists a function which is continuous only at the rationals. To answer the question we need to talk of G_δ and F_σ set. We first mention some basic definitions.

Open set : A subset G of $\mathbb{R}$ is said to be open iff for each $x \in G$ there exists $\delta_x > 0$ such that $(x - \delta_x, x + \delta_x) \subset G$.
Closed set : A subset F of $\mathbb{R}$ is said to be closed iff F contains all its limit points. A real number x is said to be a limit point of F iff for each $\delta > 0$

$$\Big((x - \delta, x + \delta) - \{x\}\Big) \cap F \neq \phi.$$

Equivalently a set F is closed iff its complement is open.
G_δ **set** : A set $A \subset \mathbb{R}$ is said to be a G_δ set iff it can be written as countable intersection of open sets.
F_σ **set** : A set $A \subset \mathbb{R}$ is said to be a F_σ set iff it can be written as countable union of closed sets.
Remark. Clearly every open set is a G_δ set and every closed set is a F_σ set. Also we can show that every open set is a F_σ set and every closed set is a G_δ set.
Let F be a closed set. For each $n \in \mathbb{N}$ let $G_n = \cup_{x \in F}(x - 1/n, x + 1/n)$. Then each G_n being arbitrary union of open sets is an open set. We claim that $F = \cap_{n \in N} G_n$ so that F becomes a G_δ set. Clearly $F \subset \cap_{n \in N} G_n$, for the converse part let $z \in \cap_{n \in N} G_n$. Let $\delta > 0$. Then there exists $n_0 \in \mathbb{N}$ such that $1/n_0 < \delta$. Now $z \in G_{n_0}$ and so $z \in (x - 1/n_0, x + 1/n_0)$ for some $x \in F$. This shows that $(z - \delta, z + \delta)$ contains some element of F so that $z \in F$. Thus F is a G_δ set. As complement of a G_δ set is F_σ set and vice versa so we can say that every open set is a F_σ set.
Dense set : A subset D of $\mathbb{R}$ is said to be everywhere dense or dense in $\mathbb{R}$ if $\bar{D} = \mathbb{R}$ i.e. if every point of $\mathbb{R}$ is either a point of D or it is a limit point of D. Thus if x is a real number then either $x \in D$ or there exists a sequence $\{x_n\} \subset D$ such that $x_n \longrightarrow x$ as $n \longrightarrow \infty$.
Nowhere Dense set : A subset D of $\mathbb{R}$ is said to be nowhere dense in $\mathbb{R}$ if $Int\ (\bar{D}) = \phi$ i.e. if there exists no open interval $(x - \delta, x + \delta),\ \delta > 0$ such that $(x - \delta, x + \delta) \subset \bar{D}$. This is equivalent to saying that $(\bar{D})^c$ is dense in $\mathbb{R}$ i.e. $\overline{(\bar{D})^c} = \mathbb{R}$.
As for example the set of rational numbers $\mathbb{Q}$ and the set of irrational numbers $\mathbb{Q}^c$ are dense in $\mathbb{R}$ whereas the set of natural numbers $\mathbb{N}$ and the set of integers $\mathbb{Z}$ are nowhere dense in $\mathbb{R}$.
It is easy to verify that a closed set is nowhere dense iff its complement is everywhere dense.
Category I : A set $A \subset \mathbb{R}$ is said to be of 1st category or category I iff it can be written as countable union of nowhere dense sets.
Category II : A set $A \subset \mathbb{R}$ is said to be of 2nd category or Category II iff it is not of 1st category.
It is easy to verify that a subset of a 1st category set is 1st category and a superset of 2nd category set is 2nd category. Null set, finite sets and countable sets are all examples of 1st category sets whereas we will see later that $\mathbb{R}$ is a set of 2nd category. So in a sense we get a feeling that 1st category sets are somewhat "small" whereas 2nd category sets are somewhat "big".
Please note that all the above notions can be defined in a metric space (X, d) by considering the open ball $B_{\delta_x}(x)$ instead of open intervals $(x - \delta_x, x + \delta_x)$ and can also be defined in a topological space by considering open sets instead of open balls.

2. Baire's theorem

We now state and prove Baire's theorem for real numbers.

Theorem 1 (Baire's theorem for real numbers). *Suppose $\{G_n : n \in \mathbb{N}\}$ be a countable collection of dense open subsets of $\mathbb{R}$. Then $\cap_{n \in \mathbb{N}} G_n$ is also dense in $\mathbb{R}$. Hence $\mathbb{R}$ is of 2nd category.*

Proof. Let $G = \cap_{n \in \mathbb{N}} G_n$. We want to show that G is dense in $\mathbb{R}$ i.e. for each $x \in \mathbb{R}$ and for each $r > 0$, $(x - r, x + r) \cap G \neq \phi$.

As G_1 is dense in $\mathbb{R}$ so $(x-r, x+r) \cap G_1 \neq \phi$. Let $x_1 \in (x-r, x+r) \cap G_1$. By the property of openness of $(x-r, x+r)$ and G_1 there exists $r' > 0$ such that

$$(x_1 - r', x_1 + r') \subset (x-r, x+r) \cap G_1.$$

Then we can find $r_1 < r'$ such that

$$[x_1 - r_1, x_1 + r_1] \subset (x_1 - r', x_1 + r') \subset (x-r, x+r) \cap G_1.$$

Without loss of generality we can assume that $r_1 < 1$. Next consider the open interval $(x_1 - r_1, x_1 + r_1)$. As G_2 is dense in $\mathbb{R}$ so $(x_1 - r_1, x_1 + r_1) \cap G_2 \neq \phi$. As before we can find $x_2 \in \mathbb{R}$ and $r_2 < 1/2$ such that

$$[x_2 - r_2, x_2 + r_2] \subset (x_1 - r_1, x_1 + r_1) \cap G_2.$$

Proceeding in this way we obtain a sequence $\{x_n\} \subset \mathbb{R}$ and $r_n < 1/n$ such that

$$[x_n - r_n, x_n + r_n] \subset (x_{n-1} - r_{n-1}, x_{n-1} + r_{n-1}) \cap G_n \ \forall \ n \in \mathbb{N}.$$

Thus $[x_1 - r_1, x_1 + r_1] \supset [x_2 - r_2, x_2 + r_2] \supset \ldots \supset [x_{n-1} - r_{n-1}, x_{n-1} + r_{n-1}] \supset [x_n - r_n, x_n + r_n] \supset \ldots$ is a nested sequence of closed and bounded intervals in $\mathbb{R}$ with diameters tending to zero. So by Cantor's nested interval theorem we get a unique point $x_0 \in \cap_{n \in \mathbb{N}} [x_n - r_n, x_n + r_n]$.
Clearly $x_0 \in G$ as $[x_n - r_n, x_n + r_n] \subset G_n, \ \forall n \in \mathbb{N}$. Also $x_0 \in (x-r, x+r)$ as $[x_n - r_n, x_n + r_n] \subset (x-r, x+r) \ \forall n \in \mathbb{N}$.
Thus $x_0 \in (x-r, x+r) \cap G$ so that $(x-r, x+r) \cap G \neq \phi$. Hence G is dense in $\mathbb{R}$.

For the next part if possible let $\mathbb{R}$ be of 1st category. Then $\mathbb{R}$ can be written as

$$\mathbb{R} = \cup_{n=1}^{\infty} B_n,$$

where each B_n is a nowhere dense subset of $\mathbb{R}$. Then we have

$$\mathbb{R} = \cup_{n=1}^{\infty} B_n \subset \cup_{n=1}^{\infty} \bar{B}_n \subset \mathbb{R}$$

so that

$$\mathbb{R} = \cup_{n=1}^{\infty} \bar{B}_n.$$

Using De'Morgan's rule we get

$$\phi = \cap_{n=1}^{\infty} (\bar{B}_n)^c \ \ldots\ldots (1)$$

For each $n \in \mathbb{N}$, $\bar{B}_n$ is a nowhere dense closed set and so $(\bar{B}_n)^c$ is dense open subset of $\mathbb{R}$. Thus by the result obtained in the first part we get $\cap_{n=1}^{\infty} (\bar{B}_n)^c$ is dense in $\mathbb{R}$. This is a contradiction to (1). Hence $\mathbb{R}$ is of 2nd category. This completes the proof.

The theorem in the same way can be proved for metric spaces which states that every complete metric space is of 2nd category.

Theorem 2 (**Baire's theorem for metric spaces**). *Every complete metric space is of 2nd category.*

Proof. The proof is exactly the same with the notion of open and closed intervals being replaced by open and closed spheres and using **Cantor's intersection property** which states that "*If (X, d) is a complete metric space and $\{F_n : n \in \mathbb{N}\}$ is nested sequence of non-empty closed subsets of X such that diameters of F_n tends to 0 as $n \to \infty$ then $\cap_{n=1}^{\infty} F_n$ is non-empty and contains exactly one point.*"

One can also prove Baire's theorem for topological spaces which states that a locally compact Hausdorff topological space is of 2nd category.

Theorem 3 (**Baire's theorem for topological spaces**). *A locally compact Hausdorff topological space X is of 2nd category.*

Proof. We show that if $\{G_n : n \in \mathbb{N}\}$ is a countable collection of dense open subsets of X then $G = \cap_{n\in\mathbb{N}} G_n$ is also dense in X.
Let U_0 be an arbitrary open set in X. Then as G_1 is dense in X so $U_0 \cap G_1 \neq \phi$. Let $y \in U_0 \cap G_1$. Then there exists an open set U_y containing y such that $U_y \subset U_0 \cap G_1$. As X is locally compact Hausdorff so we can find an open set U_1 such that $\bar{U_1} \subset U_y \subset U_0 \cap G_1$ and $y \in U_1$, $\bar{U_1}$ is compact. Now consider the open set U_1. Then $U_1 \cap G_2 \neq \phi$ and as before there exists an open set U_2 such that $\bar{U_2}$ is compact and

$$\bar{U_2} \subset U_1 \cap G_2.$$

Thus we get a sequence of compact neighbourhoods $\{\bar{U_n}\}$ such that

$$U_0 \supset \bar{U_1} \supset \bar{U_2} \supset \ldots\ldots$$

and $\bar{U_n} \subset G_n \ \forall n \in \mathbb{N}$.
As $\bar{U_1}$ is compact and $\{\bar{U_n}\}$ satisfies finite intersection property so $\cap_{n=1}^{\infty} \bar{U_n} \neq \phi$ by the property of a compact space which states that " *A topological space X is compact iff for every collection of non-empty closed subsets of X satisfying finite intersection property has a non-empty intersection*". So

$$U_0 \cap \left(\cap_{n=1}^{\infty} \bar{U_n}\right) \neq \phi.$$

As $\bar{U_n} \subset G_n, \ \forall n \in \mathbb{N}$ so it follows that $G \cap U_0 \neq \phi$. Thus G is dense in X.
The remaining part follows as before.

3. Application of Baire's theorem.

As an application of Baire's theorem we first show that there does not exist any function $f : \mathbb{R} \longrightarrow \mathbb{R}$ such that f is continuous exactly at the rational points.

Theorem 4. *Let $f : \mathbb{R} \longrightarrow \mathbb{R}$. Let D be the points of discontinuity of f. Then D is an F_σ-set in X and points of continuity of f is a G_δ-set.*
Hence there can't exist any $f : R \longrightarrow R$ which is continuous on rationals and discontinuous at irrationals.

Proof. Let $\mathbb{G}_x = \{I_\delta(x) = (x-\delta, x+\delta) : \delta > 0\}$ denotes the collection of all open intervals containing x. Then the oscillation of function f at the point x, denoted as, $\omega_f(x)$, is the non-negative real number defined by

$$\omega_f(x) = \inf_{\delta>0} \ \left\{ \ \sup_{u,v\in I_\delta(x)} |f(u) - f(v)| \ \right\}.$$

Step1. We claim that f is continuous at $x \in \mathbb{R}$ iff $\omega_f(x) = 0$.

Suppose f is continuous at $x \in \mathbb{R}$. Let $\epsilon > 0$ be arbitrary. Then there exists a $\delta > 0$ such that

$$\begin{aligned} |y - x| < \delta \quad &\Rightarrow |f(y) - f(x)| < \epsilon \\ \text{Then } u, v \in I_\delta(x) \quad &\Rightarrow |f(u) - f(v)| < 2\epsilon \\ \Rightarrow \sup_{u,v\in I_\delta(x)} \quad &|f(u) - f(v)| \leq 2\epsilon \end{aligned}$$

$$\text{Thus } \omega_f(x) = \inf_{\delta>0} \ \left\{ \ \sup_{u,v\in I_\delta(x)} |f(u) - f(v)| \right\} \leq 2\epsilon.$$

As $\epsilon > 0$ is arbitrary so we get $\omega_f(x) = 0$.
Conversely if $\omega_f(x) = 0$ then for a given $\epsilon > 0$ there exists $\delta > 0$ such that

$$\sup_{u,v\in I_\delta(x)} |f(u) - f(v)| < \epsilon.$$

Thus $|y - x| < \delta \Rightarrow |f(y) - f(x)| < \epsilon$ and hence f is continuous at $x \in \mathbb{R}$.

Step2. We claim that the set of points of continuity is a G_δ set.

For each $n \in \mathbb{N}$ we define $D_n = \{x \in \mathbb{R} : \omega_f(x) \geq 1/n\}$. From step 1 it follows that f is discontinuous at $x \in \mathbb{R}$ iff $\omega_f(x) > 0$ and so we get $D = \cup_{n=1}^{\infty} D_n$. To show that D is a F_σ set it is sufficient to show that for each $n \in \mathbb{N}$, D_n is a closed set.
Let $x \notin D_n$. Then $\omega_f(x) < 1/n$ and so there exists $\delta > 0$ such that

$$\sup_{u,v \in I_\delta(x)} |f(u) - f(v)| < 1/n.$$

Now for each $z \in I_\delta(x), z \neq x$ let $\delta' = min\{|z - x - \delta|, |z - x + \delta|\}$

$$\omega_f(z) \leq \sup_{u,v \in I'_\delta(z)} |f(u) - f(v)| \leq \sup_{u,v \in I_\delta(x)} |f(u) - f(v)| < 1/n.$$

This shows that $x \in I_\delta(x) \subset (D_n)^c$ so that $(D_n)^c$ is an open set and hence D_n is a closed set.
Thus the set of points of discontinuity is an F_σ set and so the set of points of continuity is a G_δ set.

Step3. We claim that $\mathbb{Q}$ is not a G_δ set.

If possible let

$$\mathbb{Q} = \cap_{n=1}^{\infty} G_n, \text{ where each } G_n \text{ is open in } \mathbb{R}.$$

Then for each $n \in \mathbb{N}$, $\mathbb{Q} \subset G_n$ and so $\bar{\mathbb{Q}} = \bar{G_n} = \mathbb{R}$. So each G_n is dense in $\mathbb{R}$ and hence each $(G_n)^c$ is nowhere dense in $\mathbb{R}$.
Again $\mathbb{Q}$ being countable we can write

$$\mathbb{Q} = \{x_1, x_2, \ldots, x_n, \ldots\}$$

where each $\{x_n\}$ is nowhere dense closed set. Thus

$$\mathbb{R} = \mathbb{Q} \cup \mathbb{Q}^c = \big(\cup_{n=1}^{\infty} \{x_n\}\big) \cup \big(\cup_{n=1}^{\infty} (G_n)^c\big).$$

This shows that $\mathbb{R}$ is a countable union of nowhere dense sets and it contradicts the fact that $\mathbb{R}$ is of 2nd category.
Thus there does not exist any function $f : \mathbb{R} \longrightarrow \mathbb{R}$ such that f is continuous exactly at the rational points.
An obvious corollary to the above theorem is the following one.

Corollary 1. *If A is a countable dense subset of $\mathbb{R}$ then there does not exist any function $f : \mathbb{R} \longrightarrow \mathbb{R}$ such that f is continuous exactly on A.*

The next question that arises is that

Exercise 1. *If A is a countable dense subset of $\mathbb{R}$ then can we always construct a function $f : \mathbb{R} \longrightarrow \mathbb{R}$ such that f is discontinuous exactly on A?*

Solution. As A is countable then we can write $A = \{x_1, x_2, \ldots, x_n, \ldots, \}$. Define $\phi : \mathbb{R} \longrightarrow \mathbb{R}$ by

$$\begin{aligned} \phi(x) &= 0, \ x \leq 0 \\ &= 1, x > 0 \end{aligned}$$

Then ϕ is discontinuous only at $x = 0$. Let $\sum c_n$ be a convergent series of positive real numbers. Now consider the function $f : \mathbb{R} \longrightarrow \mathbb{R}$ defined by

$$f(x) = \sum c_n \ \phi(x - x_n).$$

As $0 \leq \phi(x) \leq 1$ and $\sum c_n$ is convergent so the function f is well defined.
We first show that f is discontinuous at each of x_n. Choose $\epsilon < c_n$. Consider $\delta > 0$, however small it may be. Then

$$f(x_n + \delta) - f(x_n) \geq c_n$$

and so f fails to be continuous at x_n. Again from the property of uniform convergence of series of continuous functions it follows that the sum function $f(x)$ is continuous at all other points.

Thus f is discontinuous exactly on A. This completes the proof.

We proved that the set of points of continuity of a function $f : \mathbb{R} \longrightarrow \mathbb{R}$ is a G_δ set. Now the question arises that given a G_δ set A can we find a continuous function $f : \mathbb{R} \longrightarrow \mathbb{R}$ such that f is continuous exactly on A?

Exercise 2. *Let A be a G_δ subset of $\mathbb{R}$. Then there exists a function $f : \mathbb{R} \longrightarrow \mathbb{R}$ such that f is continuous exactly on A.*

Solution. Let $A = \bigcap_{n=1}^{\infty} G_n$ where each G_n is open in $\mathbb{R}$. Consider $U_1 = G_1$, $U_2 = G_1 \cap G_2$, $\ldots, U_n = G_1 \cap G_2 \cap \ldots G_n$. Then $\{U_n\}$ is a decreasing sequence of open sets with $A = \bigcap_{n=1}^{\infty} U_n$. We have

$$\mathbb{R} = A \cup A^c = A \cup (\bigcup_{n=1}^{\infty} U_n^c) \text{ where } U_1^c \subset U_2^c \subset \ldots \subset U_n^c \subset \ldots.$$

Define $f : \mathbb{R} \longrightarrow \mathbb{R}$ by

$$\begin{aligned} f(x) &= 0,\ x \in A \\ &= 1,\ x \in U_1^c \cap \mathbb{Q} \\ &= -1,\ x \in U_1^c \cap \mathbb{Q}^c \\ &= \frac{1}{n+1},\ x \in (U_{n+1}^c - U_n^c) \cap \mathbb{Q} \\ &= -\frac{1}{n+1},\ x \in (U_{n+1}^c - U_n^c) \cap \mathbb{Q}^c \end{aligned}$$

It is easy to verify that f is discontinuous on each of U_n^c and so f is discontinuous on A^c. We next show that f is continuous on A.
Let $x \in A$ and $x_n \longrightarrow x$. If possible let $\{f(x_n)\}$ does not converge to $f(x)$. Then there exists $\epsilon > 0$ and a subsequence $\{f(x_{n_k})\}$ such that $|f(x_{n_k})| > \epsilon\ \forall k \in \mathbb{N}$. By Archimedean property there exists $r \in \mathbb{N}$ such that $1/r < \epsilon$. This shows that $|f(x_{n_k})| > 1/r\ \forall k \in \mathbb{N}$ and so from the construction of function f it follows that $x_{n_k} \in U_{r-1}^c$. But $x \notin U_{r-1}^c$ and so it contradicts the fact that U_{r-1}^c is closed. Hence $f(x_n) \longrightarrow f(x)$ and so f is continuous at x.
Thus f is exactly continuous on A.

Acknowledgement. I thank Sourav Hait, now a Research scholar at IISc Bengaluru, for helping me in preparing this lecture.

Continuity of Thomae function

Let $f : \mathbb{R} \longrightarrow \mathbb{R}$ be defined by

$$\begin{aligned} f(x) &= 0,\ x \text{ is irrational} \\ &= 1,\ x = 0 \\ &= 1/n,\ x = \frac{\pm m}{n}, m, n \in \mathbb{N},\ \text{with } gcd(m, n) = 1 \end{aligned}$$

Then $D = \mathbb{Q}$ and $S = \mathbb{Q}^c$.

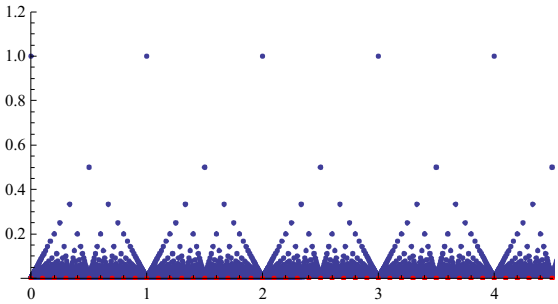

We here show that Thomae function is discontinuous on rationals and continuous on the irrationals. First we show that f is discontinuous at rationals.
Let $x = \frac{p}{q} \in \mathbb{Q}$. Then $\{x_n\}(x_n = x + \frac{\sqrt{2}}{n})$ is a sequence of irrational numbers converging to x but the sequence $\{f(x_n)\}$ does not converge to $f(x) = \frac{1}{q}$ and so f is not continuous at x. Alternatively for $q \in \mathbb{N}$ we can find $k \in \mathbb{N}$ by Archimedean property such that $k\frac{1}{q} > 1$ i.e., $\frac{1}{k} < \frac{1}{q}$. Let $\epsilon = \frac{1}{k}$. Then for $\delta > 0$, however small it may be, we get

$$y \in \mathbb{Q}^c,\ |\ y - x\ | < \delta \text{ but } |\ f(y) - f(x)\ | = \frac{1}{q} > \epsilon.$$

This shows that f is not continuous at $x \in \mathbb{Q}$.
Next we check that f is continuous at irrationals. Let ξ be an irrational number. To prove continuity of f at ξ we see whether for given $\epsilon > 0$ there exists $\delta > 0$ such that

$$|\ x - \xi\ | < \delta \Rightarrow |\ f(x) - f(\xi)\ | < \epsilon.$$

By Archimedean property there exists $k \in \mathbb{N}$ such that $\frac{1}{k} < \epsilon$. Suppose $x \in \mathbb{R}$ such that $|\ x - \xi\ | < \frac{1}{k}$. If x is irrational then $|\ f(x) - f(\xi)\ | = 0 < \epsilon$. What happens if x is rational? For $m \in \mathbb{N}$ consider the set

$$S_m = \{\pm\frac{n}{m} : n \in \mathbb{N} \cup \{0\} \&\ |\ \pm\frac{n}{m} - \xi\ | < \frac{1}{k}\}.$$

Then it is easy to check that each S_m is finite. In fact, $|\ \frac{n}{m} - \xi\ | < \frac{1}{k}$ if $-\frac{1}{k} < \frac{n}{m} - \xi < \frac{1}{k}$ i.e. if $m(\xi - \frac{1}{k}) < n < m(\xi + \frac{1}{k})$. Again $|\ -\frac{n}{m} - \xi\ | < \frac{1}{k}$ if $m(-\xi - \frac{1}{k}) < n < m(-\xi + \frac{1}{k})$. Clearly

such number of n's are finite. Now choose $0 < \delta < \frac{1}{k}$ such that $(\xi - \delta, \xi + \delta) \cap S_r = \phi$ for each $r = 1, 2, \ldots, k$. Then for rational numbers $x \in (\xi - \delta, \xi + \delta)$ we get $\mid f(x) - f(\xi) \mid = \mid f(x) \mid < \frac{1}{k} < \epsilon$. Thus f is continuous at irrationals.

Department of Mathematics, Jadavpur University, Kolkata 700032, India
E-mail address: kalloldada@gmail.com

A NOTE ON MINIMAL PRIME IDEALS IN $C([0,1])$

Bikram Banerjee
Department of Mathematics, Ranaghat College,
Ranaghat, Nadia, W.B 741201, India
email address: pbikraman@rediffmail.com

Abstract: Assuming $\beta\mathbb{N} \setminus \mathbb{N}$ contains P-points ($\beta\mathbb{N}$ is the Stone-$\check{C}$ech compactification of $\mathbb{N}$) it has been shown that if $f,g \in C([0,1])$ where $0 \leq f \leq g$, $g \in M_p = \{h \in C([0,1]) : h(p) = 0\}$ for some $p \in [0,1]$ and there exists an open set U containing p such that g vanishes nowhere on U except p then there is a minimal prime ideal Q contained in M_p such that $Q(g)$ divides $Q(f)$. We have also proved that if for every open set U containing p, g vanishes at infinitely many points of U as well as g does not vanish at infinitely many points of U then there exists a minimal prime ideal Q contained in M_p such that $Q(g)$ divides $Q(f)$.

Keywords: Tychonoff spaces, valuation domain, minimal prime ideals, rings of real valued continuous functions.

AMS Subj. Class: 54C40, 06F99.

1 Introduction

Throughout, $C(X)$ denotes the ring of real valued continuous functions on a Tychonoff space X with usual pointwise ring and lattice operations. The notation and terminology of the Gillman-Jerison text [4] will be used almost everywhere. A prime ideal P of $C(X)$ is called valuation prime if $C(X)/P$ (residue class ring of $C(X)$ modulo P) becomes a valuation domain i,e. whenever $0 < f < g \bmod P$, $\exists h \in C(X)$ such that $f - hg \in P$. Indeed every maximal ideal of $C(X)$ is valuation prime. It is known that when X is an F-space (X is called an F-space if every finitely generated ideal in $C(X)$ is principal), every prime ideal of $C(X)$ is valuation prime. Now if P is a valuation prime ideal of $C(X)$ and Q is a prime ideal of $C(X)$ containing P then $C(X)/Q$ becomes a homomorphic image of $C(X)/P$ and as the later is a valuation domain, consequently Q becomes valuation prime. On the contrary if Q is contained in P then there is no easy way to tell whether Q is a valuation prime ideal. Incidentally it was shown in [3]that there is a non maximal valuation prime ideal P of $C(\beta(\mathbb{N} \times \alpha\mathbb{N}))$ [$\alpha\mathbb{N} = \mathbb{N} \cup \{\infty\}$ is the one point compactification with '∞' be the point of infinity and βX denotes the Stone-$\check{C}$ech compactification of X] while there exists a prime ideal $Q \subsetneqq P$ which fails to be valuation prime.

If Ψ is a free ultrafilter on $\mathbb{N}$ then $P_\Psi = \{f \in C(\alpha\mathbb{N}) : z(f) \setminus \{\infty\} \in \Psi\}$, where $z(f) = \{x \in \alpha\mathbb{N} : f(x) = 0\}$, becomes a minimal prime ideal of $C(\alpha\mathbb{N})$ contained in the maximal ideal $M_\infty = \{f \in C(\alpha\mathbb{N}) : f(\infty) = 0\}$ and the correspondence $\Psi \to P_\Psi$ is a bijection between the class of all free ultrafilters on $\mathbb{N}$ onto the class of all minimal prime ideals of $C(\alpha\mathbb{N})$ contained in M_∞ (14G,[4]). It was shown in [2] that a minimal prime ideal P_Ψ of $C(\alpha\mathbb{N})$ is valuation prime if

and only if Ψ converges to a P-point in $\beta\mathbb{N} \setminus \mathbb{N}$ ($p \in X$ is called a P-point if every real valued continuous map on X becomes constant on a neighborhood of p). Now whether $\beta\mathbb{N} \setminus \mathbb{N}$ contains a P-point is undecidable in ZFC and consequently whether $C(\alpha\mathbb{N})$ contains a minimal prime ideal contained in M_∞ which is valuation prime is undecidable in ZFC. In [1] the assumption that $C(\alpha\mathbb{N})$ contains a minimal valuation prime ideal contained in M_∞ is denoted by Ωasv axiom and whether every maximal ideal $M_p = \{f \in \mathrm{C}([0,1]): f(p) = 0\}$ of $C([0,1])$, $p \in [0,1]$, contains a minimal valuation prime ideal assuming Ωasv axiom remains an open problem. In this paper we have shown (if Ωasv axiom holds) that if $f,g \in C([0,1])$ where $0 \leq f \leq g$, $g \in M_p$ for some $p \in [0,1]$ and there exists an open set U containing p such that g vanishes nowhere on U except p then there is a minimal prime ideal Q contained in M_p such that $Q(g)$ divides $Q(f)$. We have also proved that if for every open set U containing p, $U \cap z(g)$ as well as $U \cap coz(g)$ both are infinite then there exists a minimal prime ideal Q contained in M_p such that $Q(g)$ divides $Q(f)$.

2 Preliminaries and some necessary tools

If X is a topological space and $f \in C(X)$ then the set $\{x \in X : f(x) = 0\}$ is called the zero set of f and denoted by $z(f)$ and co$z(f)$ denotes $X \setminus z(f)$.

2.1 A) The collection of all maximal ideals of $C(X)$ is given by $\{M^p : p \in \beta X\}$, where $M^p = \{f \in C(X) : p \in cl_{\beta X} z(f)\}$ (Gelfand-Kolmogoroff theorem). It is customary to denote M^p by M_p if $p \in X$. In particular, if X is compact then every maximal ideal of $C(X)$ is of the form $M_p = \{f \in C(X) : p \in z(f)\}$, for some $p \in X$.

B) If P is a prime ideal of $C(X)$ then the residue class ring $C(X)$ modulo P i,e. $C(X)/\mathrm{P}$ becomes totally ordered where $P(f) \geqq 0$ means $\exists g \in P(f)$ such that $g \geqq 0$ on X.

C) Every prime ideal P of $C(X)$ is contained in a unique maximal ideal M^p and contains the z-ideal $O^p = \{f \in \mathrm{C(X)}: p \in intcl_{\beta X} z(f)\}$, for some $p \in \beta X$. It is customary to denote O^p by O_p if $p \in X$. Moreover O^p is the intersection of all minimal prime ideals of $C(X)$ contained in M^p.

D) Every maximal as well as minimal prime ideal of $C(X)$ is a z-ideal (An ideal I of $C(X)$ is called a z-ideal if $g \in I \Longleftrightarrow \mathrm{z(g)} \in Z(I) = \{z(f) : f \in I\}$).

E) Every member of a minimal prime ideal P of $C(X)$ is a zero divisor and hence if $f \in P$ then $intz(f) \neq \emptyset$.

2.2 The operation γ:
In [5] Kohls introduced a one-one correspondence γ between prime z-ideals of $C(X)$ contained properly in a maximal ideal M_p where p is a non isolated

G_δ-point of X and certain prime z-ideals of $C(X \setminus \{p\})$. In the study of the valuation prime ideals the operation γ plays a major role. Let p be a non isolated G_δ-point of X and i be the inclusion mapping from $X \setminus \{p\}$ into X. Now there exists a largest subspace X_0 of $\beta(X \setminus \{p\})$ on which i admits a continuous (definitely unique) extension ϕ onto X and consequently the set $\phi^{-1}(p)$ becomes nonempty. The following proposition describes in clear terms how the above mentioned bijection γ on the family Υ of all prime z-ideals Q of $C(X \setminus \{p\})$ such that $Z(Q)$ converges to a point of $\phi^{-1}(p)$, onto the family Δ of all non maximal prime z-ideals of $C(X)$ contained in M_p is set:

Proposition: For any $Q \in \Upsilon$, $\gamma(Q)$ is that z-ideal of $C(X)$ whose corresponding z-filter $Z(\gamma(Q))$ is given by
$Z(\gamma(Q)) = \{cl_X Y : Y \in Z(Q)\} = \{Y \cup \{p\} : Y \in Z(Q)\}$.

It is worth mentioning in this context that for any zeroset Z in $Z(Q)$, $cl_X Z = Z \cup \{p\}$ is a zeroset in X – a fact settled by Kohls in his paper [5].Furthermore for $Q \in \Upsilon$, Q is maximal in $C(X \setminus \{p\})$ if and only if $\gamma(Q)$ is an immediate prime z-ideal predecessor of M_p in $C(X)$.

2.3 P(p) z-filters:

The idea of a P(p) filter was given by Cherlin and Dickmann in 1986 [2]. Let X be a space, $p \in X$ and $\Im$ be a filter of subsets of X. $\Im$ is called a P(p) filter if for every $f \in C(X \setminus \{p\})$, $0 \leqq f \leqq 1$, there exists $Y \in \Im$ such that $\lim_{x \to p} f_{/Y}$ exists.

It is clear from the above definition that any filter containing a P(p)-filter is again a P(p)-filter. The interrelation between valuation prime ideals of $C(X)$ and P(p) z-filters on X is reflected by the following proposition:

Proposition: Let P be a non maximal valuation prime ideal of $C(X)$ contained in a maximal ideal (definitely unique) M_p, for some $p \in X$. If Q is a minimal prime ideal contained in P then $Z(Q)$ becomes a P(p)z-filter(2.2.2 [2]).

As already mentioned that any filter containing a P(p)-filter is again a P(p)-filter also every prime ideal of $C(X)$ always contains a minimal prime ideal, therefore if P is a non maximal valuation prime ideal of $C(X)$ contained in a maximal ideal M_p, for some $p \in X$; then $Z(P)$ becomes a P(p) z-filter.

3 Main Results

By Ωasv axiom we will understand the assumption that the ring $C(\alpha\mathbb{N})$ contains a minimal valuation prime ideal P contained in the maximal ideal M_∞ i,e. $P \subset M_\infty$ is a minimal prime ideal such that $C(\alpha\mathbb{N})/P$ is a valuation domain. We start with the following theorem:

Theorem 3.1 Let Ωasv hold and $p \in [0,1]$. Then there exists a non maximal valuation prime ideal Q of $C([0,1])$ contained in M_p.

Proof. Let $\{x_n\}_{i=1}^{\infty} \subset [0,1]$ be a sequence of distinct elements converging to p and $Y = \{x_n\}_{i=1}^{\infty} \cup \{p\}$. Clearly $Y \approx \alpha\mathbb{N}$. As Ωasv holds, therefore there exists a minimal (non maximal) valuation prime ideal P of $C(Y)$ contained in the maximal ideal $\{f \in C(Y) : f(p) = 0\}$. Let φ be the restriction mapping of $C([0,1])$ onto $C(Y)$. As Y is compact therefore C-embedded in [0,1] and so φ is an epimorphism. Then clearly $C([0,1])/\varphi^{-1}(P) \cong C(Y)/P$ and as the latter is valuation domain so also is the former and therefore $Q = \varphi^{-1}(P)$ becomes a non maximal valuation prime ideal of $C([0,1])$ contained in M_p.

Remark: As every closed subset of a metrizable space is a zero set, therefore $\exists\ g \in C([0,1])$ such that $z(g) = Y$. Then $g_{/Y} = 0 \in P$ and consequently $g \in i^{-1}(P) = Q$. But $int_{[0,1]}z(g) = \emptyset$. Thus Q is not minimal in $C([0,1])$. Now if T is a prime ideal of $C([0,1])$ properly contained in Q, there is no easy way to tell whether T also becomes valuation prime. One of the reasons behind it may be the fact that the structure of prime ideals of $C([0,1])$ is exceedingly rich.

Theorem:3.2 Suppose $p \in [0,1]$ and $g \in C([0,1])$ is such that $g \geqq 0$ on $[0,1]$ and $g(p) \neq 0$ or there is an open set U of $[0,1]$ containing p such that $z(g) \cap U = \{p\}$. If Ωasv holds then there is a minimal prime ideal $Q \subset M_p$ such that whenever $0 \leq f \leq g$, the coset mod Q of g divides coset mod Q of f.

Proof : Let $X = [0,1]$. We will prove this for $p = 0$ only. The case with other maximal ideals M_p of $C(X)$ with $p \neq 0$, can be dealt with analogously. Let $\{x_n\}_1^{\infty} \subset [0,1]$ be a convergent sequence of distinct elements with limit 0. Clearly $Y = \{x_n\}_1^{\infty} \cup \{0\} \approx \alpha\mathbb{N}$. As Ωasv holds therefore $\exists$ a minimal (non-maximal)valuation prime ideal P of $C(Y)$ contained in the maximal ideal $\{f \in C(Y) : f(0) = 0\}$ of $C(Y)$. Let φ be the restriction map of $C(X)$ onto $C(Y)$ which is an epimorphism as Y being compact is C-embedded in X. Clearly $\varphi^{-1}(P)$ becomes a valuation prime ideal of $C(X)$ contained in M_0. Let $Q \subset \varphi^{-1}(P)$ be a minimal prime ideal of $C(X)$ and $0 \leqq f \leqq g$; in particular $z(g) \subset z(f)$. Now if $g(0) \neq 0$ then Q(g) being a unit of $C(X)/Q$, becomes invertible and so $Q(g)/Q(f)$.

Now let $g(0) = 0$ and $[0,a)$ be an open set of $[0,1]$ containing 0 such that g does not vanish anywhere on $(0,a)$. Let $b \in (0,a)$; then g also does not vanish on $(0,b]$. Again as $\varphi^{-1}(P)$ is a non-maximal valuation prime ideal and $Q \subset \varphi^{-1}(P)$ therefore $Z(Q)$ becomes a $P(0)$ z-filter (proposition 2.3) . Now we define a map h on $(0,b]$ by $h(x) = f(x)/g(x)$; clearly $0 \leq h \leq 1$. As $(0,b]$ is closed in $(0,1]$ it is C^*-embedded. Let $h_1 \in C^*((0,1])$ be an extension of h and without loss of generality we can assume $0 \leqq h_1 \leqq 1$. Now as $Z(Q)$ is a $P(0)$ z-filter therefore there exists a member $Z \in Z(Q)$ such that $\lim_{x\to 0} h_1/Z$ exists. Now $[0,b] \in Z(Q), Z \in Z(Q) \Rightarrow [0,b] \cap Z \in Z(Q)$. Again as $lim_{x\to 0}h_1/Z$ exists therefore $lim_{x\to 0}h_1/[0,b] \cap Z$ also exists and $lim_{x\to 0}h_1/[0,b] \cap Z = \alpha$ (say). Let us define $h_1' : Z \cap [0,b] \to \mathbb{R}$ as follows: $h_1'(0) = \alpha$ and $h_1'(x) = h_1(x)$ if $0 < x \leqq b$ and $x \in Z$. Thus h_1' becomes continuous on $[0,b] \cap Z$. As $[0,b] \cap Z$ is closed therefore h_1' admits an extension say $h^* \in C(X)$. Now clearly if $x \in [0,b] \cap Z$

and $x \neq 0$ then $h^*(x) = h_1'(x) = h(x) = f(x)/g(x)$ and $h^*(0) = \alpha$. We further recall that $f(0) = g(0) = 0$, hence $f(x) = h^*(x)g(x)$ on $[0,b] \cap Z$. Now as $[0,b] \cap Z \in Z(Q)$, so we get a member of $Z(Q)$ on which $f = h^*g$ and since Q in minimal therefore it is a z-ideal. Hence $Q(f) = Q(h^*)Q(g)$ and consequently $Q(g)/Q(f)$.

Note: If $0 < Q(f) \leqq Q(g)$ then there is no loss of generality in assuming that $0 \leqq f \leqq g$, because $Q(f) = Q(0 \vee f)$ and $Q(g) = Q(0 \vee f \vee g)$.

The following proposition which follows from the work of C.W. Kohls in 1958 (3.5, [5]) will be required for our last theorem.

Proposition 3.3 Let X be compact, $p \in X$ be a non isolated G_δ-point and let S be a sequence of distinct points of $X \setminus \{p\}$ converging to p. Clearly $S \cup \{p\} \approx \alpha\omega$ and let φ be the restriction mapping of $C(X)$ onto $C(S \cup \{p\})$. Now if P is a minimal (non maximal) prime ideal of $C(S \cup \{p\})$ then the prime ideal $\varphi^{-1}(P)$ of $C(X)$ is the image by the map γ of a maximal ideal M^q of $C(X \setminus \{p\})$ where $q \in \beta(X \setminus \{p\}) \setminus (X \setminus \{p\})$ and therefore maximal among prime z-ideals of $C(X)$ properly contained in M_p.

Theorem:3.4 Let $f, g \in C([0,1])$ such that $0 \leq f \leq g$ and $g(p) = 0$ for some $p \in [0,1]$. Also let for every open set U containing p in $[0,1]$, both $U \cap z(g)$ and $U \cap coz(g)$ be infinite. If Ωasv holds then there exists a minimal prime ideal $Q \subset M_p$ such that coset mod Q of g divides coset mod Q of f.

Proof: From the assumptions it follows that $\exists$ a sequence $\{x_n\}_1^\infty \subset coz(g)$ converging to p. Let $Y = \{x_n\}_1^\infty \cup \{p\} (\approx \alpha\mathbb{N})$. and φ be the restriction of $C([0,1])$ onto $C(Y)$. As Ωasv holds therefore $\exists$ a minimal (non-maximal) valuation prime ideal P of $C(Y)$ contained in $\{h \in C(Y) : h(p) = 0\}$. Clearly $\varphi^{-1}(P)$ is a valuation prime z-ideal of $C([0,1])$ properly contained in M_p. Now as $Z(g/Y)$ is finite (in fact $z(g/Y) = \{p\}$) and every member of a (non maximal) minimal prime ideal of $C(\alpha\mathbb{N})$ has an infinite zero set, therefore $g \notin \varphi^{-1}(P)$. Let $X = [0,1] \setminus \{p\}$. Now $\exists$ a maximal ideal M^q of $C(X)$ for some $q \in \beta X \setminus X$ such that $\varphi^{-1}(P) = \gamma(M^q)$, where $Z(\gamma(M^q)) = \{cl_{[0,1]}Z : Z \in Z(M^q)\} = \{Z \cup \{p\} : Z \in Z(M^q)\}$ [By proposition 3.3]. But as $z(g) \setminus \{p\}$ is a zero set of X and $g \notin \varphi^{-1}(P) \subset \gamma(M^q)$, therefore $z(g) \setminus \{p\} \notin Z(M^q)$ [Because $z(g) \setminus \{p\} \in Z(M^q) \Rightarrow z(g) \in Z(\gamma(M^q)) = Z(\varphi^{-1}(P)) \Rightarrow g \in \varphi^{-1}(P)$ as $\varphi^{-1}(P)$ is a prime z-ideal of $C([0,1])$ – which is a contradiction]. Hence by Gelfand Kolmogoroff theorem q does not belong to $cl_{\beta X}(z(g)\setminus\{p\})$. Therefore $\exists$ a zero set neighborhood V of q in βX such that $V \cap (z(g)\setminus\{p\}) = \emptyset$. Clearly $V \cap X \in Z(O^q)$ and consequently we get a member $V \cap X (= Z, say)$ of $Z(O^q)$ on which g does not vanish. Let $Q' \subset M^q$ be a minimal prime ideal of $C(X)$. Then $\gamma(Q') = Q$ (say) becomes a minimal prime ideal of $C([0,1])$ (as γ is a bijection and order preserving in set inclusion sense) contained in $\gamma(M^q) (= \varphi^{-1}(P))$ where $Z(\gamma(Q')) = \{cl_{[0,1]}Z : Z \in Z(Q')\} = \{Z \cup \{p\} : Z \in Z(Q')\}$. We will show $Q(g)/Q(f)$. Now $Z \in Z(O^q) \Rightarrow Z \in Z(Q')$ as $O^q \subset Q'$ and this implies

$cl_{[0,1]}Z = Z \cup \{p\} \in Z(\gamma(Q')) = Z(Q)$. As g does not vanish on Z hence we can define a map $h(x) = f(x)/g(x)$ on Z. Clearly $0 \leq h \leq 1$. As Z is a zero set of X, therefore closed and C-embedded in X and consequently we can get a bounded extension h_1 of h over X and without loss of generality we take $0 \leqq h_1 \leqq 1$. Again $\varphi^{-1}(P)$ is a non maximal valuation prime ideal and Q is a minimal prime ideal contained in $\varphi^{-1}(P)$. Hence $Z(Q)$ becomes a $P(p)$ z-filter (proposition 2.3). Hence $\exists Z_1 \in Z(Q)$ such that $\lim_{x\to p} h_1/Z_1$ exists. Now as $Z \cup \{p\} \in Z(Q)$ and $Z_1 \in Z(Q)$ therefore $(Z \cup \{p\}) \cap Z_1 \in Z(Q)$. Let $(Z \cup \{p\}) \cap Z_1 = Z'$. Thus $\lim_{x\to p} h_1/Z'$ also exists and let $\lim_{x\to p} h_1/Z' = a$. Now we define $(h_1'/Z')(p) = a$ and $(h_1'/Z')(x) = (h_1/Z')(x)$ if $x \in Z'$ with $x \neq p$ and thus h_1'/Z' becomes continuous on Z'. But as Z' is a zero set of $[0,1]$ and hence C-embedded in $[0,1]$ so h_1'/Z' has an extension $h^* \in C([0,1])$. Now if $x \in Z'$ and $x \neq p$ then $h^*(x) = (h_1/Z')(x) = h(x) = \frac{f(x)}{g(x)}$ and at $x = p$ $f(p) = 0 = g(p)$. So $f = gh^*$ on Z'.Thus we get a member Z' of $Z(Q)$ on which f agrees with gh^* and as Q is minimal prime ideal of $C([0,1])$, therefore a z-ideal; consequently $Q(f) = Q(g) \cdot Q(h^*)$ i.e. $Q(g)/Q(f)$.

References

1. Bikram Banerjee and Melvin Henriksen, *Ways in which $C(X)$ mod a Prime Ideal Can be a Valuation Domain; Something Old and Something New, Positivity Trends in Mathematics, Birkhäuser Verlag Basel / Switzerland.*(2007) 1-25.

2. G. Cherlin and M. Dickmann, *Real closed rings I*, Fund. Math. 126 (1986), 147-183.

3. H.G. Dales and W. H. Woodin, *Super-Real Fields*, Claredon Press, Oxford, 1994.

4. L. Gillman and M. Jerison, *Rings of Continuous Functions*, Springer-Verlag, New York, 1976.

5. C.W.Kohls, *Prime ideals in rings of continuous functions II* , Duke Math. J.25 (1958), 447-458.

6. M. Henriksen and R. Wilson, *When is $C(X)/P$ a valuation ring for every prime ideal P?*. Topology and Appl. 44 (1992), 175-180.

7. M. Henriksen and M. Jerison, *The space of minimal prime ideals of a commutative ring,* Trans. Amer. Math. Soc. 115 (1965), 110-130.

Recurrence in Complex Dynamics

Gorachand Chakraborty

Department of Mathematics, Govt. General Degree College at Manbazar II, Purulia (W.B)

Tarakanta Nayak

School of Basic Sciences, Indian Institute of Technology Bhubaneswar, India.

Abstract

In this paper, we studied the location of recurrent critical point of a transcendental meromorphic function f. We show that if a is a recurrent point of a transcendental meromorphic function f then either a is in Julia set of f or a is in one of the rotational domains (Herman ring or Siegel Disc). Moreover if a is a recurrent critical point of f then a is in Julia set of f.

Keywords: Recurrent critical point, Julia set, Herman ring and Transcendental meromorphic function.

1. Introduction

Let $f : \mathbb{C} \to \widehat{\mathbb{C}}$ be a transcendental meromorphic function. The iterates of f, denoted by f^n, generate a dynamical system. The family $\{f^n\}_{n>0}$ of functions on a domain $\Omega \subseteq \mathbb{C}$ is said to be *normal in* Ω if every sequence of functions in $\{f^n\}_{n>0}$ contains a subsequence which converges either to a limit function $f \not\equiv \infty$ or to ∞ uniformly on each compact subset of Ω. The set of points in a neighborhood of which the sequence of iterates $\{f^n\}_{n>0}$ is defined and forms a normal family is called the *Fatou set* of f and is denoted by $\mathcal{F}(f)$. The *Julia set*, denoted by $\mathcal{J}(f)$, is the complement of $\mathcal{F}(f)$ in $\widehat{\mathbb{C}}$. The *Fatou set* is open

Email address: gorachand11@gmail.com (Gorachand Chakraborty)

and the *Julia set* is perfect. An introduction to the properties of these sets can be found in [1]. A maximal connected subset of the Fatou set is called a *Fatou component*. For a *Fatou component* U, U_k denotes the *Fatou component* containing $f^k(U)$.A Fatou component U is called *wandering* if $U_n \neq U_m$ for all $n \neq m$. We say a multiply connected Fatou component U surrounds a point $a \in \mathbb{C}$ if there exists a bounded component of $\widehat{\mathbb{C}} - U$ containing a.

Definition 1.1. *(**Baker wandering domain**) A Baker wandering domain is a wandering component U of $\mathcal{F}(f)$ such that, for n large enough, U_n is bounded, multiply connected and surrounds 0, and $f^n(z) \to \infty$ as $n \to \infty$ for $z \in U$.*

Note that if f has a Baker wandering domain then all the Fatou components including the Baker wandering domains are bounded. A *Fatou component* U is called p-periodic if p is the smallest natural number satisfying $U_p \subseteq U$. Periodic Fatou components are of five types, namely Attracting domain, Parabolic domain, Siegel disk, Herman ring and Baker domain.

Definition 1.2. *A periodic Fatou component H is called a p-periodic Herman ring if there exists an analytic homeomorphism $\phi : H \to A = \{z : 1 < |z| < r, r > 1\}$ such that $\phi(f^p(\phi^{-1}(z))) = e^{2\pi i\alpha}z$ for all $z \in A$ and for some $\alpha \in \mathbb{R}\setminus\mathbb{Q}$.*

Clearly, there are uncountably many f^p-invariant Jordan curves in H. Each such curve separates the two components of $\widehat{\mathbb{C}} \setminus H$. In Herman ring, recurrence is a very natural thing. By definition of Herman ring, every point in the Herman ring is recurrent point.

Herman rings have some interesting and significant properties. On Herman

rings (as well as Siegel disc) the limit functions of the sequence of iterates $\{f^n\}$ are non-constant which is not the case for other Fatou components. Also Herman rings are doubly connected by definition whereas in case of other Fatou component,(other than Siegel disc) the connectivity can be anything.

We call a point $a \in \widehat{\mathbb{C}}$ a singular value of f if for every open neighborhood U of a, there exists a component V of $f^{-1}(U)$ such that $f : V \to U$ is not bijective. The singular values of a function play very crucial role in studying the dynamics of the function. Denote the set of singular values of f by $S(f)$. This set is the closure of critical values and asymptotic values of f. A critical value is the image of a critical point, that is, $f(z_0)$ where $f'(z_0) = 0$. A point $a \in \widehat{\mathbb{C}}$ is an asymptotic value of f if there exists a curve $\gamma : [0, \infty) \to \mathbb{C}$ with $\lim_{t\to\infty} \gamma(t) = \infty$ such that $\lim_{t\to\infty} f(\gamma(t)) = a$. A more general definition of singular values is given below [2].

For $a \in \widehat{\mathbb{C}}$ and $r > 0$, let $D_r(a)$ be a disk (in the spherical metric) and choose a component U_r of $f^{-1}(D_r(a))$ in such a way that $U_{r_1} \subset U_{r_2}$ for $0 < r_1 < r_2$. There are two possibilities.

1. $\bigcap_{r>0} U_r = \{z\}$ for $z \in \mathbb{C}$: Then $f(z) = a$. The point z is called an ordinary point if (i) $f'(z) \neq 0$ and $a \in \mathbb{C}$, or (ii) z is a simple pole. The point z is called a critical point if $f'(z) = 0$ and $a \in \mathbb{C}$, or z is a multiple pole. In this case, a is called a critical value and we say that a critical point or algebraic singularity lies over a.
2. $\bigcap_{r>0} U_r = \phi$: The choice $r \to U_r$ defines a transcendental singularity of f^{-1}. We say a transcendental singularity lies over a. The singularity lying

over a is called direct if there exists $r > 0$ such that $f(z) \neq a$ for all $z \in U_r$. The singularity lying over a is called logarithmic if $f : U(r) \to D_r(a) \setminus \{a\}$ is a universal covering for some $r > 0$. A singularity is indirect if it is not direct.

A value $z_0 \in \widehat{\mathbb{C}}$ is said to be an *omitted value* for the function f if $f(z) \neq z_0$ for any $z \in \mathbb{C}$. An omitted value is always an asymptotic value but converse need not be true. It is clear that the singularities lying over an omitted value are always direct.

Definition 1.3. *(**Baker omitted value**) An omitted value $a \in \widehat{\mathbb{C}}$ of an entire or meromorphic function f is said to be Baker omitted value, in short bov, if there exists $r_0 > 0$ such that for all r satisfying $0 < r < r_0$, each component of the boundary of $f^{-1}(D_r(a))$ is bounded.*

It follows that $f^{-1}(D_r(a))$ is infinitely connected and each component of $\mathbb{C} \setminus f^{-1}(D_r(a))$ is bounded [3]. The *bov* is the only asymptotic value of the function [3]. Consequently, the *bov* of an entire function must be ∞ and the *bov* of a meromorphic function is always finite.

In Section 2, we have discussed some preliminary definitions. Section 3 contains the results about the location of recurrent critical point and their proofs. In Section 4, some related results are discussed.

2. Some Definitions

Definition 2.1. ω-limit set:

Let $\alpha \in \mathbb{C}$ and f be a transcendental meromorphic function then ω- limit set of

α, *denoted by* $\omega(\alpha)$, *is defined by*

$$\omega(\alpha) = \{z \in \widehat{\mathbb{C}} : \textit{there exists a subsequence } \{n_k\} \textit{ such that } f^{n_k}(\alpha) \to z\}$$

Definition 2.2. Recurrent Point:

A point c *in the complex plane is called recurrent point of* f *if* $c \in \omega(c)$.

The point which are not recurrent is called non recurrent point. From the above definition of recurrent point, we can say if $c \notin \omega(c)$ then c is a non-recurrent point. In [4] dynamics of the map $z \longmapsto \exp(z)/z$ on the punctured plane $\mathbb{C}^* = \mathbb{C} \setminus \{0\}$ have been studied. The ω-limit set of z is equal to $\{0, \infty\}$.In particular, 0 and ∞ are the only recurrent point for the above map.

Definition 2.3. Recurrent Critical Point:

Let c *be a critical point of* f. *Then* c *is called recurrent critical point of* f *if* $c \in \omega(c)$.

Definition 2.4. Recurrent Critical Value:

Let c *be a critical value of* f. *Then* c *is called recurrent critical value of* f *if* $c \in \omega(c)$.

3. Result and its proof

Lemma 3.1. *Let* U *be either Attracting domain or Parabolic domain or Baker domain or Wandering domain of a transcendental meromorphic function* f. *If* $a \in U$ *then* a *is not a recurrent point of* f.

Proof. Case-1: U is Attracting domain

Let $a \in U$ be a point such that a is not an attracting periodic point. Let w be

the attracting periodic point. Then we will get a subsequence $\{n_k\}$ such that $f^{n_k}(a) \to w$ as $k \to \infty$.

But $f^{n_k}(a) \to a$ never happens since a is not an attracting periodic point. Thus a is not a recurrent point.

Suppose a be the attracting periodic point. Then there exists subsequence $\{n_k\}$ such that $f^{n_k}(a) = a$. But $f^{n_k}(a) \nrightarrow a$ i.e, forward orbit of a under $\{n_k\}$ does not accumulate at a. So, a is not the limit point of the forward orbit. Thus if $a \in U$ then a is a non-recurrent point.

Case-2: U is Parabolic domain

Proof is same as before.

Case-3: U is Baker domain

By definition of Baker domain U can not contain any recurrent point.

Case-4: U is Wandering domain

If U is Wandering domain then $a \in U$ can not be a recurrent point. Let there exists $\{n_k\}$ such that $f^{n_k}|U \to b$ then we can prove that $b \in J(f)$. Suppose $b \in F(f)$ then there exists a neighborhood of b where f is normal. Then boundary of w_0 (w_0 be the domain such that $w_0 = f^{-1}(b)$ in the path in which $f^{n_k}|U$ approaches to b) goes to boundary of b under f. But $\partial w_0 \subset J(f)$. Since $J(f)$ is completely invariant, ∂w_0 can not go to neighborhood of b which is in Fatou set. Thus $b \in J(f)$. Thus $b \notin U$.

□

Therefore if some recurrent point of f lies in $F(f)$ then the recurrent point

must be in either Herman ring or Siegel disc of f. Then the following theorem is obvious.

Theorem 3.1. *Let $a \in F(f)$. Then a is recurrent point if and only if a is in either Herman ring or Siegel disc of f.*

Suppose a is a recurrent point of f then either $a \in J(f)$ or a is in one of the rotational domains (Herman ring or Siegel disc).

Theorem 3.2. *If a is a recurrent critical point of f then a is in Julia set of f.*

Proof. Let H_0 be a Herman ring or Siegel disc. If $a \in H_0$ then $f : H_0 \to f(H_0)$ is not one one since a is a critical point of f. But for any Herman ring or Siegel disc H_0, $f : H_0 \to f(H_0)$ must be one one. This is a contradiction. So $a \notin H_0$. Thus by previous result, a is in Julia set of f. □

Lemma 3.2. *If a is the Baker omitted value of f and also recurrent critical value of f. Then a can not be in Herman ring or Siegel disc. Thus $a \in J(f)$.*

Proof. Let H_0 be a Herman ring or Siegel disc. If $a \in H_0$ then all the components of $f^{-1}(H_0)$ are unbounded since H_0 contains an omitted value. Also from [5], we have for any component of $f^{-1}(H_0)$, f is not one one. That is $f : f^{-1}(H_0) \to H_0$ is not one one. Thus H_0 can not be a Herman ring or Siegel disc. Thus $a \in J(f)$. □

4. Conclusion

In [6] we have seen that

Theorem 4.1. *Let $f : \widehat{\mathbb{C}} \to \widehat{\mathbb{C}}$ be a rational function and Γ be the boundary of a Siegel disk or a connected component of the boundary of a Herman ring. Then there exists a recurrent critical point c such that $\omega(c) \supset \Gamma$.*

Above result gives us a notion that recurrent critical point is more important than non recurrent critical point for determining the dynamics. Theorem 4.1 is true for rational functions. We will try to investigate that result of the Theorem 4.1 remains true for transcendental functions or not.

Suppose $h \in E$ has Baker wandering domain U then h has infinitely many critical values [1] and ∞ is a limit function of $\{f^n|_U\}$ by definition of Baker wandering domain . By [7], $\infty \in (P(f))'$. Now our question is

Question : If $h \in E$ has Baker wandering domain U then $\infty \in \omega(c)$ for some recurrent critical point c or not ?

References

[1] W. Bergweiler, *Iteration of meromorphic functions*, Bull. of Amer. Math. Soc. **29** (1993), no. 2, 151–188.

[2] W. Bergweiler and A. Eremenko, *On the singularities of the inverse to a meromorphic function of finite order*,, Rev. Mat. Iberoamericana 11(1995), no.2, 355-373.

[3] T.K. Chakra, G. Chakraborty and T. Nayak, *Baker omitted value*,, Complex Variables and Elliptic Equations, (2016) DOI: 10.1080/17476933.2016.1174216.

[4] Guo Ping ZHAN, *Non-recurrence of* $\exp(z)/z$, Acta Mathematica Sinica, English Series, Apr. 2013, Vol. 29, No. 4, pp.703-716.

[5] A. Bolsch, *Periodic Fatou components of meromorphic functions*,, Bull. London Math. Soc. 31(1999), no.5, 543-555.

[6] Ricardo Mane, *On a Theorem of Fatou*, Bol. Soc. Bras. Mat., Vol. 24, N. 1, 1-11,(1992).

[7] Jian-Hua Zheng *Singularities and limit functions in iteration of meromorphic functions*., J. Lond. Math. Soc.(2) 67 (2003) 195-207.

Intersection forms in Closed Simply-connected 4−manifold

Sourav Kanti Patra
Department of Mathematics,
Ramakrishna Mission Vidyamandira,
Belur Math,Howrah-711202,West Bengal,India
email:souravkanipatra@gmail.com

September 16, 2016

Abstract

A topological manifold is a Hausdorff, second countable topological space, which is locally euclidean. We can put compatibility condition on the charts of a manifold to define smooth manifolds. Classification of manifolds is one of the fundamental problem in topology and geometry. Low-dimensional manifolds are classified by geometric structure; high-dimensional manifolds are classified by surgery theory. For example there is a unique connected 0-dimensional manifold, namely the point, and disconnected 0-dimensional manifolds are just discrete sets, classified by cardinality. A connected 1-dimensional manifold without boundary is either circle(if compact) or the real line(if not compact).

1 Introduction

For any finitely presented group, it is easy to construct a (smooth) compact 4-manifold with it as its fundamental group. As there is no algorithm to tell whether two finitely presented group are isomorphic(even if one is known to be trivial) there is no algorithm to tell if two 4-manifolds have the same fundamental group.

This is one reason why much work on 4-manifolds just considers the simply-connected case. The general case of many problem is already known to be intractable. The Freedman's theorem says that all simply connected closed 4-manifolds can be classified upto homeomorphism using intersection forms and Kerby-Siebemann invariant. Here we concentrate on intersection forms to classify the closed simply connected 4-manifolds up to homotopy.

2 Few Results

Theorem 1 ***(Milnor, Whitehead)*** *Two simply connected* $4-$*manifold are homotopy equivalence if and only if they have isomorphic intersection forms*

Theorem 2 ***(Freedman)***

(a). Two simply-connected closed topological 4−manifold are homeomorphic if and only if they have isomorphic intersection forms and the same Kirby-Siebenmann invarient.

(b). Given any even unimodular symmetric bilinear form q over $\mathbb{Z}$ there is, up to homeomorphism, a uuique simply connected topological 4−manifold with intersection form q.

(c). Given any odd unimodular symmetric bilinear form q over $\mathbb{Z}$ there are, up to homeomorphism, precisely two simply connected 4−manifold with intersection form q one of them has non-trivial Kriby-Siebemann invarient and therefore can not be given a smooth structure.

So to classify simply-connected closed 4−manifolds, we need to know at least about the intersection forms. Here we briefly study about intersection forms and calculate the intersection form of some manifold.

3 Intersection forms

Definition 1 *Given any closed oriented 4−manifold M, its intersection form is the symmetric 2−form defined as follows*

$$Q_M : H^2(K;\mathbb{Z}) \times H^2(M;\mathbb{Z}) \longrightarrow \mathbb{Z}$$
$$Q_M(\alpha,\beta) = (\alpha \smile \beta)[M]$$

This forms is bilinear and is represented by a matrix of determinant ± 1.
For convenience, we will often denote $Q_M(\alpha,\beta)$ by $\alpha \cdot \beta$. Further, we will identify without comment a cohomology class $\alpha \in H^2(M;\mathbb{Z})$ with its poincare-dual homology class $\alpha \in H_2(M;\mathbb{Z})$.

For defining Q_M more geometrically, we will represent α and β from $H_2(M;\mathbb{Z})$ by embedded surface S_α and S_β and then equivalently define $Q_M(\alpha,\beta)$ as intersection number of S_α and S_β

$$Q_M(\alpha,\beta) = S_\alpha \cdot S_\beta$$

Given a closed oriented 4-manifold M, we defined its intersection form as

$$Q_M : H_2(M;\mathbb{Z}) \times H_2(M;\mathbb{Z}) \to \mathbb{Z} \quad Q_M(\alpha,\beta) = S_\alpha \cdot \ S_\beta,$$

where S_α and S_β are any two surfaces representing the classes α and β.

Notice that, if M is simple-connected then $H_2(M;\mathbb{Z})$ is a free $\mathbb{Z}$-module and there are isomorphisms $H_2(M;\mathbb{Z}) \approx \oplus m\mathbb{Z}$, where $m = b_2(M)$. If M is not simple connected, then $H_2(M;\mathbb{Z})$ inherits the torsion of $H_1(M;\mathbb{Z})$, but by linearity the intersection form will always vanish on these torsion classes; thus, when studying intersection form, we can safely pretend that $H_2(M;\mathbb{Z})$ is always free. Here we will prove some lemmas

Lemma 1 *The form $Q_M(\alpha,\beta) = S_\alpha \cdot S_\beta$ on $H_2(M;\mathbb{Z})$ coincides modulo poincare duality with the pairing*

$$Q_M(\alpha^*,\beta^*) = (\alpha^* \smile \beta^*)[M]$$

on $H^2(M;\mathbb{Z})$

Proof : Given any class $\alpha \in H_2(M;\mathbb{Z})$, denoted by α^* its Poincare-dual from $H^2(M;\mathbb{Z}$; we have $\alpha^* \frown [M] = \alpha$. We wish to show that the pairing

$$Q_M(\alpha^*,\beta^*) = (\alpha^* \smile \beta^*)[M]$$

on $H^2(M,\mathbb{Z})$ defines the same bilinear form as the one defined above.We will use the general formula(more often written Kronecer pairing as

$$\langle \alpha^* \smile \beta^*, [M]\rangle = \langle \alpha^*, \beta^* \frown [M]\rangle),$$

$(\alpha^* \smile \beta^*)[M] = \alpha^*[\beta \frown [M]]$, from which it follows that $Q_M(\alpha^*,\beta^*) = \alpha^*[\beta]$, or

$$Q_M(\alpha^*,\beta^*) = \alpha^*[S_\beta] \tag{1}$$

Therefore we need to show that
$\alpha^*[S_\beta] = S_\alpha.S_\beta$.

Since Q_M vanishes on torsion classes, it is enough to check the last formula including the free part of $H^2(M;\mathbb{Z})$ into $H^2(M;\mathbb{R})$ and by interpreting the latter as the de Rham Cohomology of exterior 2-forms.

Moving into de Rham cohomology translates cup products into wedge products and cohomology/ homology pairing into integrations. We have for example,

$$Q_M(\alpha^*,\beta^*) = \int_{S_\beta} \alpha^* \wedge \beta^* \quad and \quad \alpha^*[S_\beta] = \int_{S_\beta} \alpha^* \,\mathrm{d}x$$

for all 2-forms $\alpha^*, \beta^* \in \Gamma(\Lambda^2(I^*_M))$.

In this setting, given a surface S_α, one can find a 2-form α^* dual to S_α so that it is non-zero only close to S_α. Further, one can choose some local oriented coordinates $\{x_1, x_2, y_1, y_2\}$ so that S_α coincides locally with the plane $\{y_1 = 0; y_2 = 0\}$, oriented by $dx_1 \wedge dx_2$. One can then choose α^* to be locally written as $\alpha^* = f(x_1, x_2)dy_1 \wedge dy_2$, for some suitable bump-function f on $\mathbb{R}^2$, supported only around $(0,0)$ and with integral $\int_{\mathbb{R}^2} f = 1$.

If S_β is some surface transverse to S_α and we arrange that, around the intersection points of S_α and S_β, we have S_β described by $\{x_1 = 0; x_2 = 0\}$, then clearly

$$\int_{S_\beta} \alpha^* = S_\alpha \cdot S_\beta \tag{2}$$

with each intersection point of S_α and S_β contributing ± 1 depending on weather $dy_1 \wedge dy_2$ orients S_β positively or not.

Unimodularity and Dual classes:

The intersection form Q_M is $\mathbb{Z}$-bilinear and symmetric. As a consequence of Poincare duality, the form Q_M is also **unimodular**, meaning that the matrix representing Q_M is invertible over $\mathbb{Z}$. This is the same as saying that

$$detQ_M = \pm 1.$$

Unimodularity is furthe equivalent to the property that, for every $\mathbb{Z}$-linear function $f : H_2(M;\mathbb{Z}) \to \mathbb{Z}$, there exists a unique $\alpha \in H_2(M;\mathbb{Z})$ so that $f(x) = \alpha \cdot x$.

Lemma 2 *The intersection form Q_M of a 4-manifold is unimoduler.*

Proof. The intersection form is unimoduler if and only the map

$$\hat{Q}_M : H_2(M;\mathbb{Z}) \to Hom_{\mathbb{Z}}(H_2(M;\mathbb{Z}),\mathbb{Z})$$
$$\alpha \mapsto x \mapsto \alpha \cdot x$$

is an isomorphism. We will argue that this last map coincides with the Poincare duality morphism. Indeed, Poincare duality is the homomorphism

$$H_2(M;\mathbb{Z}) \to H^2(M;\mathbb{Z})$$
$$\alpha \mapsto \alpha^*$$

with α^* characterized by $\alpha * \cap[M] = \alpha$. Assume for simplicity that $H_2(M;\mathbb{Z})$ is free.If not free, a similar argument is made on the free part $H^2(M;\mathbb{Z})/Ext(H_1(M;\mathbb{Z});\mathbb{Z})$ of $H^2(M;\mathbb{Z})$,which is all that matters since Q_M vanishes on torsion. Then the universal coefficient theorem shows that we have an isomorphism

$$H_2(M;\mathbb{Z}) \xrightarrow{\approx} Hom(H_2(M;\mathbb{Z}),\mathbb{Z})$$
$$\alpha^* \mapsto x \mapsto \alpha^*[x]$$

Combining Poincare duality with the latter yields the isomorphism

$$H_2(M;\mathbb{Z}) \xrightarrow{\approx} Hom(H_2(M;\mathbb{Z}),\mathbb{Z})$$
$$\alpha \mapsto x \mapsto \alpha^*[x].$$

However, as argued in the preceding subsection, we have $Q_M(\alpha, x) = \alpha^*[x]$, and therefore the above isomorphism coincides with the map $\hat{Q_M}$. That proves that the intersection form Q_M is unimodular.

Further, the unimodularity of Q_M is equivalent to the fact that, for every basis $\{\alpha_1, ..., \alpha_m\}$ of $H_2(M;\mathbb{Z})$, there is a unique dual basis $\{\beta_1, ..., \beta_m\}$ of $H_2(M;\mathbb{Z})$ so that $\alpha_k \cdot \beta_k = +1$ and $\alpha_i \cdot \beta_j = 0$ if $i \neq j$.
To see this start with the basis $\{\alpha_1, ..., \alpha_m\}$ in $H_2(M;\mathbb{Z})$, pick the familiar dual basis $\{\alpha_1^*, ..., \alpha_m^*\}$ in the dual $\mathbb{Z}$ module $Hom(H_2(M;\mathbb{Z}),\mathbb{Z})$, then transport it back to $H_2(M;\mathbb{Z})$ by using Poincare duality (or $\hat{Q_M}$) and hence obtain the desire basis $\{\beta_1, ..., \beta_m\}$.

Lemma 3 *If M and N have intersection forms Q_M and Q_N, then their connected sum $M \# N$ will have intersection form*

$$Q_{M\#N} = Q_M \oplus Q_N.$$

Proof. Since M^o and N^o can be viewed as M and N without a 4-handle (or a 4-cell), and since 2-homology is influenced only by 1-, 2- and 3-handles, it follows that the 2-homology of $M\#N$ will marely be the friendly gathering of the 2-homology of M and M, intersections and all.

Invariants of intersection forms: To start to distinguish between the various possible intersection forms,we define the following simple algebric inveriants:

- The **rank** of Q_M:
  It is the size of Q_M's domain,defined simply as

$$rankQ_M = rank_{\mathbb{Z}} H^2(M;\mathbb{Z}),$$

or $rankQ_M = dim_{\mathbb{R}} H^2(M;\mathbb{R})$. In the other words, the rank is the second Betti number $b_2(M)$ of M.

- The **signature** of Q_M:

It is obtained as follows: first diagonalize Q_M as a matrix over $\mathbb{R}$ (or $\mathbb{Q}$), separate the resulting positive and negative eigenvalues, then subtruct their counts; that is

$$signQ_M = dimH^2_+(M;\mathbb{R}) - dimH^2_-(M;\mathbb{R})$$

where $H^2_\pm$ are any maximal positive or negative-definite subspaces for Q_M. We can set partial Betti numbers $b_2^\pm = dimH^2_\pm$, and thus we can read sign $Q_M = b^+(M) - b^-(M)$.

- The **definiteness** of Q_M (definite or indefinite):

If for all non-zero classes α we always have $Q_M(\alpha,\alpha) > 0$, then Q_M is called **positive definite.**

If, on the contrary, we have $Q_{\mathbb{M}}(\alpha,\alpha) < 0$ for all non-zero $\alpha's$, then Q_M is called **negative definite.**

Otherewise, if for some α_+ we have, $Q_M(\alpha_+,\alpha_+) > 0$ and for some α_- and we have $Q_M(\alpha_-,\alpha_-) < 0$, then Q_M is called **indefinite.**

- The **parity** of Q_M (even or odd):

If, for all classes α, we have that $Q_M(\alpha,\alpha)$ is even, then Q_M is called **even.** Otherwise, it is called **odd.** Notice that is enough to have one class with odd self-intersection for Q_M to be called odd.

Remark Signature are additive,

$$sing(Q' \oplus Q'') = signQ' + signQ''$$

In particular

$$sign(M\#N) = signM + signN$$

Also, changing orientation of M will change the sign of the signature

$$sign\overline{M} = -signM$$

Since it obviously changes the sign of its intersection form: $Q_{\overline{M}} = -Q_M$

4 Developing the Tools

Theorem 3 ***(The Hurewicz Theorem)***

If a space X is $(n-1)$-connected, $n \geq 2$, then $\tilde{H}_i(X) = 0$ for $i \lneq n$ and $\amalg_n(X) \approx H_n(X)$. If a pair (X, A) is $(n-1)$-connected, $n \geq 2$, with A simply connected and non-empty, then $H_i(X, A) = 0$ for $i \lneq n$ and $\Pi_n(X, A) \approx H_n(X, A)$.

Corollary 1 *A map $f : X \to Y$ between simply connected CW complexes is a homotopy equivalence if $f_* : H_n(X) \to H_n(Y)$ is an isomorphism for each n.*

Proof After replacing Y by the mapping cylinder M_f we may take f to be an inclusion $X \hookrightarrow Y$. Since X and Y are simply connected, we have $\Pi_1(Y, X) = 0$. The relative Hurewicz theorem then says that the first nonzero $\Pi_n(Y, X)$ is isomorphic to the first nonzero $H_n(Y, X)$. All the groups $H_n(Y, X)$ are zero from the long exact sequence of homology, so all the groups $\Pi_n(Y, X)$ also vanish. this means that the inclusion $X \hookrightarrow Y$ induces isomorphism on all homotopy groups, and therefore this inclusion is a homotopy eqivalence.

5 Proof of Main Theorem(Milnor, Whitehead)

Proof Take a simply connected 4-manifold M. Then $H_1(M; \mathbb{Z}) = 0$, so by Poincare duality we have $H^3(M; \mathbb{Z}) = H_1(M; \mathbb{Z}) = 0$.

Now, by universal coefficient theorem, $H_3(M; \mathbb{Z}) = 0$. Hence by Hurewicz's theorem,

$$\amalg_2(M) \approx H_2(M, \mathbb{Z}).$$

Since M is simply connected , $H_2(M, \mathbb{Z})$ has no torsion and then is isomorphic to some $\mathbb{Z}^m$. Hence the isomorphism $\amalg_2 \approx H_2$ can be realized by a map,

$$f : S^2 \cdots \vee S^2 \longrightarrow M.$$

Such f induces an isomorphism on 2-homology, and thus on all homology groups but the fourth.

To remedy this defect, we can cut out a small 4-ball from M and thus annihilate its

H_4. The remainder, denoted by M°, is now homotopy-equivalent to $S^2 \vee \cdots \vee S^2$: Indeed the map f can be easily arranged to avoid the missing 4-ball, and it then induces an isomorphism of the whole homologies of the two spaces. Invoking result of Whitehead implies that f is infact a homotopy equivalence

$$M^\circ \sim S^2 \vee \cdots \vee S^2.$$

Since M can be reconstructed by gluing the 4-ball back to M°, we deduce that the homotopy type of M can equivalently be obtained from $\bigvee_m S^2$ by gluing a 4-ball $\mathbb{D}^4$ to it:

$$M \sim \bigvee_m S^2 \cup_\phi \mathbb{D}^4.$$

The attachment of the ball is made through some suitable map

$$\phi : \partial\mathbb{D}^4 \longrightarrow \bigvee_m S^2.$$

In conclusion, the homotopy type of M is completely determined by the homotopy class of this ϕ; this class should be viewed as an element of $\Pi_3(\bigvee_m S^2)$.

To prove whitehead's theorem, we need only show that the homotopy class of ϕ is completely determined by the intersection form of M.

At the outset, it is worth noticing that, through the homotopy equivalence $M \sim \bigvee_m S^2 \cup_\phi \mathbb{D}^4$, the fundamental class $[M] \in H_4(M;\mathbb{Z})$ corresponds to the class of the attached 4-ball $\mathbb{D}^4$; indeed, since the latter has its boundary entirely contained in the 2-skeleton $\bigvee_m S^2$, as $\partial\mathbb{D}^4 = S^3$ and $\bigvee_m S^2 \cup_\phi \mathbb{D}^4$ has no 3-skeleton; it represents a 4-cycle.

Think of each S^2 as a copy of $\mathbb{CP}^1$ inside $\mathbb{CP}^\infty$. Then embed

$$S^2 \vee \cdots \vee S^2 \subset \mathbb{CP}^\infty \times \cdots \times \mathbb{CP}^\infty,$$

and consider the exact homotopy sequence

$$1\!1_4(\times_m \mathbb{CP}^\infty) \to 1\!1_4(\times_m \mathbb{CP}^\infty, \bigvee_m S^2) \to 1\!1_3(\bigvee_m S^2) \to 1\!1_3(\times_m \mathbb{CP}^\infty).$$

Since $\mathbb{CP}^\infty$ is an Eilenberg-MacLane $K(\mathbb{Z},2)$-space, the only nonzero homtopy group of $\times_m \mathbb{CP}^\infty$ is π_2, and thus the above sequence exhibits an isomorphism

$$1\!1_4(\times_m \mathbb{CP}^\infty, \bigvee_m S^2) \approx 1\!1_3(\bigvee_m S^2).$$

The above π_4 is made of maps $\mathbb{D}^4 \to \times_m \mathbb{CP}^\infty$ that take $\partial\mathbb{D}^4$ to $\bigvee_m S^2$. The isomorphism associates to $\pi : \partial\mathbb{D}^4 \to \bigvee_m S^2$ in π_3 the class of any of its extensions

$$\tilde{\phi} : \mathbb{D}^4 \longrightarrow \times_m \mathbb{CP}^\infty.$$

Now, we have an exact homotopy sequence:

$$\amalg_3(\times_m \mathbb{CP}^\infty) \to \amalg_3(\times_m \mathbb{CP}^\infty, \bigvee_m S^2) \to \amalg_2(\bigvee_m S^2) \xrightarrow{\cong} \amalg_2(\times_m \mathbb{CP}^\infty) \to$$

$$\amalg_2(\times_m \mathbb{CP}^\infty, \bigvee_m S^2) \to \amalg_1(\bigvee_m S^2) \to \amalg_1(\times_m \mathbb{CP}^\infty) \to \amalg_1(\times_m \mathbb{CP}^\infty, \bigvee_m S^2) \to 0$$

Since the inclusion $\bigvee_m S^2 \subset \times_m \mathbb{CP}^\infty$ induces an isomorphism on $\amalg_2$. Hence the homotopy exact sequence implies that both $\prod_1, \amalg_2$ and $\prod_3$ of the pair $(\times_m \mathbb{CP}^\infty, \bigvee_m S^2)$ must vanish. Therefore, Hurewicz's theorem shows that we have a natural identification

$$\amalg_4(\times_m \mathbb{CP}^\infty, \bigvee_m S^2) \approx H_4(\times_m \mathbb{CP}^\infty, \bigvee_m S^2; \mathbb{Z}).$$

through this identification, the class of $\tilde{\phi}$ from $\prod_4$ is sent to the class

$$\tilde{\phi}_*[\mathbb{D}^4] \in H_4(\times_m \mathbb{CP}^\infty, \bigvee_m S^2; \mathbb{Z},)$$

where $\tilde{\phi}_*$ is the morphism induced on homology by the map $\tilde{\phi}$.

Also, we have the homology exact sequence:

$$H_4(\bigvee_m S^2; \mathbb{Z}) \to H_4(\times_m \mathbb{CP}^\infty; \mathbb{Z}) \to H_4(\times_m \mathbb{CP}^\infty, \bigvee_m S^2; \mathbb{Z}) \to H_3(\bigvee_m S^2; \mathbb{Z}) \to$$

$$H_3(\times_m \mathbb{CP}^\infty; \mathbb{Z}) \to H_3(\times_m \mathbb{CP}^\infty, \bigvee_m S^2; \mathbb{Z}) \to H_2(\bigvee_m S^2) \to H_2(\times_m \mathbb{CP}^\infty) \to$$

$$H_2(\times_m \mathbb{CP}^\infty, \bigvee_m S^2) \to H_1(\bigvee_m S^2) \to H_1(\times_m \mathbb{CP}^\infty).$$

Since both H_4 and H_3 of $\bigvee_m S^2$ vanish, the homology exact sequence makes appear the isomorphism

$$H_4(\times_m \mathbb{CP}^\infty, \bigvee_m S^2; \mathbb{Z}) \approx H_4(\times_m \mathbb{CP}^\infty; \mathbb{Z}).$$

For example, since $\tilde{\phi}_*[\mathbb{D}^4]$ represents a 4-class and its boundary is included in the 2-skeleton of $\times_m \mathbb{CP}^\infty$, it follows that $\tilde{\phi}_*[\mathbb{D}^4]$ can be viewed as a 4-cycle directly in $H_4(\times_m \mathbb{CP}^\infty; \mathbb{Z})$.

Owing to the lack of torsion, we also have a natural duality

$$H^4(\times_m \mathbb{CP}^\infty; \mathbb{Z}) = Hom(H_4(\times_m \mathbb{CP}^\infty; \mathbb{Z}), \mathbb{Z}).$$

This shows that, in order to determine $\tilde{\phi}_*[\mathbb{D}^4]$ in H_4, it is enough to evaluate all classes from H^4 on it. In other words, the class $\phi \in \prod_3(\bigvee_m S^2)$ (and thus the homotopy type of M) are completely determined by the set of values $\alpha_k(\tilde{\phi}_*[\mathbb{D}^4])$ for some basis $\{\alpha_k\}_k$ of $H^4(\times_m \mathbb{CP}^\infty; \mathbb{Z})$.

Such a basis can be immediately obtained by cupping the classes dual to each S^2, that is to say we have

$$H^4(\times_m \mathbb{CP}^\infty; \mathbb{Z}) = \mathbb{Z}\{\omega_i \smile \omega_j\}_{i,j},$$

where ω_k denotes the 2-class dual to $\mathbb{CP}^1$ inside the k^{th} copy of $\mathbb{CP}^\infty$. Furthermore, since

$$H_2(\times_m \mathbb{CP}^\infty; \mathbb{Z}) \approx H^2(\bigvee_m S^2; \mathbb{Z}) \approx H^2(M^\circ; \mathbb{Z}) \approx H^2(M; \mathbb{Z}),$$

we see that each class of ω_k of $\times_m \mathbb{CP}^\infty$ can be in fact viewed as a 2-class ω_k of M itself.

Specifically, the inclusion $\iota : \bigvee_m S^2 \subset \times_m \mathbb{CP}^\infty$ extends by $\tilde{\phi}$ to the map

$$M \sim \bigvee_m S^2 \cup_\phi \mathbb{D}^4 \xrightarrow{\iota + \tilde{\phi}} \times_m \mathbb{CP}^\infty.$$

The ω_k's appear as the pull backs $\omega_k = (\iota + \tilde{\phi})^* \omega_k$ and make up a basis of $H^2(M; \mathbb{Z})$.

Evaluating $\omega_i \smile \omega_j$ on $\tilde{\phi}_*[\mathbb{D}^4]$ inside $\times_m \mathbb{CP}^\infty$ yields the same result as pulling ω_i and ω_j back to M, cupping there, and the evaluating on $[\mathbb{D}^4]$:

$$\begin{aligned}(\omega_i \smile \omega_j)(\tilde{\phi}_*[\mathbb{D}^4]) &= ((\iota + \tilde{\phi})^*(\omega_i \smile \omega_j))[\mathbb{D}^4] \\ &= ((\iota + \tilde{\phi})^* \omega_i) \smile ((\iota + \tilde{\phi})^* \omega_j)[\mathbb{D}^4] \\ &= (\omega_i \smile \omega_j)[\mathbb{D}^4].\end{aligned}$$

However, as we noticed at the outset, the class $[\mathbb{D}^4]$ coincides with the fundamental class $[M]$ of M, and hence

$$(\omega_i \smile \omega_j)[\mathbb{D}^4] = Q_M(\omega_i, \omega_k).$$

Since $\{\omega_1, \cdots \omega_m\}$ is a basis in $H^2(M; \mathbb{Z})$, we deduce that the set of values $Q_M(\omega_i, \omega_k)$ fills-up a complete matrix for the intersection form Q_M of M.

On the other hand, as we have argued, by staying in $\times_m \mathbb{CP}^\infty$ and evaluating all the $\omega_i \smile \omega_j$'s on $\tilde{\phi}_*[\mathbb{D}^4]$ we fully determine the class of ϕ in $\amalg_3(\bigvee_m S^2)$ and thus fix the homotopy type of M.

This concludes the proof of Whitehead's theorem.

6 Computation of intersection forms of some manifolds

For a closed R-orientable n-manifold M, consider the cup product pairing,

$$\begin{aligned}H^k(M; R) \times H^{n-k}(M; R) &\to R \\ (\phi, \psi) &\mapsto (\phi \smile \psi)[M]\end{aligned}$$

Such a bilinear pairing $A \times B \to R$ is said to be non-singular if the maps $A \to Hom(B, R)$ and $B \to Hom(A, R)$, obtained by viewing the pairing as a function of each variable separately, are both isomorphism.

Proposition: The cup product pairing is nonsingular for closed R orientable manifolds when R is a field, or when $R = \mathbb{Z}$ and torsion in $H^*(M;\mathbb{Z})$ is factored out.

Proof: Consider the composition

$$H^{n-k}(M;R) \xrightarrow{h} Hom_R(H_{n-k}(M;R),R) \xrightarrow{D^\star} Hom_R(H^k(M;R),R)$$

where h is the map appearing in the universal coefficient theorem, induced by evaluation of cochains on chains, and D^* is the Hom-dual of the Poincare duality map $D : H^k \to H_{n-k}$. the composition D^*h sends $\psi \in H^{n-k}(M;R)$ to the homomorphism $\phi \mapsto \psi([M] \frown \phi) = (\phi \smile \psi)[M]$. For field coefficients or integer coefficients with torsion factored out, h is an isomorphism. Nonsingularity of the pairing in one of its variables is then equivalent to D being an isomorphism. Nonsingularity in the other variable follows by commutativity of the cup product.

Corollary 2 *If M is a closed connected orientable n-manifold, then for each element $\alpha \in H^k(M;\mathbb{Z})$ of infinite order that is not a proper multiple of another element $\beta \in H^{n-k}(M;\mathbb{Z})$ such that $\alpha \smile \beta$ is a generator of $H^n(M;\mathbb{Z}) \approx \mathbb{Z}$. With coefficient in a field the same conclusion holds for any $\alpha \neq 0$*

Proof: The hypothesis on α means that it generates a $\mathbb{Z}$ summand of $H^k(M;\mathbb{Z})$. There is then a homomorphism $\phi : H^k(M;\mathbb{Z}) \to \mathbb{Z}$ with $\phi(\alpha) = 1$. By the nonsingularity of the cup product pairing $\beta \in H^{n-k}(M;\mathbb{Z})$ and evaluating on $[M]$, so $\alpha \smile \beta$ generates $H^n(M;\mathbb{Z})$. The case of field coefficients is similar.
A. The sphere (S^4)**:** It does not have any 2−homology, it has no intersection form worth mentioning.

B. The complex projection plane ($\mathbb{C}P^2$)**:**
We know that $H^*(\mathbb{C}P^2,\mathbb{Z}) = \mathbb{Z}[\alpha]/(\alpha^3)$ with $|\alpha| = 2$
By Corrolary (2), $\exists \beta \in H^2(\mathbb{C}P^2,\mathbb{Z})$ such that $\alpha \smile \beta$ generates $H^4(\mathbb{C}P^2,\mathbb{Z})$
let $\beta = m\alpha$
Now, $(\alpha \smile \beta)[\mathbb{C}P^2] = 1 \Rightarrow m(\alpha \smile \alpha)[\mathbb{C}P^2] = 1 \Rightarrow m = \pm 1$, without loss of generality $m = 1, \therefore \alpha \smile \alpha[\mathbb{C}P^2] = 1$
Thus it has intersection form $Q_{\mathbb{C}P^2} = (+1)$. Since $H_2(\mathbb{C}P^2;\mathbb{Z}) = \mathbb{Z}\{[\mathbb{C}P^1]\}$ where $\mathbb{C}P^1$ is the class of a projective line, and since the two projective lines always meet in a point. The opposite oriented manifold $\mathbb{C}P^2$ has intersection form

$$Q_{\overline{\mathbb{C}P^2}} = (-1)$$

C. Sphere Bunde ($S^2 \times S^2$)**:** We have by Kunneth Formula

$$\begin{aligned} &H^2(S^2 \times S^2;\mathbb{Z}) \\ &\cong H^2(S^2;\mathbb{Z}) \otimes_{\mathbb{Z}} H^0(S^2;\mathbb{Z}) \oplus H^1(S^2;\mathbb{Z}) \otimes_{\mathbb{Z}} H^1(S^2;\mathbb{Z}) \oplus H^0(S^2,\mathbb{Z}) \otimes_{\mathbb{Z}} H^2(S^2,\mathbb{Z}) \\ &= \mathbb{Z} \oplus \mathbb{Z} \end{aligned}$$

Also, by Kunneth formula:

$$
\begin{aligned}
&H^4(S^2 \otimes S^2; \mathbb{Z}) \\
&\cong H^4(S^2;\mathbb{Z}) \otimes_{\mathbb{Z}} H^0(S^2;\mathbb{Z}) \oplus H^3(S^2;\mathbb{Z}) \otimes_{\mathbb{Z}} H^1(S^2;\mathbb{Z}) \oplus H^2(S^2;\mathbb{Z}) \otimes_{\mathbb{Z}} H^2(S^2;\mathbb{Z}) \\
&\oplus H^1(S62;\mathbb{Z}) \otimes_{\mathbb{Z}} H^3(S^2;\mathbb{Z}) \oplus H^0(S^2;\mathbb{Z}) \otimes_{\mathbb{Z}} H^4(S^2;\mathbb{Z}) \\
&\cong H^2(S^2;\mathbb{Z}) \otimes_{\mathbb{Z}} H^2(S^2;\mathbb{Z}) [\because H^i(S^2;\mathbb{Z}) = 0 \quad \text{for} \quad i \neq 0, 2] \\
&\cong \mathbb{Z} \otimes_{\mathbb{Z}} \mathbb{Z} \\
&\cong \mathbb{Z}
\end{aligned}
$$

We know that,

$$H^*(S^2;\mathbb{Z}) \cong \mathbb{Z}[\alpha]/(\alpha^2) \quad \text{where} \quad |\alpha| = 2$$

$$\therefore H^2(S^2 \times S^2;\mathbb{Z}) \cong \mathbb{Z}[\alpha,\beta]/(\alpha^2,\beta^2) \quad \text{where} \quad |\alpha| = |\beta| = 2$$

$$\therefore \alpha \smile \alpha = \beta \smile \beta = 0$$

Now, by the corollary, for $\alpha \in H^2(S^2 \times S^2;\mathbb{Z})$, $\exists \gamma \in H^2(S^2 \times S^2;\mathbb{Z})$ such that $\alpha \smile \gamma$ is a generator of $H^4(S^2 \times S^2;\mathbb{Z})$.
Let $\gamma = a\alpha + b\beta$
$\alpha \smile \gamma = \alpha \smile (a\alpha + b\beta) = a(\alpha \smile \alpha) + b(\alpha \smile \beta) = b(\alpha \smile \beta)$
Since $\alpha \smile \gamma$ generates $H^4(S^2 \times S^2;\mathbb{Z})$, we have:

$$
\begin{aligned}
&(\alpha \smile \gamma)[S^2 \times S^2] = 1 \\
&\Rightarrow b(\alpha \smile \beta)[S^2 \times S^2] = 1 \\
&b = \pm 1
\end{aligned}
$$

Without loss of generality let $b = 1$, Then $(\alpha \smile \beta)[S^2 \times S^2] = 1$
Hence the intersection form of $S^2 \times S^2$ is:
$Q_{S^2 \times S^2} = \begin{pmatrix} 0 & 1 \\ 1 & 0 \end{pmatrix}$

For the twisted product $S^2 \tilde{\times} S^2$; the intersection form is $Q_{S^2 \tilde{\times} S^2} = \begin{pmatrix} 1 & 1 \\ 1 & 0 \end{pmatrix}$ so $Q_{S^2 \tilde{\times} S^2} = \begin{pmatrix} 1 & 0 \\ 0 & -1 \end{pmatrix} = (+1) \oplus (-1)$

$$S^2 \tilde{\times} S^2 \cong \mathbb{C}P^2 \# \overline{\mathbb{C}P^2}$$

D. The manifold E_8: Freedman's E_8 manifold is $M_{E_8} = P_{E_8} \cup_{\Sigma_p} \Delta$. This topological 4-manifold was build by plumbing on the E_8 diagram and capping with a fake 4-ball. Its intersection form can be read from the plumbing diagram to be

$$
Q_{M_{E_8}} = \begin{pmatrix}
2 & 1 & & & & & & \\
1 & 2 & 1 & & & & & \\
 & 1 & 2 & 1 & & & & \\
 & & 1 & 2 & 1 & & & \\
 & & & 1 & 2 & 1 & & 1 \\
 & & & & 1 & 2 & 1 & \\
 & & & & & 1 & 2 & \\
 & & & & 1 & & & 2
\end{pmatrix}
$$

Lemma 4 *The E_8-form is positive-definite, even, and of signature 8.*

Proof: We will perform elementary operations on the rows and colums of the E_8-matrix. First off, notice that these operations must be applied symmetrically, corresponding to change of basis in $H_2(M;\mathbb{Z})$. That is to say when for example we subtract $3/2$ times the first row from the third, we must afterwards also subtract $3/2$ times the first column from the third column. Indeed, since the matrix A of a bilinear form acts on $H_2 \times H_2$ by $(x,y) \mapsto x^t A y$, any elementary change of basis $I + \lambda E_{ij}$ on H_2 will transform A into $(I + \lambda E_{ij}) A (I + \lambda E_{ij})$.

Debote by $(1),(2),(3),(4),(5),(6),(7),(8)$ the eight rows / columns of the E_8-matrix, and let us start: We write down the E_8-matrix, then subtract $1/2 \times (1)$ from (2):

$$\begin{pmatrix} 2 & 1 & & & & & & \\ 1 & 2 & 1 & & & & & \\ & 1 & 2 & 1 & & & & \\ & & 1 & 2 & 1 & & & \\ & & & 1 & 2 & 1 & & 1 \\ & & & & 1 & 2 & 1 & \\ & & & & & 1 & 2 & \\ & & & & 1 & & & 2 \end{pmatrix} \quad \textit{then} \quad \begin{pmatrix} 2 & & & & & & & \\ & 3/2 & 1 & & & & & \\ & 1 & 2 & 1 & & & & \\ & & 1 & 2 & 1 & & & \\ & & & 1 & 2 & 1 & & 1 \\ & & & & 1 & 2 & 1 & \\ & & & & & 1 & 2 & \\ & & & & 1 & & & 2 \end{pmatrix}$$

Subtract $2/3 \times (2)$ from (3), then subtract $3/4 \times (3)$ from (4):

$$\begin{pmatrix} 2 & & & & & & & \\ & 3/2 & & & & & & \\ & & 4/3 & 1 & & & & \\ & & 1 & 2 & 1 & & & \\ & & & 1 & 2 & 1 & & 1 \\ & & & & 1 & 2 & 1 & \\ & & & & & 1 & 2 & \\ & & & & 1 & & & 2 \end{pmatrix} \quad \textit{then} \quad \begin{pmatrix} 2 & & & & & & & \\ & 3/2 & & & & & & \\ & & 4/3 & & & & & \\ & & & 5/4 & 1 & & & \\ & & & 1 & 2 & 1 & & 1 \\ & & & & 1 & 2 & 1 & \\ & & & & & 1 & 2 & \\ & & & & 1 & & & 2 \end{pmatrix}.$$

Subtract $4/5 \times (4)$ from (5), then subtract $1/2 \times (8)$ from (5):

$$\begin{pmatrix} 2 & & & & & & & \\ & 3/2 & & & & & & \\ & & 4/3 & & & & & \\ & & & 5/4 & & & & \\ & & & & 6/5 & 1 & & 1 \\ & & & & 1 & 2 & 1 & \\ & & & & & 1 & 2 & \\ & & & & 1 & & & 2 \end{pmatrix} \quad \textit{then} \quad \begin{pmatrix} 2 & & & & & & & \\ & 3/2 & & & & & & \\ & & 4/3 & & & & & \\ & & & 5/4 & & & & \\ & & & & 7/10 & 1 & & \\ & & & & 1 & 2 & 1 & \\ & & & & & 1 & 2 & \\ & & & & & & & 2 \end{pmatrix}$$

Subtract $10/7 \times (5)$ from (6), then subtract $7/4 \times (6)$ from (7):

$$\begin{pmatrix} 2 & & & & & & & & \\ & 3/2 & & & & & & & \\ & & 4/3 & & & & & & \\ & & & 5/4 & & & & & \\ & & & & 7/10 & & & & \\ & & & & & 4/7 & 1 & & \\ & & & & & 1 & 2 & & \\ & & & & & & & 2 & \end{pmatrix} \quad \textit{then} \quad \begin{pmatrix} 2 & & & & & & & & \\ & 3/2 & & & & & & & \\ & & 4/3 & & & & & & \\ & & & 5/4 & & & & & \\ & & & & 7/10 & & & & \\ & & & & & 4/7 & & & \\ & & & & & & 1/4 & & \\ & & & & & & & 2 & \end{pmatrix}.$$

We have diagonalized E_8, and its signature is 8. It is positive-definite. Its determinant is $\det E_8 = 1$ and hence E_8 is unimodular, as claimed.

References

[1] *Algebraic Topology.* Allan Hatcher

[2] *The wild world of* 4*-manifolds.* Alexandru Scorpan

[3] *Algebra.* Michael Artin.

On Stanley's theorem & It's Generalizations

Suprokash Hazra

July 10, 2016

Abstract

In this paper we go on to discuss about Stanley's theorem in Integer partitions. We give two different versions for the proof of the generalization of Stanley's theorem illustrating different techniques that may be applied to profitably understand the underlying structure behind the theorem.

KEYWORDS: Stanley's theorem,Tilings,Partition identities.

Introduction:

Stanley's theorem is an important result in the theory of partitions. Various generalizations have been made to it over the course of time including Elder's theorem[1] and Dastidar & Gupta's[2] subsequent generalization.In their paper they go on to show how the sum of the number of distinct members of the partition is not just equal to the number of 1's present in the partition of the same number but is also equal to the sum of the number of i's in the partitions of all the numbers from n to (n+i-1), where i can be any positive integer. In this paper we go on to provide different combinatorial arguments to prove such generalizations. A proof of the generalization involves the use of tilings of a

1x∞ board. This concept can be further generalised to cover similar properties for overpartitions as well. To prove the generalization we first make use of some lemmas which follow subsequently in the article.

LEMMA 1.1 :

Let n and k be two positive integers with $k \leq n$, then for each positive integer i, $(1 \leq i \leq n)$, we have $n + i = q_i k + r_i$, where $0 \leq r_i < k$,

then $q_i = q_0$, for all $1 \leq i \leq s - 1$

$= q_0 + 1$, for all i $\geq$ s

And $r_i = r_0 + i$, for all 1 $\leq$i $\leq$s-1,

$= i - s$, for all i $\geq$s where $s = k - r_0$

Proof of lemma 1.1 :

Let us consider the two integers n+i and k,

then by division algorithm there exists two integers q_i and r_i

such that,$n + i = q_i k + r_i$ with $0 \leq r_i < k$. Now, $n = q_0 k + r_0$.

We assume, $k - r_0 = s$

Then we have the following,

$n = q_0 k + r_0$;

$n + 1 = q_0 k + (r_0 + 1)$;

$n + 2 = q_0 k + (r_0 + 2)$

...

$n + s - 1 = q_0 k + (r_0 + s - 1)$

$n + s = (q_0 + 1)k$

$n + s + 1 = (q_0 + 1)k + 1$

$n + s + 2 = (q_0 + 1)k + 2$

.....

$n+k-1=(q_0+1)k+(r_0-1)$

By the above formula it is clear that

$q_i = q_0$ for all $1 \leq i \leq s-1$

$=q_0+1$ for all $i \geq s$

Hence the lemma 1.1

Notation: $Q_k(n+i)$:=Number of occurences of k

in the unordered partitions of $(n+i)$

$B(n)$:=Sum of the total number of distinct members

in all the partitions of n.

$A(n) = \sum_{i=0}^{k-1} Q_k(n+i)$=Sum of all the number of occurrences of k in all

unordered partitions of n+i for all $0 \leq i \leq k-1$

LEMMA 1.2 :

$Q_k(n+i) = \sum_{j=1}^{q_i} P(n+i-jk)$, for some fixed i.

Proof of lemma 1.2 :

For a fixed i, considering the two integers n+i and k, then by division

algorithm there exists two integers q_i and r_i such that, $n+i = q_i k + r_i$

with $0 \leq r_i < k$ (as mentioned in lemma 1.1)

For a fixed i, the number of partitions of n+i,

where k occurs exactly once is $P(n+i-k) - P(n+i-2k)$,

the number of partitions of n+i,

where k occurs exactly twice is $P(n+i-2k) - P(n+i-3k)$,

The number of partitions of n+i, where k occurs

exactly $(q_i - 1)$ times is $P(n+i-(q_i-1)k) - P(n+i-q_ik)$

And , the number of partitions of n+i, where k occurs

exactly q_i times is $P(r_i)$.

So $Q_k(n+i)$

= The number of occurrences of k in all unordered partitions of n+i

$= P(n+i-k) - P(n+i-2k) + 2[P(n+i-2k) - P(n+i-3k)] + \ldots.$

$\ldots + (q_i - 1)[P(n+i-(q_i-1)k) - P(n+i-q_ik)] + q_iP(r_i)$

$= P(n+i-k) + P(n+i-2k) + P(n+i-3k) + \ldots..$

$\ldots + P(n+i-(q_i-1)k) - (q_i-1)P(n+i-q_ik) + q_iP(r_i)$

$= P(n+i-k) + P(n+i-2k) + P(n+i-3k) + \ldots..$

$\ldots + P(n+i-(q_i-1)k) - q_iP(n+i-q_ik) + P(n+i-q_ik) + q_iP(r_i)$

$= P(n+i-k) + P(n+i-2k) + P(n+i-3k) + \ldots..$

$\ldots.. + P(n+i-(q_i-1)k)) + P(n+i-q_ik)[since, n+i-q_ik = r_i]$

$= \sum_{j=1}^{q_i} P(n+i-jk),$

Hence the lemma 1.2.

Observation: When $t\varepsilon\{1, 2, ..., n\}$ is fixed for all $1 \leq$ i $\leq$n ,we have,

$\sum_{i=0}^{k-1}[P(n+i-tk)] = P(n-tk) + P(n+1-tk) + P(n+2-tk) + \ldots..$

$+P(n+k-1-tk)$

$= P(n-tk) + P(n-(tk-1)) + P(n-(tk-2)) + \ldots. + P(n-((t-1)k+1)).$

Now we come to our main theorem which states that,

THEOREM 1 :

$A(n) = B(n)$ for all integers n

Proof of theorem:

We consider $A(n) = \sum_{i=0}^{k-1} Q_k(n+i) = \sum_{i=0}^{k-1}[\sum P(n+i-jk)]$

{By lemma 1.2}

$=\sum_{i=0}^{k-1}[P(n+i-k)]+\sum_{i=0}^{k-1}[P(n+i-2k)+\ldots.$

$+\sum_{i=0}^{k-1}[P(n+i-(q_i-1)k))]+\sum_{i=0}^{k-1}[P(n+i-q_ik)]$

from which it follows that $A(n)$

$=[P(n-1)+P(n-2)+P(n-3)+\ldots.+P(n-k)]+[P(n-(k+1))+$

$P(n-(k+2))+\ldots..+P(n-2k)]\ldots\ +[P(n-((q_0-1)k+1)+$

$P(n-((q_0-1)k+2)+\ldots..+P(n-q_0k)]+\sum_{i=s}^{k-1}[P(n+i-q_ik)]$

(by above observation)

$=P(n-1)+P(n-2)+P(n-3)+\ldots.+P(n-q_0k)+\sum_{i=s}^{k-1}P(r_i)$

(Using lemma 1.1)

$=P(n-1)+P(n-2)+P(n-3)+\ldots.+P(r_0)+$

$[P(r_0-1)+P(r_0-2)+\ldots.+P(1)+1]$

This is the expression for A(n). Now to find the expression for B(n) using $P(1),P(2),\ldots.,P(n-1)$. For finding the expression for B(n),we will look at this sum to count the number of partitions of n in which the number i appears and sum those result for all $1\leq i\leq n$.Now the number of partitions of n in which i appears is $P(n-i)$ for all $1\leq i\leq n-1$ and with the special case $i=n$ is 1. Hence $B(n)=1+P(1)+P(2)+\ldots.+P(n-3)+P(n-2)+P(n-1)$.

Hence A(n)= B(n)

This completes our proof.

2. A TILLING PROOF OF THE EXTENSION OF STANLEY'S THEOREM

We consider a 1x∞ board. We will tile this board using white squares and finitely many black squares. We allow the stacking of the black squares. Let T be the set of all such tilings. Let a white tile will have measure 1 and a black tile in position i will have measure q^i. Now we define the measure of a tiling to be M(t)= $\prod$ m(t). (where the product runs over all the squares for a particular tiling tε T. And m denotes the measure of the squares for a particular tiling t.

Partition representation of a tiling:

Suppose we assume a partition of $m = \mu_1 + \mu_2 + \ldots..\mu_K$, denoting this partition by μ. Then we associate a tiling t_{μ} such that, it has a black tiles in position $\mu_1, \mu_2 ..., \mu_K$. Now as the numbers $\mu_1, \mu_2, .., \mu_K$ may not all distinct so we can have more than one black tiles in some position. Also we obtain $M(t_{\mu}) = q^{\mu_1+\mu_2+\ldots..\mu_K}$

Now we need these following lemmas in order to prove the theorem.

LEMMA 2.1 :

For each $1 \leq i \leq k-1$, the number of partitions of n with atleast (k-i) times r = Number of partitions of n+ir with atleast r times k.

Proof of lemma 2.1 :

Consider A= Set of all tilings with atleast (k-i) black tiles in position r.

And B=Set of all tilings with atleast r black tiles in position k.

Now we define T: A$\rightarrow$B, by the following way,

We take a tiling from A, then we remove (k-i) black tiles from position r and

add r black tiles in position k.

Then T is well defined map. In order to prove T is bijective

we define a mapping S:B→A, by the following way,we take a tiling from B,

then we remove r black tiles from position k and add (k-i) black tiles in

position r. Then S is well defined map. Also S T = Id_A and T S = Id_B,

the identity mappings on A and B respectively.

Now clearly the change of measure under the map T is $q^{-r(k-i)+kr} = q^{ir}$.

Now take A*=Set of all tilings of A with measure q^n.

Then for each tiling of A* we obtain a bijective Correspondence with a tiling

of B of measure q^{n+ir}.

Now every tiling gives a partitions and vice versa.

So by the Partition representation of a tiling,

we have that, the number of partitions of n

with atleast (k-i) times r = number of partitions of n+ir

with atleast r times k.

Hence the lemma 2.1.

LEMMA 2.2 :

Number of partitions of n with atleast i times r = The number of partitions of n with atleast r times i.

Proof of lemma 2.2:

Consider M= Set of all tilings with atleast i black tiles in position r. And N=Set of all tilings with atleast r black tiles in position i. Now we define Q: M→N, by the following way, We take a tiling from M, then we remove i black tiles from position r and add r black tiles in position i. Then Q is well defined map. In order to prove Q is bijective we define a mapping Z:N→M, by

the following way,we take a tiling from N, then we remove r black tiles from position i and add i black tiles in position r. Then Z is well defined map. Also QZ= Id_N and ZQ = Id_M, the identity mappings on N and M respectively. Now clearly there is no change of measure under the map Q. Now take M*=Set of all tilings of A with measure q^n. Then for each tiling of A* we obtain a bijective Correspondence with a tiling of N of measure q^n . Now every tiling gives a partitions and vice versa. So by the Partition representation of a tiling, we have the lemma 2.2.

LEMMA 2.3 :

The number of partitions of n with atleast 1 times r = The number of partitions of (n+kj-r) with atleast j times k. we assume $n = qk+r$,and $1 \leq j \leq q$. In particular,$V_j^k(n+kj-r) = V_s^k(n+ks-r)$, for all $1 \leq j, s \leq n$ Where $V_p^q(m)$= The number of partitions of m with atleast p times q.

Proof of lemma 2.3:

Let C = Set of all tilings with atleast 1 black tiles in position r. And D= Set of all tilings with atleast j black tiles in position k. Now we define F: C$\rightarrow$D, by the following way, We take a tiling from C, then we remove 1 black tiles from position r and add j black tiles in position k. Then F is well defined map. In order to prove F is bijective we define a mapping G:D$\rightarrow$C, by the following way, we take a tiling from D, then we remove j black tiles from position k and add 1 black tiles in position r. Then G is well defined map. Also GF = $\mathrm{Id}_C$and FG = Id_D, the identity mappings on C and D respectively. Now clearly the change of measure under the map F is q^{kj-r}.

$C^{\#}$=Set of all tilings of C with measure q^n. Then for each tiling of $C^{\#}$ we obtain a bijective Correspondence with a tiling of D of measure q^{n+kj-r}.

Now every tiling gives a partition and vice versa. So by the Partition representation of a tiling, we have that, the number of partitions of n with atleast 1 times r = number of partitions of n+kj-r with atleast j times k.

So notationally, $V_j^k(n+kj-r) = V_1^r(n)$.

Since the right hand side of the above expression does not depend on j,so clearly we have that, $V_j^k(n+kj-r) = V_s^k(n+ks-r)$, for all $1 \leq j, s \leq n$

Hence the lemma 2.3.

Now we come to our main theorem.

Proof of theorem :

First we put r=1 in lemma 2.1.

Then we get, the number of partitions of n with atleast (k-i) times 1 = number of partitions of n+i with atleast 1 times k.

Notationally $V_{(k-i)}^1(n) = V_1^k(n+i)$ for all $1 \leq i \leq k-1$ We sum this over all $1 \leq i \leq k-1$ and obtain, $\sum_{i=1}^{k-1} V_{(k-i)}^1(n) = \sum_{i=1}^{k-1} V_1^k(n+i)$ ..... (1)

Now we put r=1 in lemma 2.2. and obtain, $V_i^1(n) = V_1^i(n)$ We sum this over all $k \leq i \leq n$ and obtain, $\sum_{i=k}^{n} V_i^1(n) = \sum_{i=k}^{n} V_1^i(n)$ .....(2)

We add (1) and (2),we obtain

$\sum_{i=1}^{k-1} V_{(k-i)}^1(n) + \sum_{i=k}^{n} V_i^1(n) = \sum_{i=1}^{k-1} V_1^k(n+i) + \sum_{i=k}^{n} V_1^i(n)$

$\sum_{i=1}^{n} V_i^1(n) = \sum_{i=1}^{k-1} V_1^k(n+i) + \sum_{i=k}^{n} V_1^i(n)$

Number of 1's present in the all unordered

partitions of n

$= \sum_{i=1}^{k-1} V_1^k(n+i) + \sum_{i=k}^{n} V_1^i(n)$

$= \sum_{i=1}^{k-1} V_1^k(n+i) + V_1^k(n) + \sum_{i=k+1}^{n} V_1^i(n)$

$= \sum_{i=0}^{k-1} V_1^k(n+i) + \sum_{i=k+1}^{n} V_1^i(n)$..... (4)

Now by lemma 2.3

$\sum_{i=k+1}^{n} V_1^r(n) = \sum_{i=k+1}^{n} V_j^k(n+kj-r)$

$\sum_{i=k+1}^{n} V_1^r(n) = \sum_{i=k+1}^{2k} V_j^k(n+kj-r) + \sum_{i=2k+1}^{3k} V_j^k(n+kj-r) + \ldots\ldots$
$+\sum_{i=(q-1)k+1}^{qk}(V_j^k(n+kj-r))$

$\sum_{i=k+1}^{n} V_1^r(n) = \sum_{i=k+1}^{2k} V_2^k(n+2k-r) + \sum_{i=2k+1}^{3k} V_3^k(n+3k-r) + \ldots\ldots$
$\ldots.\sum_{i=(q-1)k+1}^{qk}(V_q^k(n+kq-r))$

$\sum_{i=k+1}^{n} V_1^r(n) = \sum_{i=0}^{k-1} V_2^k(n+i) + \sum_{i=0}^{k-1} V_3^k(n+i) + \ldots\ldots\ldots\ldots\ldots\ldots$
$\ldots + \sum_{i=0}^{k-1} V_q^k(n+i)\ldots\ldots\ldots$ (6)

Now by (4) and (6) we have that, Number of 1's present in the all unordered partitions of n

$= \sum_{i=0}^{k-1} V_1^k(n+i) + \sum_{i=0}^{k-1} V_2^k(n+i) + \sum_{i=0}^{k-1} V_3^k(n+i) + \ldots\ldots\ldots\ldots$
$\ldots + \sum_{i=0}^{k-1} V_q^k(n+i)$

$= \sum_{j=1}^{q} V_j^k(n) + \sum_{j=1}^{q} V_j^k(n+1) + \ldots\ldots\ldots + \sum_{j=1}^{q} V_j^k(n+k-1)$

$= Q_k(n) + Q_k(n+1) + Q_k(n+2) + \ldots\ldots\ldots\ldots\ldots + Q_k(n+k-1)$

$= \sum_{i=0}^{k-1} Q_k(n+i)$

This completes our proof.

Conclusion:

In this paper we have tried to demonstrate how simple combinatorial proofs can be effectively applied to problems involving unordered partitions. Similar to the extension of Stanley's theorem, we can apply similar techniques to prove further extensions of Elder's theorem and not just for regular partitions but for all classes of overpartitions. The concept of tilings could also pe profitably extended to study similar results in the area of planar partition

References

[1] Wolfram Mathworld. Elder's Theorem. 2010. Available at http://mathworld.wolfram.com/EldersTheorem.html

[2] Dastidar, Gupta. Generalization of a few results in integer partitions

[3] Andrews, George, The Theory of Partitions, in "Encyclopedia of Mathematics and Its Applications," Vol. 2, Addison-Wesley, Reading, MA, 1976.

WAVELETS AND APPLICATIONS
(Quadrature rules involving Daubechies wavelets)

B. N. Mandal
(Retired)
Physics and Applied Mathematics Unit
Indian Statistical Institute

Co-workers: Dr. M. M. Panja, Mr Swaraj Paul Department of Mathematics,Visva Bharati, Santiniketan

Plan of talk

- **Introduction to wavelets**
- **Daubechies wavelet**
- **One-point qudrature formula**
- **Evaluation of regular integrals**
- **Evaluation of singular integrals**

Weakly singular (Abel)
Strongly singular (Cauchy)
Combination of Abel and Cauchy

- **Further works**
- **References**

Introduction to wavelets

Some simple ideas

A very brief history

Wavelet analysis is a new (?) development in the area of **applied mathematics.**

It was first introduced in seismology to locate underground oil deposits. Petroleum geologists usually locate underground oil deposits by making loud sound noises.

Why?

- Because sound waves travel through different materials at different speeds, and geologists can infer what kind of material lies under the surface by sending seismic waves and measuring how quickly they rebound.

- Unfortunately, seismic signals contain lots of transients - abrupt changes in wave as it passes through one layer to another. Fourier analysis spreads that spatial information out **all over** the place.

- Jean Morlet , an engineer, in nineteen hundred and eighties, developed his own way of analyzing the seismic signals to create components that were localized in space, which he called wavelets of constant shape. Morlet, in his personal computer, could separate a wave into its wavelet components and then reassemble them into original wave. But he was not sure if this is mathematically sound. He found the answer from Alex Grossman, a physicist at the Centre de Physique Theorique , Marseills. Both of them collaborated and found that *waves could be reconstructed from their wavelet decompositions.* They coined the word wavelet and published their paper in 1984

- **Yves Meyer** heard about this work in the same year and is the first to realize the connection between Morlet's wavelet and earlier mathematical works of Littlewood, Paley. He discovered a new kind of wavelet, with a mathematical property called **orthogonality** that made the wavelet transform as easy to work with and manipulate as Fourier transform. *Orthogonality* means that the information captured by one wavelet is completely independent of the information captured by another.

- In 1986, **Stephane Mallat,** a student of Meyer, linked the theory of wavelets to the existing literature on subband coding and quadrature mirror filters. Thanks to Mallat's work, wavelets became much easier.

- **Ingrid Daubechies,** a post doc in Courant Institute, fired the final great salvo in the wavelet revolution in 1987. She discovered a whole new class of wavelets, which are not only orthogonal but which could be implemented using simple digital filtering ideas.

- The Daubechies wavelets have surprising features, such as intimate connections with the theory of **fractals.** These turn the theory into a practical tool that can be easily programmed and used by **anyone with a minimum of mathematical training.**

To summarize the history we have the following table.

- 1910, Haar families
- 1981, Morlet, wavelet concept
- 1984, Morlet and Grossman, **wavelet**
- 1985, Meyer, orthogonal wavelet
- 1987, International conference in France
- 1988, Mallat and Meyer, multiresolution
- 1988, Daubechies, compactly supported orthogonal wavelet

Mathematical Background

In mathematics, representing a complicated function $f \in \Omega$, abstract space of functions with the aid of some simpler functions $\{f_n\} \in \Omega$ by

$$f = \sum_n c_n \, f_n \qquad (1)$$

for unique set of coefficients $\{c_n\}$, has been employed since the era of Lagrange. Representation (1) may be regarded as the decomposition of complicated function (phenomenon) into the sum of many simple pieces in such a way that the study of each of these pieces might be easier. For instance, if T is a operator (linear, in particular) on Ω and its action on $f_n \in \Omega$ are known, one can find the action of T on an arbitrary function $f \in \Omega$, as

$$Tf = \Sigma_n c_n T f_n \qquad (2)$$

Whenever the abstract space Ω is a separable Hilbert space H, a countable set of functions $\{f_n\} \in \mathrm{H}$ is said to be *Riesz basis* if every f of the space can be written uniquely as in (1) and there is a bounded invertible operator on H, mapping $\{f_n\}$ onto an orthonormal basis for H.

If the functions $\{f_n\} \in \Lambda$ is the sequence of orthonormal functions, the formal infinite series (1) is called Fourier series of f and the functions f_n's are called harmonics.

Examples are:

i) **System of trigonometric functions** :

$$\frac{1}{\sqrt{2\pi}}, \frac{1}{\sqrt{2\pi}}\cos x, \frac{1}{\sqrt{2\pi}}\sin x, \ldots\ldots, \frac{1}{\sqrt{2\pi}}\cos nx, \frac{1}{\sqrt{2\pi}}\sin nx, \ldots\ldots.$$

or $\frac{1}{\sqrt{2\pi}} e^{inx}, n = 0, \pm 1, \pm 2, \ldots\ldots,$

ii) **System of Strum-Liouville functions**:

Solutions of the homogeneous self-adjoint linear ordinary differential equation

$$\frac{d}{dx}\left(p(x)\frac{du}{dx}\right) + q(x)u + \lambda u = 0, \alpha \le x \le \beta$$

with some well behaved functions $p(x)$ and, $q(x)$ for all possible values of λ satisfying boundary condition $\frac{du}{dx} + h\,u = 0$ at $x = \alpha$ and $\frac{du}{dx} + g\,u = 0$ at $x = \beta$.

To analyze a function it is helpful to use some basic tools (*i.e.,* basis) that look like the function itself.

Now the question arises, *does there exist at all an orthonormal function system with the property that every continuous function (**even not in the space containing the basis**) can be expanded in the Fourier manner into a uniformly convergent series, according to the function of this system?* The answer is **negative**, has been shown a long ago by Haar in his dissertation work at Gottingen in 1909. In the same vein Haar prescribed a complete set of orthonormal discontinuous functions based on a single function $\chi_{[0,1]}$ (characteristic function on [0,1]) such that the Fourier series with respect to the proposed set of orthonormal functions of a function f converges to this function at every point of continuity $'x'$ of f.

Haar's mother wavelet function

$$\psi(t) = 1, 0 < t < \frac{1}{2}$$
$$= -1, \frac{1}{2} \leq t < 1$$
$$= 0, \text{otherwise}$$

Its scaling function is

$$\varphi(t) = 1, 0 \leq t < 1$$
$$= 0 \text{ , otherwise}$$

$$\varphi_{jk}(t) = 2^{\frac{j}{2}}\varphi\left(2^j t - k\right), j, k \in \mathbb{Z}$$

$$\mathbb{Z} = \{\dots\dots, -2, -1, 0, 1, 2, \dots\dots\}$$
$$\psi_{jk}(t) = 2^{\frac{j}{2}}\psi\left(2^j t - k\right), j, k \in \mathbb{Z}$$

Support of $\psi_{jk}(t)$ is $I_{j,\,k} = [\, k\,2^{-j}, (k+1)\,2^{-j})$

$$\int_{\mathbb{R}} \psi_{jk}(t)dt = 0$$

$$\int_{\mathbb{R}} {\psi_{jk}}^2(t)dt = 1$$

The Haar functions are pairwise orthogonal,

$$\int_{\mathbb{R}} \psi_{jk}(t)\,\psi_{mn}(t)dt = \delta_{jm}\delta_{kn}$$

The **Haar system** on the real line is the set of functions $\{\psi_{jk}(t), j, k \in \mathbb{Z}\}$.

It is complete in $L^2(\mathbb{R})$: *The Haar system on the line* $\mathbb{R}$ *is an orthonormal basis in* $L^2(\mathbb{R})$.

Properties of Haar wavelets

1. Any continuous real function with compact support can be approximated uniformly by linear combinations of $\varphi(t), \varphi(2t), \varphi(2^2t), \ldots, \varphi(2^jt)$.

and their shifted functions $\varphi_{jk}(t)$. This extends to those function spaces where any function therein can be approximated by continuous functions.

2. Any continuous real function on [0, 1] can be approximated uniformly on [0, 1] by linear combinations of the constant function 1(const), $\psi(t), \psi(2t), \psi(2^2t), \ldots, \psi(2^jt)$ and their shifted functions $\psi_{jk}(t)$

3. Orthogonality in the form

$$\int_{\mathbb{R}} \psi_{jk}(t)\,\psi_{mn}(t)dt = \delta_{jm}\delta_{kn}$$

After seventy years of its inception, the work of Haar initiated a new scheme for representing functions, now known as wavelet expansion in mathematics, wavelet transform of signal in engineering [Daubechies]. It also developed a novel scheme for the systematic analysis of the convergence of the expansion known as the multiresolution analysis (MRA) [Mallat & Meyer].

Wavelet expansion are similar to the Fourier expansion but the different functions f_n's (like $\frac{1}{\sqrt{2\pi}} e^{inx}$ or $u_n(\lambda_n, x)$ nonzero almost everywhere within the domain of definition of

the function) in the basis are replaced by $\varphi_{j,k}(x) \in I_{j,k} \subset \mathcal{R}$ indexed by the collection of all subintervals. Note that these functions are all copies (by translation and change of scale) of the same regular function $\varphi(x)$, localized in a finite domain in $\mathcal{R}$.

A MRA of the Hilbert space H of square integrable functions $L^2(\mathcal{R})$ is defined as a sequence of closed subspaces $V_j \subset \mathrm{H}$, $j \in \mathrm{Z}$, with the following properties:

i) $V_j \subset V_{j+1}$

ii) $v(x) \in V_j \Leftrightarrow v(2x) \in V_{j+1}$;

iii) $v(x) \in V_0 \Leftrightarrow v(x+1) \in V_0$;

iv) $\bigcup_{j=-\infty}^{j=\infty} V_j$ is dense in $L^2(\mathcal{R})$ and $\bigcap_{j=-\infty}^{j=\infty} V_j = \{0\}$;

v) A function $\varphi \in V_0$, known as scale function, with a nonvanishing integral exists such that the collection $\{\varphi(x-l) \mid l \in Z\}$ is a Riesz basis of V_0.

Moreover, a sequence $\{h_k\} \in \ell^2(Z)$, known as filter coefficients or masks, exist such that the scale function satisfies the relation

$$\varphi(x) = \sqrt{2} \sum_k h_k \varphi(2x - k) \qquad (3)$$

goes by several different names: ***refinement*** equation, the ***dilation*** equation, the ***two scale difference*** equation, ***renormalization*** equation etc.

Interestingly, it can be shown that the collection of functions $\{\varphi_{j,k} \mid k \in Z\}$ with $\varphi_{j,k}(x) = 2^{\frac{j}{2}} \varphi(2^j x - k)$ is a Riesz basis of V_j.

It is important to note that in the scale function φ – dependent analysis of wavelet expansion of $L^2(R)$, the filter coefficient or mask h_k plays the dominant role. For example,

i) Support of the scale function φ depends on the number of nonzero h_k 's. If the number of nonzero h_k is finite, the scale function φ has compact support.

ii) The Fourier transform $\hat{\varphi}(\xi)$ of $\varphi(x)$ also depends on h_k through the relation

$$\hat{\varphi}(\xi) = \frac{1}{\sqrt{2\pi}} \prod_{j=1}^{\infty} m_0\left(\frac{\xi}{2^j}\right)$$

with

$$H(\xi) = \sum_k h_k e^{-i k \xi} \left(\equiv \sqrt{2}\, m_0(\xi)\right).$$

It has been found that although Daubechies scale function can generate sets of orthonormal basis for multiresolution approximation of any function $f \in L^2(\mathcal{R})$defined over the entire real line $\mathcal{R}$, it looses this aspect whenever the domain of definition becomes finite. The origin of this difficulty lies in the loss of the translational invariance (condition (iii) of MRA) of the scale function near the edges of the finite intervals. Consequently, straightforward use of MRA is no longer possible.

To overcome such hindrance, some researchers tried to regain MRA either with the aid of biorthogonal system or by constructing a set of orthonormal basis with the help of the scale functions having full and partial supports within the finite domain. Unfortunately, the process of construction of the orthonormal basis swallows many advantages of the method achieved in case of whole real line.

It has been observed that *orthogonality is no longer a significant issue for wavelet bases of Sobolev spaces. Instead, the size of the support of a scale function or wavelet turns out to be an important criterion for its performance.*

Multiscale analysis has found its way into diverse fields, from differential or integral equations, numerical analysis in mathematics to signal and image processing in computer science and electrical engineering.

- **Daubechies wavelets**

Ingrid Daubechies (December 2005)
DOB: 17.8.1954,
POB: Houthalen-Helchteren, Belgium

Short Biography

Daubechies was born in Houthalen, Belgium, as the daughter of Marcel Daubechies (a civil mining engineer) and Simonne Duran (then a homemaker, later a criminologist). Ingrid remembers that when she was a little girl and could not sleep, she did not count numbers, as you would expect from a child, but started to multiply numbers by two from memory. Thus, as a child, she already familiarized herself with the properties of exponential growth. Her parents found out that mathematical conceptions, like cone and tetrahedron, were familiar to her before she reached the age of 6. She excelled at the primary school, moved up a class after only 3 months. According to her parents she was able to derive the area of an ellipse by means of integral calculation at the age of 11. After completing the Lyceum in Turnhout she entered

the Vrije Universiteit Brussel at 17. Daubechies completed her undergraduate studies in physics at the Vrije Universiteit Brussel in 1975. During the next few years, she visited the CNRS Center for Theoretical Physics in Marseille several times, where she collaborated with Alex Grossmann; this work was the basis for her doctorate in quantum mechanics. She obtained her Ph.D. in theoretical physics in 1980, and continued her research career at the Vrije Universiteit Brussel until 1987, rising through the ranks to positions roughly equivalent with research assistant-professor in 1981 and research associate-professor 1985, funded by a fellowship from the NFWO (Nationaal Fonds voor Wetenschappelijk Onderzoek).

In 1985 Daubechies met mathematician Robert Calderbank, then on a 3-month exchange visit from AT&T Bell Laboratories, New Jersey to the Brussels-based mathematics division of Philips Research; they married in 1987, after Daubechies had spent most of 1986 as a guest-researcher at the Courant Institute of Mathematical Sciences. At Courant she made her best-known discovery: based on quadrature mirror filter-technology she constructed compactly supported continuous **wavelets** that would require only a finite amount of processing, in this way enabling wavelet theory to enter the realm of digital signal processing. In July 1987, Daubechies joined the Murray Hill AT&T Bell Laboratories' New Jersey facility. In 1988 she published the result in Communications on Pure and Applied Mathematics.

From 1994 to 2010, Daubechies was a professor at Princeton University, where she was active especially within the Program in Applied and Computational Mathematics. She was the first female full professor of mathematics at Princeton. In January 2011 she moved to Duke University to serve as a professor of mathematics.

In 2012 King Albert II of Belgium granted her the title of Baroness.

*Daubechies and Calderbank h*ave two children, Michael and Carolyn Calderbank.

The name Daubechies is widely associated with

- the orthogonal Daubechies wavelet
- and the biorthogonal CDF wavelet.

Daubechies used the idea of multiresolution analysis to create her own family of wavelets. These wavelets were of course named the Daubechies Wavelets. Daubechies wavelet family satisfies a number of wavelet properties. They have compact support, orthogonality, regularity, and continuity. The property of orthogonality is satisfied because the inner products of all of the various translates of the Daubechies wavelets are zero. The regularity property is satisfied because the Daubechies wavelets can reproduce linear functions. Finally, the continuity property is satisfied because the Daubechies wavelet functions are continuous even though they are not very smooth and not differentiable everywhere. Although it is not a very good one, there is an example of the Daubechies scaling function shown below.

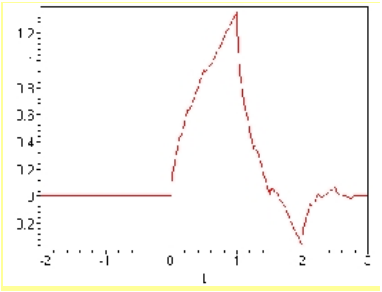

Mathematically, wavelets with compact support
proposed by Daubechies, as the generalization of Haar function, are sets of L^2functions generated from a single function called father function or scale function or refinable function satisfying the most important scale relation.

Most surprising aspect of this function is
that one need not know the explicit form of
the function at all for its use. Instead, only knowledge on the coefficients of two-scale relation, usually called mask or filter coefficients, are enough for its application
to the appropriate problem.

In comparison to representing L^2 functions
in terms of orthogonal L^2 bases (usually having infinite support or support over entire domain of interest) Daubechies scale function offers much convenient role for representing L^2 functions of physical origin.

1. Basic properties of Daubechies scale functions

Here we will discuss the basic properties of Daubechies scale function with a compact support mainly within a finite interval $I = [a, b] \subset \mathbb{R}$ (a, b are integers) so that a small programme can generate requisite values effectively. Our emphasis here lies on the scale functions having three vanishing moments of their wavelets.

1.1 Refinement equations

On $\mathbb{R}$, the scale function φ with compact support $[0,2K-1]$, $K \in \mathcal{N}$ is assumed to satisfy the refinement equation

$$\varphi(x) = \sqrt{2}\, \boldsymbol{H^I \Phi}(2x) \qquad (1)$$

with the mask

$$\boldsymbol{H^I} \equiv \boldsymbol{H^I_{1\times 2K}} = (h_0, h_1, \dots\dots\dots, h_{2K-1}),$$

$$\boldsymbol{\Phi}(2x) = (\varphi(2x), \varphi_1(2x), \dots\dots\dots, \varphi_{2K-1}(2x))^T \quad (2)$$

is a $2K \times 1$ matrix with

$$\varphi_k(x) = \varphi(x-k)\ . \quad (3)$$

In concurrence to the def. (1), define another function $\psi(x)$ as

$$\psi(x) = \sqrt{2}\ \boldsymbol{G^I}\boldsymbol{\Phi}(2x), \quad (4)$$

where

$$\boldsymbol{G^I} \equiv \boldsymbol{G^I}_{1\times 2K} = (g_0, g_1, \dots\dots\dots, g_{2K-1})$$

with

$$g_i = (-1)^i h_{2K-1-i}, i = 0, 1, \dots\dots\dots 2K-1.$$

Masks (coefficients h_l) for Daubechies scale function in $\mathbb{R}$ which maintains orthonormality with its dyadic dilation and integer translates

$$\varphi_{jk}(x) = 2^{\frac{j}{2}}\varphi\left(2^j - k\right), k \in Z$$

at a particular resolution j and vanishing moment up to order $K-1$ for $\psi(x)$, can be evaluated.

Table 1: filter coefficients (h_l) for $K = 3$ ($l = 1,2, \dots\dots, 2\times 3-1$)

l	h_l
0/5	$\frac{1+\sqrt{10}\pm\sqrt{5+2\sqrt{10}}}{16\sqrt{2}}$
1/4	$\frac{5+\sqrt{10}\pm 3\sqrt{5+2\sqrt{10}}}{16\sqrt{2}}$
2/3	$\frac{10-2\sqrt{10}\pm\sqrt{5+2\sqrt{10}}}{16\sqrt{2}}$

Using the dilated functions $\varphi_{jk}(x)$ and $\psi_{jk}(x)$ ($j,k \in \mathbb{Z}$) one can develop the multi- resolution analysis (MRA) for$L^2(\mathbb{R})$.

However, it is important to note that translational invariance and orthonormality of $\varphi_{jk}(x)$ ($k \in \mathbb{Z}$) and $\psi_{jk'}(x)$ ($j \geq j_0$; $k, k' \in \mathbb{Z}$), have been lost whenever the domain of independent variable x is restricted to a finite interval $I = [a, b]$. To deal with this situation, we divide the translates of refinable functions
at a particular resolution j as well as wavelet
into three classes

$$\Lambda_j^{LT} = \{\varphi_{jl}^{LT} = \varphi_{jl}(x)\chi_I(x), l = a2^j - 2K + 2, \dots\dots, a2^j - 1\},$$

$$\Lambda_j^{I} = \{\varphi_{jl}^{I} = \varphi_{jl}(x), l = a2^j, \dots\dots, b2^j - 2K + 1\},$$

$$\Lambda_j^{RT} = \{\varphi_{jl}^{RT} = \varphi_{jl}(x)\chi_I(x), l = b2^j - 2K + 2, \dots\dots, b2^j - 1\}, \quad (5)$$

Here $\chi_I(x) = 1$ when $x \in I$ and 0 otherwise.

Although the refinement equation for interior scale function of Λ_j^I remains unchanged as given in (1), the two- scale relation for other classes viz., Λ_j^{RT} and Λ_j^{LT} can be recast into

$$\varphi^{RT}(x) = \sqrt{2}(\boldsymbol{H}^{RT}_{(2K-2)\times(2K-2)}, \boldsymbol{H}^{IRT}_{(2K-2)\times(2K-2)}) \times (\boldsymbol{\Phi}^{RT}(2x), \boldsymbol{\Phi}^{IRT}(2x))^T \quad (6)$$

and

$$\varphi^{LT}(x) = \sqrt{2}(\boldsymbol{H}^{LT}_{(2K-2)\times(2K-2)}, \boldsymbol{H}^{ILT}_{(2K-2)\times(2K-2)}) \times (\boldsymbol{\Phi}^{LT}(2x), \boldsymbol{\Phi}^{ILT}(2x))^T \quad (7)$$

Here the notations $\boldsymbol{H}^s$ and $\boldsymbol{\Phi}^s$,
$s = RT, LT, IRT, ILT$ are defined by

$\boldsymbol{H}^{RT}_{pq} = [H^{RT}_{pq}]$ where $H^{RT}_{pq} = h_{q-2p}, -2K + 2 \leq p.q \leq 1$, and 0 otherwise

and

$$H^{IRT}_{pl} = \begin{cases} h_{l-2p} & -2K + 2 \leq p \leq -1, \\ & 0 \leq l \leq 2K - 3 \\ 0 & \text{otherwise;} \end{cases} \quad (8)$$

$$H_{p\,q}^{LT} = \begin{cases} h_{q-2p} & -2K+2 \le p,q \le -1 \\ 0 & \text{otherwise} \end{cases}$$

and

$$H_{p\,l}^{ILT} = \begin{cases} h_{l-2p} & -2K+2 \le p \le -1, \\ & -4K+4 \le l \le -2K+1 \\ 0 & \text{otherwise;} \end{cases} \quad (9)$$

with

$$h_l = \begin{cases} \text{mask in (2.1)} & 0 \le l \le 2K-1, \\ 0 & \text{otherwise;} \end{cases} \quad (10)$$

$\boldsymbol{\Phi}^{RT}(x) = (\varphi_{-2K+2}^{RT}(x), \dots\dots, \varphi_{-1}^{RT}(x))^T,$

$\boldsymbol{\Phi}^{IRT}(x) = (\varphi_0^I(x), \dots\dots, \varphi_{2K-3}^I(x))^T$; (11)

and

$\boldsymbol{\Phi}^{LT}(x) = (\varphi_{-2K+2}^{LT}(x), \dots\dots, \varphi_{-1}^{LT}(x))^T,$

$\boldsymbol{\Phi}^{ILT}(x) = (\varphi_{-4K+4}^{I}(x), \dots\dots, \varphi_{2K-1}^{I}(x))^T$ (12)

The abbreviations RT and LT in (11)-(12) stand for the overlapping of right tail and left tail of support of the refinable function with the interval I.

NOTE (*Imp.*)

In contrast to the functions in the class Λ^I which are orthonormal and the integer translates of a single function $\varphi(x)$ follows single scale equation (1), functions in the classes Λ^{RT} or Λ^{LT} are neither orthonormal nor follow the single refinement equation. Instead, they are independent and each of them follows different refinement like equations (6) and (7) separately. Consequently, moments and normalizations for scale functions in Λ^{RT} or Λ^{LT} are different from the same for the scale functions in Λ^I.

1.2 Moments and product integrals

We just outline the recursive formulae for the evaluation of moments of scale functions belonging to all three classes Λ^{RT}, Λ^I and Λ^{LT}.

1.2a Moments of $\varphi_k^I(x) \in \Lambda^I$

The kth moment, M^k for the scale function $\phi(x)$ can be obtained by using the refinement equation (1) in the formula

$$M^k = \int_{-\infty}^{\infty} x^k \phi(x) dx$$

$$= \sqrt{2} \sum_{l=0}^{2K-1} h_l \int_{-\infty}^{\infty} x^k \varphi(2x - l) dx$$

$$= \frac{1}{2^k - 1} \frac{1}{\sqrt{2}} \sum_{r=0}^{2K-1} \binom{k}{r} \left(\sum_{l=1}^{2K-1} h_l l^{k-r} \right) M^r \quad (13)$$

with $M^0 = 1$. Given M^k's, k^{th} moment M_{jl}^k of translated and dilated scale functions $\varphi_{jl}(x)$ of φ are given by the formula

$$M_{jl}^k = \int_{-\infty}^{\infty} x^k \varphi_{j\,k}(x) dx$$

$$= \frac{1}{2^{j(k+\frac{1}{2})}} \sum_{n=0}^{k} \binom{k}{n} l^{k-n} M^n \quad (14)$$

Formulae (13) and (14) are essential to determine moments of scale functions in the classes Λ^{RT} and Λ^{LT}.

1.2b Moments of $\phi \in \Lambda^{RT}$, Λ^{LT}

If we denote

$\boldsymbol{R}^k = \int_0^{\infty} x^k \boldsymbol{\Phi}^{RT}(x) dx$ (15)

and

$\boldsymbol{L}^k = \int_{-\infty}^{0} x^k \boldsymbol{\Phi}^{LT}(x) dx$ (16)

for the scale functions $\boldsymbol{\Phi}^{RT}(x)$ and $\boldsymbol{\Phi}^{LT}(x)$, then $\boldsymbol{R}^k$ and $\boldsymbol{L}^k$ (components) respectively are the solutions of the linear equations

$$(1_{(2K-2)\times(2K-2)} - \frac{1}{2^{k+1}} \boldsymbol{H}^{RT}) \boldsymbol{R}^k = \frac{1}{2^{k+1}} \boldsymbol{H}^{IRT} \boldsymbol{M}^{kIRT} \quad (17)$$

and

$$(1_{(2K-2)\times(2K-2)} - \frac{1}{2^{k+1}} \boldsymbol{H}^{LT}) \boldsymbol{L}^k = \frac{1}{2^{k+1}} \boldsymbol{H}^{ILT} \boldsymbol{M}^{kILT} \quad (18)$$

with

$$\boldsymbol{M}^{kIRT} = (M_{00}^k, M_{01}^k, \ldots\ldots, M_{02K-3}^k)^T, \quad (19)$$

$$\boldsymbol{M}^{k\,ILT} = (M^k_{0-4K+4}, M^k_{0-4K+5}, \dots\dots, M^k_{0-2K+1})^T. \qquad (20)$$

Values of M^k_{jl} s in (19) and (20) are obtained
by simultaneous use of (13) and (14).

Partial moments for functions belonging to Λ^{RT} and Λ^{LT} at higher resolution j can be found by using results of (17) and (18) in the formulae

$$\boldsymbol{R}^k_j = \int_0^\infty x^k \boldsymbol{\Phi}^{RT}_j(x)dx = \frac{1}{2^{j(k+\frac{1}{2})}}\boldsymbol{R}^k \qquad (21)$$

and

$$\boldsymbol{L}^k_j = \int_{-\infty}^0 x^k \boldsymbol{\Phi}^{LT}_j(x)dx = \frac{1}{2^{j(k+\frac{1}{2})}}\boldsymbol{L}^k . \qquad (22)$$

The accuracy of the values of $\boldsymbol{R}^k$ and $\boldsymbol{L}^k$ for
different $= 0, 1, 2, \cdots\cdots$, can be verified from the consistency condition

$$\boldsymbol{R}^k + \boldsymbol{L}^k = \left(M^k_{0-2K+2}, M^k_{0-2K+3}, \dots\dots, M^k_{0-1}\right)^T. \qquad (23)$$

1.2c Product integrals

By construction, the mask $\boldsymbol{H}^I$ in (1) is determined with the requirement that

$$N^I_{\varphi\ l_1 l_2} = \int_{-\infty}^{\infty} \varphi^I_{j\,l_1}\varphi^I_{j\,l_2}dx = \delta_{l_1\,l_2} \qquad (24)$$

where $\delta_{l_1 l_2}$ is the Kronecker delta symbol.
However, this property does not hold when φ 's
belong to Λ^{RT} and Λ^{LT} separately. Their numerical values

$$N^s_{\varphi\ p\,q} = \begin{cases} \int_0^\infty \varphi^{RT}_{j\,l_1}(x)\ \varphi^{RT}_{j\,l_2}(x)\,dx & s = RT \\ \int_{-\infty}^0 \varphi^{LT}_{j\,l_1}(x)\ \varphi^{LT}_{j\,l_2}(x)\,dx & s = LT \end{cases} \qquad (25)$$

are solutions of the system of linear equations

$$\boldsymbol{N}^s - \boldsymbol{H}^s\boldsymbol{N}^s(\boldsymbol{H}^s)^T = \boldsymbol{H}^{Is}(\boldsymbol{H}^{Is})^T,\ s = RT \text{ or } LT \qquad (26)$$

where $\boldsymbol{H}^{RT}$, $\boldsymbol{H}^{IRT}$, $\boldsymbol{H}^{LT}$, $\boldsymbol{H}^{ILT}$ are given by (8) and (9) respectively.

It must be noted that
$\int_0^\infty \varphi_{j\,p}^{RT}(x)\,\varphi_{j\,l}^{I}(x)\,dx$ or $\int_{-\infty}^{0} \varphi_{j\,p}^{LT}(x)\,\varphi_{j\,l}^{I}(x)\,dx$

vanishes identically and $\boldsymbol{N}^s$ ($s = RT$, LT) follow the consistency condition
$\boldsymbol{N}_{\varphi}^{RT} + \boldsymbol{N}_{\varphi}^{LT} = \boldsymbol{I}_{(2K-2)\times(2K-2)}$. (27)

2. One-point quadrature formula for Daubechies scale function with partial support

(Panja and Mandal (2011) Appl Math Comput)

There is a considerable progress in the use
of wavelet in the numerical estimate of functions satisfying differential equations or integral equations or some mathematical operations which appear in diverse fields of science and engineering. In spite of a considerable success, there still exist some important problems which are yet to be solved satisfactorily. For example, numerical evaluation of integrals of products of scale fuctions or wavelets having partial support within the range multiplied by an ordinary function, may not be easy to perform. Except for a few special cases, it is not possible in general to compute these integrals directly by finding their premitives.

Since Daubechies scale functions or wavelets
with compact support have no explicit forms, it is a formidable task to find the primitive of any integral consisting of the product of Daubechies scale function or wavelet and any ordinary function $f(x)$.

Here the one-point quadrature rule for
Daubechies scale function and wavelet with
full support in the real line R is extended
to those with partial support in the finite
interval $[a,b] \subset R$. This rule gives very accurate numerical results for the integrals of product of a function $f(x) \in L^2[a,b]$
and Daubechies scale function with partial
support within $[a,b]$.

2.1 One point quadrature rule for truncated
scale function

The one-point quadrature rule

$$\int f(x)\,\varphi_{j\,k}(x)\,dx \approx \frac{1}{2^{\frac{j}{2}}} f\left(\frac{k+ < x >}{2^j}\right) \quad (28)$$

to estimate the numerical value of the integral

involving product of a smooth functions
$f(x)$ and the scale functions $\varphi_{jk}^{L}(x)$ for $k = 2^j a, \ldots\ldots, 2^j b - (2K-1)$ was established by Sweldens and Piessen(1994) SIAM J Num Analysis and Kessler et al (2003) provided the values of the moments are known.

However, this rule is not valid when $k \in L$ or R.

Kessler et al(2003) suggested using $(K+1)$ point Gauss-Legendre type quadrature rule with weights determined by solving a system of linear equations obtained by the requirement that the quadrature rule reproduces the lowest order moments up to order K for evaluating such integrals.

But the method will face considerable difficulties in reproducing the value of the function from the raw images (i.e. the
coefficients of expansion of $f(x)$ in the scale function (Daubechies) basis).

It is thus desirable to formulate one-point quadrature rule even for truncated scale functions with minimum possible error so that all the scale functions can be treated on equal footing so far as the evaluation of their integrals is concerned.

Keeping this in mind, one-point quadrature rule for integrals involving non-normalised truncated scale functions is now developed.

We choose two constants, weight ω and
node $\bar{x}$ such that

$$\int_a^b f(x)\, \varphi_{j\,k}^{L\ or\ R}(x)\, dx \approx \omega_{j\,k}^{L\ or\ R} f(\bar{x}_{j\,k}^{L\ or\ R}) \quad (29)$$

produces exact results up to polynomial of
degree one in x.

The choice $f(x) = 1$ in (29) then yields

$$\begin{aligned} \omega_{j\,k}^{L\ or\ R} &= \int_a^b \varphi_{j\,k}^{L\ or\ R}(x)\, dx \\ &= \frac{1}{2^{\frac{j}{2}}} \langle x^0 \rangle_{[a\,2^j-k,\,2K-1]\ or\ [0,b\,2^j-k]} \end{aligned} \quad (30)$$

The choice

$$f(x) = x - \bar{x}_{j\,k}^{L\ or\ R} \text{ for } f(x)$$

in (29) produces

$$\bar{x}_{j\,k}^{L\ or\ R} = \frac{1}{2^j}\frac{I_k^{L\ or\ R}(1)}{I_k^{L\ or\ R}(0)} = \frac{k + \frac{\langle x\rangle_{[a\,2^j-k,2K-1]\ or\ [0,b\,2^j-k]}}{\langle x^0\rangle_{[a\,2^j-k,2K-1]\ or\ [0,b\,2^j-k]}}}{2^j} \quad (31)$$

In Tables 2a and 2b, some representative values of weights and nodes in the one-point quadrature rule for truncated scale functions for Daubechies-3 scale function are given (calculated by using the data given in Chen et al
(1996) Int. J. Num. Meth. Engg.)

Table 2a
Weights and nodes for boundary
integrals for RT

$k-2^j a$	$w_{j\,k}^L$	$\bar{x}_{j\,k}^L$
-4	$\frac{0.00034091099275035397}{2^{\frac{j}{2}}}$	$a+\frac{0.00797276023564402}{2^j}$
-3	$\frac{0.01451327379758438}{2^{\frac{j}{2}}}$	$a+\frac{0.01549128074837215}{2^j}$
-2	$\frac{-0.09671144714834012}{2^{\frac{j}{2}}}$	$a+\frac{0.0313956584750341}{2^j}$
-1	$\frac{0.39925843016888396}{2^{\frac{j}{2}}}$	$a+\frac{0.02883810457561126}{2^j}$

Table 2b: Weights and nodes for boundary integrals for LT

$k-2^j b$	w_{jk}^R	$\bar{x}_{jk}^R$
-4	$\frac{0.9996590890072496}{2^{\frac{j}{2}}}$	$b-\frac{3.1836869040537943}{2^j}$
-3	$\frac{0.9854867262024156}{2^{\frac{j}{2}}}$	$b-\frac{2.2149701293285116}{2^j}$
-2	$\frac{1.0967114471483401}{2^{\frac{j}{2}}}$	$b-\frac{1.075544999271151}{2^j}$
-1	$\frac{0.600741569031116}{2^{\frac{j}{2}}}$	$b-\frac{0.32312178530544267}{2^j}$

2.2 Error analysis

If $E_{jk}^{L,R}$ denote the error in the evaluation of the integrals $\int_a^b f(x)\varphi_{jk}^{L,R}(x)dx$ by the one-point quadrature rule (29), then

$$E_{jk}^{L,R} = \int_a^b f(x)\,\varphi_{jk}^{L,R}(x)\,dx - \omega_{jk}^{L,R} f(\bar{x}_{jk}^{L,R}). \tag{32}$$

Thus

$$E_{jk}^{L} \le \frac{1}{2^{2j+\frac{j}{2}+1}}(f''(\zeta_k^+)\eta_k^L + \{f''(\zeta_k^-) - f''(\zeta_k^+)\}\lambda_k^L) \tag{33}$$

where

$$\eta_k^L = \int_{2^j a-k}^{2^j b-k} (z-\bar{z}_{2^j a-k}^L)^2\,\varphi(z)\,dz\,, \tag{34}$$

$$\lambda_k^L = \sum_{n=1}^{\Lambda_k^-} \int_{\alpha_{k,n}^-}^{\beta_{k,n}^-} (z-\bar{z}_{2^j a-k}^L)^2\,\varphi(z)\,dz\,. \tag{35}$$

Following a somewhat similar analysis with appropriate modifications, the error E_{jk}^{R} satisfies the inequality

$$E_{jk}^{R} \leq \frac{1}{2^{2j+\frac{j}{2}+1}}(f''(\zeta_k^{+})\eta_k^{R}+\{f''(\zeta_k^{-})-f''(\zeta_k^{+})\}\lambda_k^{R}) \tag{36}$$

where η_k^{R} and λ_k^{R} have obvious meanings.

2.3 Illustrative Example

To demonstrate the efficiency of the one-point quadrature formula (29) with the weight and node given by the formulae (30) and (31) respectively, the numerical results for the integral

$$\int_0^4 \varphi_{-1}(x)dx$$

for Daubechies-3 scale function obtained by the present method are compared with those obtained by Xiao et al (2006) Appl Math Comp
using Gauss-Legendre 7-point and wavelet Gauss n-point $(n = 1,2,3,4)$ rules. The results are presented in Tables 3a , 3b, 3c.

Table 3a: Values and errors in one-point quadrature rule

j	$Q_j^{1-Pt.}$	$E_j^{1-Pt.}$
0	1.15122605(−2)	1.0(−02)
1	2.07411405(−2)	2.0(−03)
2	2.16616669(−2)	3.2(−04)
3	2.17657328(−2)	5.7(−05)

Table 3b: Values and errors Gauss-Legendre 7-pt. quadrature rule in M subintervals

M	$Q_j^{1-Pt.}$	$E_j^{1-Pt.}$
20	2.184308(−02)	6.3(−05)
50	2.174802(−02)	3.2(−05)
80	2.178428(−02)	4.2(−06)
100	2.178000(−02)	1.0(−07)

Table 3c: Values and errors in wavelet Gauss n-point quadrature rule ($2n$ mode)

n	Q_n^{WG}	E_n^{WG}
1	4.62366468	4.6(00)
2	3.95942437(−1)	4.2(−01)
3	3.59686182(−2)	1.4(−02)
4	2.15099945(−2)	1.8(−04)

The Tables 3a, 3b, 3d show that the results obtained by the one-point quadrature rule presented here are comparable to those obtained by multi-point Gauss-Legendre and wavelet-Gauss quadrature rules. It is obvious that the one-point rule is easy to implement compared to the multi-point in obtaining the same order of accuracy.

To verify the consistency of the rule we consider two more examples, viz.

$\int_0^4 x^{\frac{7}{2}}\,\varphi_{-1}(x)dx$ and $\int_0^4 \frac{x^{\frac{7}{2}}}{\sqrt{1+x^3}}\,\varphi_{-1}(x)dx$.

Since weights and nodes for wavelet-Gauss n-point quadrature rule proposed by Xiao et al (2006) are not readily available and the values of $\varphi_{-1}(x)$ cannot be well approximated at the nodes of the Gauss-Legendre quadrature rule, we have calculated all the three integrals approximated by using the one-point quadrature rule proposed here and Simpson's one-third rule at several resolutions and presented them in Table 3d.

Table 3d: Absolute errors in values obtained by using one-point quadrature rule and Simpson's one-third rule for $\int_0^4 \sin x\,\varphi_{-1}(x)dx$,
$\int_0^4 x^{\frac{7}{2}}\,\varphi_{-1}(x)dx$ and $\int_0^4 \frac{x^{\frac{7}{2}}}{\sqrt{1+x^3}}\,\varphi_{-1}(x)dx$.

$f(x)$	j	Abs Error in One-point	Abs Error in Simpson's-$\frac{1}{3}$
$Sin(x)$	0	0.01	0.40
	1	0.001	0.017
	2	0.0001	0.0.004
	3	0.000014	0.00053
$x^{\frac{7}{2}}$	0	0.02	0.49
	1	0.003	0.21
	2	0.0004	0.02
	3	0.00005	0.001
$\frac{x^{\frac{7}{2}}}{\sqrt{1+x^3}}$	0	0.062	0.01
	1	0.006	0.02
	2	0.0007	0.005
	3	0.00008	0.0008

Comparison of the results confirms that the one-point quadrature rule provides very accurate results at each resolution compared to the existing ones.

It may be noted that the values of the integral

$$\int_0^4 \sin x \, \varphi_{-1}(x)dx,$$

for higher resolution are obtained by using the rule

$$\int_a^b f(x)\,\varphi_{j\,k}(x)\,dx = \frac{1}{2^{\frac{j_1}{2}}} \sum_{l_{j_1}=0}^{2K-1} \sum_{l_{j_1-1}=0}^{2K-1} \cdots\cdots \times$$

$$\sum_{l_1=0}^{2K-1} h_{l_{j_1}} h_{l_{j_1-1}} \cdots h_{l_1} \times$$

$$\int_{2^{j_1}a}^{2^{j_1}b} f(\frac{x}{2^{j_1}}) \varphi_{2(2^{j_1-1}k+2^{j_1-2}l_1+\cdots+l_{j_1-1})+l_{j_1}}(x)c$$

$$\approx \frac{1}{2^{\frac{j_1}{2}}} \sum_{l_{j_1}=0}^{2K-1} \sum_{l_{j_1-1}=0}^{2K-1} \cdots\cdots \sum_{l_1=0}^{2K-1} h_{l_{j_1}} h_{l_{j_1-1}} \cdots h_{l_1} \times$$

$$\omega_{2(2^{j_1-1}k+2^{j_1-2}l_1+\cdots+l_{j_1-1})+l_{j_1}} \times$$

$$f(\frac{\bar{x}_{2(2^{j_1-1}k+2^{j_1-2}l_1+\cdots+l_{j_1-1})+l_{j_1}}}{2^{j_1}\omega_{2(2^{j_1-1}k+2^{j_1-2}l_1+\cdots+l_{j_1-1})+l_{j_1}}}).$$

Remarks

1. Here one-point quadrature formula for evaluation of integrals containing product of smooth function and scale function with partial support has been obtained. The bound for the error in the quadrature formula has been analysed purely based on scale function, without using the properties of wavelets.

2. From the numerical results for the integral

$$\int_0^4 \sin x \, \varphi_{-1}(x)dx,$$

it appears that the error at resolution zero is found to be $1.0 \times 10{-}2$. The estimates (33) shows that this error decreases roughly at the rate of $\frac{1}{2^{\frac{5}{2}}} \approx 0.18$ per resolution as the resolution increases. Thus, one can easily guess

the level of resolution j at which the desired order of accuracy can be attained (which is an essential information for the development of a self adaptive numerical method).

It opens the possibility to develop scale function based quadrature formula for numerical evaluation of integrals (nonsingular and singular) in a finite interval by considering integrals of products of a integrable function and a scale function with partial as well as full support uniformly.
\
This has been done recently in the following paper (which is however not discussed here).

Gauss-type quadrature rule with complex nodes and weights for integrals involving Daubechies scale functions and wavelets, Panja, M M and Mandal, B N., *J. Comput. Appl. Math* 290 (2015) 609-632.

Regular and weakly singular integrals

3. Quadrature rule for weakly singular Integrals

Weakly singular integrals appear in diverse fields of mathematical sciences. Since most of them cannot be evaluated analytically, several numerical methods have been developed for evaluation of their approximate numerical values.

Observing the success of representing $f(x) \in L^2[a,b]$ in Daubechies scale function based Meyer basis we now develop a quadrature rule in terms of raw image of $f(x)$ (coefficients $f_{jk}^{L \text{ or } I \text{ or } R}$) for numerical evaluation of weakly singular integrals with singularities at the edges a and b.

3.1 Raw image of bounded $f(x) \in L^2[a,b]$

The coefficients of the expansion of $f(x)$ in the scale function basis are known as raw image. Similar to the expansion of $f(x) \in L^2[\mathbb{R}]$, we represent $f(x) \in L^2[a,b]$ as the sum

$$f(x) \approx \sum_{k=a\,2^j-(2K-2)}^{b\,2^j-1} f_{j\,k}\,\varphi_{j\,k}(x)\chi_{[a,b]}, \quad (37)$$

where $\chi_{[a,b]}$ is the characteristic function in $[a,b]$. The range of k in the summation can be justified since $x \in [a,b]$ and the support of $\varphi_{jk}(x)$ is $[\frac{k}{2^j}, \frac{k+2K-1}{2^j}]$. However, due to finite support of $\varphi_{jk}(x)$, whenever $k \in \{a\,2^j-(2K-2), \cdots\cdots, a2^j-1\}$, or $k \in \{b2^j-(2K-2), \cdots\cdots, b2^j-1\}$, only some part of the support of $\varphi_{jk}(x)$ overlaps with $[a,b]$. Consequently, all the $\varphi_{jk}(x)$'s with supports having nonempty overlaps with $[a,b]$ need to be classified into three categories as mentioned in section earlier in section 1.1.

We have seen in the same section that whenever $k \in L \text{ or } R, \varphi_{jk}^{B}(x)$'s are not normalized and integrals of their product within $[a,b]$ do not satisfy orthonormality conditions. So, the determination of coefficients f_{jk}'s in the expansion (37) for $k \in L \text{ or } R$, are not straightforward as in the case of L^2 [$\mathbb{R}$]. In order to evade the intertwining of $f_{jk}, k \in L$ and $f_{jk}, k \in R$, we choose the resolution j such that $\varphi_{jk}^{L}(x), k \in L$ and $\varphi_{jk}^{R}(x), k \in R$ have no common support. As a result

$$\int_a^b \varphi_{jl}^{L}(x)\, \varphi_{jr}^{R}(x) dx = 0 \qquad (38)$$

whenever $l \in L$ and $r \in R$. Multiplying both sides of (37) by $\varphi_{jk}(x)$ and integrating over $[a,b]$ and using normalization conditions we obtain

$$\begin{pmatrix} N^L & 0 & 0 \\ 0 & I_{(b-a)2^j-(2K-2)\times(b-a)2^j-(2K-2)} & 0 \\ 0 & 0 & N^R \end{pmatrix} \times$$

$$\begin{pmatrix} f^L \\ f^I \\ f^R \end{pmatrix} = \begin{pmatrix} \omega^L f(\bar{x}^L) \\ \omega^I f(\bar{x}^I) \\ \omega^R f(\bar{x}^R) \end{pmatrix} \qquad (39)$$

where $\mathbf{N}^I = \mathrm{I}_{\{(b-a)2^j-2K-2\}\times\{(b-a)2^j-2K-2\}}$
and $\mathbf{N}^{L \text{ or} R} = [N_{mn}^{L \text{ or} R}]$.

Eqn (39) can be split into three sets of linear equations

$$\begin{aligned} N^L f^L &= \omega^L f(\bar{x}^L), \\ N^I f^I &= \omega^I f(\bar{x}^I), \\ N^R f^R &= \omega^R f(\bar{x}^R). \end{aligned} \qquad (40)$$

From second set of eqs.(40) it appears that the coefficients for interior scale functions in the expansion (37) are decoupled from each other. They give the direct relationship between the value of the function at the nodes and the raw image f_{jk} (as in the case of L^2 [$\mathcal{R}$]) as

$$f_{jk}^{I} = \frac{1}{2^j} f\left(\frac{k+<x>}{2^j}\right). \qquad (41)$$

However, this is not true whenever $k \in L$ or R.
Solving first and third sets of eqs. (40) one can obtain the coefficients for boundary scale functions in terms of values of the function at different nodes as

$$f_{jk}^{L} = \sum_{l=a2^{j}-(2K-2)}^{a2^{j}-1} (N^{L})^{-1}_{k-a2^{j},\, l-a2^{j}}\, \omega_{jl}^{L} f(\bar{x}_{jl}^{L});$$

$$k \in \{a\,2^{j} - (2K-2), \cdots\cdots, a\,2^{j} - 1\} \quad (42)$$

$$f_{jk}^{R} = \sum_{r=b2^{j}-(2K-2)}^{b2^{j}-1} (N^{R})^{-1}_{k-b2^{j},\, r-b2^{j}}\, \omega_{jr}^{R} f(\bar{x}_{jr}^{R})$$

$$k \in \{b\,2^{j} - (2K-2), \cdots\cdots, b\,2^{j} - 1\} \quad (43)$$

Thus, any function $f(x) \in L^2[a,b]$ can be expressed in terms of Daubechies-K scale function in resolution $j \geq \frac{4K-2}{b-a}$ with full and partial support and the expansion coefficients are given by the formulae (42) and (43).

3.2a Quadrature formula for regular Integrand

In order to develop Daubechies scale function based quuadrature rule for numerical evaluation of the integral of $f(x) \in L^2[a,b]$, we integrate both sides of (37) over $[a,b]$ and use dilation property in combination with the normalizations satisfied by $\varphi_{jk}^{I}(x)$,$k \in I$ to get

$$\int_a^b f(x)dx \approx Q^{Reg}[f] \equiv \sum_{k \in L} f_{jk}^{L}\, \omega_{jk}^{L} + \sum_{k \in I} f_{jk}^{I}\, \omega_{jk}^{I} + \sum_{k \in R} f_{jk}^{R}\, \omega_{jk}^{R} \qquad (44)$$

Although the evaluation of f_{jk}^{I} is trivial, it depends only upon the nodes $\frac{k+<x>}{2^{j}}, k \in I$, estimation of $f_{jk}^{L \text{ or } R}$ requires somewhat heavy calculations for each resolution j. Using (42)- (43) in the R.H.S. of (44) and interchanging the sum over l and k whenever they take their values in L or R, one gets

$$Q^{Reg}[f; a, b] = \sum_{l=a2^{j}-(2K-2)}^{a2^{j}-1} \Omega_{jl}^{L}\, \omega_{jl}^{L}\, f(\bar{x}_{jl}^{L}) +$$

$$\sum_{i=a2^j}^{b2^j-(2K-1)} (\omega_{j\,i}^I)^2\ f(\bar{x}_{j\,i}^I) +$$

$$\sum_{r=b2^j-(2K-2)}^{b2^j-1} \Omega_{j\,r}^R\ \omega_{j\,r}^R\ f(\bar{x}_{j\,r}^R), \qquad (45)$$

where

$$\Omega_{j\,l}^L = \sum_{k=a2^j-(2K-2)}^{a2^j-1} (N^L)_{k-a2^j,\,l-a2^j}^{-1}\ \omega_{j\,k}^L, \qquad (46)$$

$$\Omega_{j\,r}^R = \sum_{k=b2^j-(2K-2)}^{b2^j-1} (N^R)_{k-b2^j,\,r-b2^j}^{-1}\ \omega_{j\,k}^R. \qquad (47)$$

The values of each of $\Omega^{L\text{ or }R}$ for Daubechies $K = 3$ scale function is $\frac{1}{2^{\frac{j}{2}}}$, and thus the quadrature rule (45) simplifies to

$$Q^{Reg}[f;a,b] = \frac{1}{2^j}\Bigg[\sum_{l=a2^j-(2K-2)}^{a2^j-1} \omega_l^L\ f(\bar{x}_{j\,l}^L) +$$

$$\sum_{i=a2^j}^{b2^j-(2K-1)} f(\bar{x}_{j\,i}^I) +$$

$$\sum_{r=b2^j-(2K-2)}^{b2^j-1} \omega_r^R\ f(\bar{x}_{j\,r}^R)\Bigg], \qquad (48)$$

where ω_l^L and ω_r^R are given in first rows of Tables 3a and 3b in reverse order.

Table -3a Partial moments $I_k^L(m) = \int_k^{2K-1} x^m \varphi(x)\, dx$

k m	1	2	3	4
0	0.39925843016888396	0.0967114471483401 2	0.01451327379758 438	0.000340910992750 353
1	0.4107722865307886	- 0.1964592138619757	0.04376465059172 918	0.001366361972608 421
2	0.36058536336405395	- 0.3860728286663880 3	0.13140232857401 3	0.005472847072422 5
3	0.1979965650492068	- 0.7163592582754439	0.39255641017926 9	0.021906236564613 5
4	-0.089889970488100	- 1.1889468759534776	1.16595862431149 9	0.087621917481467 0
5	-0.224798155972725	- 1.4864435793368804	3.44014629236384 6	0.350212291754873 0
6	1.3172165028297727	0.0172739817709077 8	10.0737997576725 2	1.398641487428037 7
7	10.53358287064466	9.558447281179674	29.2515264020680 6	5.581105888813937
8	48.17528203128408	48.41482738882302	84.1632347058770 4	22.25129265804047 3
9	181.31393039851662	184.7805665186955	239.868747129752 6	88.63263987297731

Table -3b Partial moments $I_k^R(m) = \int_0^k x^m \varphi(x)\, dx$

k m	1	2	3	4
0	0.600741569831116	1.0967114471483401	0.9854867262024156	0.9996590890072496
1	0.406628881280091	1.013860381672856	0.773636517219151	0.8160348058382718
2	0.307559305774537	1.054217497804979	0.5367423405645771	0.6626718220661685
3	0.247463479864190	1.161819303188841	0.0529036347341277	0.4235538083487836
4	0.207116317494341	1.3061732229597185	-1.048732277305258	0.0296044295247737
5	0.178147065382211	1.4397924887463665	-3.48679738295436	-0.396863382345387
6	0.156328838077650	1.4562713591365153	-8.600254416765106	0.0749038534793853
7	0.139297997719183	1.114433587184168	-18.5786455337042	5.091774979549905
8	0.125629888270937	-0.11391546926800807	-35.8623227863220	26.04961926151454
9	0.114414815561820	-3.352221304617066	-58.44040191567418	92.79570534110113

3.2b Estimation of total error

In the process of obtaining the quadrature
rule (48) two types of approximations are involved. One is the ommission of the detail space in the multiresolution approximation and the other is the numerical evalution of coefficients through the formulae

(46)-(47) in the approxiamtion space.

The bound in the error of the first can be approximated by Jackson's inequality

$$||f - P_j f|| \leq \frac{c}{(2^j)^{K-1}} \max ||D^{K-1} f||$$

where $||\cdot||$ denotes the usual L^2 norm while the error for the evaluation of f_{jl}'s are given by the formulae (33) and (36).

If the error in the expansion of $f(x)$ in (37) is denoted by $E_j(x)$, then

$$f(x) = \sum_{k=a2^j-(2K-2)}^{b2^j-1} f_{j\,k} \varphi_{j\,k}(x) + E_j(x) \quad (49)$$

where

$$||E_j(x)||_{L^2[a,b]} \leq \frac{\tau}{(2^j)^{K-1}} C. \qquad (50)$$

In (50), C depends on the basis functions $\varphi_{jk}(x)$
and

$$\tau = [\int_a^b |f^{(K-1)}(x)|^2 \, dx]^{\frac{1}{2}}.$$

(cf. Cohen et al (1995)).

Now integrating both sides of (49) between a to b after substituting $f_{jk} = f_{jk}^{1-pt.} + \epsilon_{jk}^{1-pt.}$, $k \in L, I$ or R we obtain

$$|\int_a^b f(x)\, dx - Q^{Reg}[f]| \leq$$

$$|\sum_{k=a2^j-(2K-2)}^{b2^j-1} w_{j\,k}^{1-Pt} \epsilon_{j\,k}^{1-Pt}| + |\int_a^b E_j(x)\, dx|. \qquad (51)$$

It may be noted that the function $f(x) = x$ can be expanded in terms of Daubechies- 3 scale function in exact form, and thus there will be no error in the corresponding scale function based quadrature rules. If the present one-point quadrature rule is employed to evaluate $\int_{-1}^{1} x\, dx$, then also there will be no error.

We have compared the numerical results of some definite integrals of some regular functions evaluated by the present method and by Hashish et al (2009) and these are shown in Tables 4a and 4b.

Table 4a: $\int_0^1 \sqrt{x^2 - 4x + 1}\, dx$

j	Present method	Hashish et al
7	6.2×10^{-10}	1.5×10^{-6}
9	9.7×10^{-12}	9.8×10^{-8}
11	1.5×10^{-13}	5.0×10^{-9}

Table 4b: $\int_0^1 cos(x^2)\, dx$

j	Present method	Hashish et al
7	4.2×10^{-8}	2.0×10^{-5}
9	6.6×10^{-10}	1.3×10^{-6}
11	1.0×10^{-11}	9.1×10^{-8}

From the Tables 4a and 4b it is obvious that present method produces far better accurate results than the method used by Hashish et al (2009).

Weakly singular integrals

3.3a Evaluation of integrals of the form

$$\int_a^b \frac{\varphi_{jk}(x)}{(x-a)^{\mu}} dx, \quad 0 < \mu < 1$$

Let us consider the integral

$$\omega_{jk}^{L}[\mu, a] = \int_a^b \frac{\varphi_{j\,k}(x)}{(x-a)^{\mu}} dx \qquad 0 < \mu < 1. \tag{52}$$

Using the scale transformation followed by the change of the variable in (24) we get

$$\omega_{jk}^{L}[\mu, a] = 2^{(\mu-\frac{1}{2})j} \omega_{k-2^j a}^{L}[\mu] \tag{53}$$

where

$$\omega_{k'}^{L}[\mu] = \int_0^{2^j(b-a)} \frac{\varphi_{k'}(x)}{x^{\mu}} dx. \tag{54}$$

For the evaluation of $\omega_{k'}^{L}[\mu]$, we assume

the choice of j satisfies the condition $2^j(b-a) >> (2K-1)$ to assure enough interior scale functions within $[0, 2^j(b-a)-(2K-1)]$. Using the two-scale relation for $\varphi_{k'(x)}$ in (54), a recurrence relation for $\omega_{k'}^{L}[\mu]$ is found as

$$\omega_{k'}^{L}[\mu] = 2^{\mu-\frac{1}{2}} \sum_{l=0}^{2K-1} h_l \, \omega_{2k'+l}^{L}(\mu). \qquad (55)$$

From this relation it is obvious that the determination of $\omega_{k'}^{L}[\mu]$ for particular $k' > 0$, involves numerical values [ ] for > '. These quantities, usually called asymptotic values, can be evaluated following the fact that within the support of ( ) >> *1*, the factor $\frac{1}{}$ behaves like a regular function. Therefore, one may evaluate '[ ]'s, >> *1* but within [*0, 2* (−) − (*2* − *1*)] by either of the results obtained by using one-point quadrature rule

$$[\ ] \approx \frac{1}{(\ +<\ >)}$$

or by using the series

$$[\ ] \approx \frac{1}{} \sum_{=0} \frac{(\ )}{} \quad {}_0 \qquad (\ ).$$

Once the asymptotic values are known, '[ ]'s for other positive values of ' can be easily evaluated with the help of the formula (55).

The values of '[ ]'s for −(*2* − *2*) ≤ ' ≤ *0*, are determined by solving a system of linear simultaneous equations generated with the help of (53) whose solution for Daubechies-3 scale function for $= \frac{1}{2}$ are presented in Table 5a.

Table 5a Numerical values of − *2* $\left[\frac{1}{2}\right]$

$k-a2^j$	w_{0k}^W
-4	0.002418025890650
-3	0.074507561327850
-2	-0.383612087110153
-1	1.438658438411280
0	1.171967541211238

Again, for $2^j(b-a)-(2K-2) \le k' \le 2^j(b-a)-1$, the scale function has the artial support within the domain of integration $[0, 2^j(b-a)]$. However, due to the regular behavior of $\frac{1}{x^\mu}$ within the partial support of $\varphi_{k'}(x)$ one may estimate $\omega_{k'}^L[\mu]$ by using either one-point quadrature rule

$$\omega_{k'}^L[\mu] \approx w_{k'}^R \frac{1}{(k' + < x >_{[0,2^j(b-a)-k']})^\mu},$$

or by summing the series

$$\omega_{k'}^L[\mu] \approx \frac{1}{(k')^\mu} \sum_{r=0}^{r_{max}} \frac{(-1)^r(\mu)_r}{r!(k')^r} I_{2^j(b-a)-k'}^R(r)$$

3.3b Integrals of the form $\int_a^b \frac{\varphi_{jk}(x)}{(b-x)^\nu} dx, 0 < \nu < 1$.

Following a similar method with appropriate modification, this integral can be estimated by using the formula

$$\omega_{jk}^{R}[\nu, b] = \int_a^b \frac{\varphi_{j\,k}(x)}{(b-x)^{\nu}} dx$$

$$= 2^{(\nu-\frac{1}{2})j} \int_{2^j a}^{2^j b} \frac{\varphi_k(x)}{\left(2^j b - x\right)^{\nu}} dx, \; 0 < \nu < 1 \quad (56)$$

where the two-scale relation for $\boldsymbol{\omega_{jk}^{R}}$ is found as

$$\omega_{j\,k}^{R}[\nu, b] = 2^{\nu-\frac{1}{2}} \sum_{l=0}^{2K-1} h_l \, \omega_{j+1\,2k+l}^{R}[\nu, b]. \quad (57)$$

The numerical values of $\boldsymbol{\omega_{jk}^{R}}$ without prefactors for Daubechies-3 scale fumction are presented in Table 5b.

Table-5b Numerical values of $\omega_{k-b2^j}^{R}[\frac{1}{2}]$

$k - b2^j$	w_{0k}^{W}
-5	0.4888247649751728
-4	0.5607046201248957
-3	0.6826054160639504
-2	0.9542008763684104
-1	1.6438144798009484

3.3c Quadrature formula for Integrals of the type $\int_a^b \frac{F(x)}{(x-a)^{\mu}(b-x)^{\nu}} dx, \; 0 < \mu, \nu < 1$

We are now well equipped to develop quadrature formula for numerical evaluation of above integral in terms of raw image in the Daubechies scale function dependent Meyer basis. We first split the above integral into

$$I[F; \mu, \nu] = \int_a^b \frac{F(x)}{(b-x)^{\nu}\,(x-a)^{\mu}} dx$$

$$= \int_a^{\frac{a+b}{2}} \frac{f_b(x)}{(x-a)^{\mu}} dx + \int_{\frac{a+b}{2}}^b \frac{f_a(x)}{(b-x)^{\nu}} dx, \quad (58)$$

with

$$f_b(x) = \frac{F(x)}{(b-x)^{\nu}} \qquad (59)$$

and

$$f_a(x) = \frac{F(x)}{(x-a)^{\mu}}. \qquad (60)$$

Substituting expansion (37) for the regular functions $\boldsymbol{f_b(x)}, \boldsymbol{f_a(x)}$ within their domain $\left[a, \frac{a+b}{2}\right]$ and $\left[\frac{a+b}{2}, b\right]$ respectively, and then using the values of the integrals whenever they appear, the estimate for the weakly singular integral in (58) can be found as

$$I[F;\mu,\nu] = \sum_{l=a2^j-(2K-2)}^{(\frac{a+b}{2})2^j-1} f_{b,\,j\,l}\,\omega_{j\,l}^{L} + \sum_{r=(\frac{a+b}{2})\,2^j}^{b2^j-1} f_{a,\,j\,r}\,\omega_{j\,r}^{R}, \qquad (61)$$

where the raw images $f_{b,jl}$'s and $f_{a,jr}$'s for $\boldsymbol{f_b(x)}$ and $\boldsymbol{f_a(x)}$ are determined easily.

This formula can be written in terms of values of the function $f_a(x)$ and $f_b(x)$ at different nodes by reversing the summation over $\boldsymbol{l}$ **or** $\boldsymbol{r}$ and $\boldsymbol{k}$ as

$$I[F;\mu,\nu] = \sum_{l=a2^j-(2K-2)}^{a2^j-1} \Omega_{j\,l}^{L}(\mu)\ \omega_{j\,l}^{L} f(\bar{x}_{j\,l}^{L})$$

$$+ \sum_{l=a2^j}^{\frac{a+b}{2}2^j-K} \omega_{j\,l}^{L}(\mu,\ a)\omega_{j\,l}^{I} f(\bar{x}_{j\,l}^{I})$$

$$+ \sum_{r=(\frac{a+b}{2})\,2^j-K+1}^{b2^j-(2K-1)} \omega_{j\,r}^{R}(\nu,\ b)\omega_{j\,r}^{I} f(\bar{x}_{j\,r}^{I})$$

$$+ \sum_{r=b2^j-(2K-2)}^{b2^j-1} \Omega_{j\,r}^{R}(\nu)\omega_{j\,r}^{R}(\nu) f(\bar{x}_{j\,r}^{R}). \qquad (62)$$

The quantities ( ) and ( ) aed given by

$$\Omega_{j\,l}^{L}(\mu) = \sum_{k=a2^j-(2K-2)}^{a2^j-1} (N^{L})^{-1}_{k-a2^j,\,l-a2^j}\ \omega_{j\,k}^{L}(\mu,a), \qquad (63)$$

$$\Omega_{j\,r}^{R}(\nu) = \sum_{k=b2^j-(2K-2)}^{b2^j-1} (N^{R})^{-1}_{k-b2^j,\,r-b2^j}\ \omega_{j\,k}^{R}(\nu,b). \qquad (64)$$

To check the efficiency of our formula (63) or (64) for evaluation of numerical values of weakly singular integrals a comparison of results for the integrals

$$\int_0^1 \frac{e^x}{\sqrt{x}}\,dx$$

and

$$\int_{-1}^{1} \frac{|x|}{\sqrt{1-x^2}}\,dx$$

have been presented in Tables 6a and 6b.

Table 6a : Relative error for $\int_0^1 \frac{e^x}{\sqrt{x}}\,dx$

j	Method adopted here	Method adopted by Hashish et al
7	5.9×10^{-7}	3.2×10^{-2}
9	3.4×10^{-7}	1.6×10^{-2}
11	1.5×10^{-7}	8.1×10^{-3}

Table 6b: Relative error for $\int_{-1}^1 \frac{|x|}{\sqrt{1-x^2}}\,dx$

j	Method adopted here	n	Method adopted by n-point formula
4	3.4×10^{-5}	20	1.3×10^{-2}
5	8.4×10^{-6}	40	4.5×10^{-3}
7	4.8×10^{-7}	80	1.6×10^{-3}

These tables (6a, 6b) show that the method adopted here is superior to the methods adopted by Hashish et al [2009] and Jung et al [??] for evaluating the weakly singular integrals.

Strongly singular integrals

3.4 Quadrature Rule for Cauchy principal value integrals

Numerical evaluation of Cauchy principal value(CPV) integrals within a finite domain by using scale function is a major issue when wavelet analysis is invoked to boundary integral approach for boundary value problems.
Encouraged by the successful application of Daubechies scale function based raw image dependent quadrature formula for evaluating regular or weakly singular integrals within a finite interval, we now try to develop quadrature rule for CPV integrals

$$I^C[f,t] = \int_a^b \frac{f(x)}{x-t}\,dx \qquad f(x) \in L^2[a,b], \quad (65)$$

with singularity t within the interval (a,b). The underlying idea behind the construction of formula is the application of formula (37) for $f(x)$ in the integral of (65) and then evaluation of the integrals involving product $\frac{1}{x-t}$ and $\phi_{jk}(x)$ within the interval $[a,b]$. So, the prime objective of numerical estimate of Cauchy singular integral is the evaluation of the integral

$$\omega^C_{j\,k}[t] = \int_a^b \frac{\varphi^{L\ or\ I\ or\ R}_{j\,k}(x)}{x-t}\,dx;$$

$$2^j a - (2K-2) \le k \le 2^j b - 1. \qquad (66)$$

Using dilation followed by transformation of variables, (66) can be recast into the form

$$\omega^C_{j\,k}[t] = 2^{\frac{j}{2}}\omega^C_k[2^j t], \qquad (67)$$

where

$$\omega^C_k[2^j t] = \int_{2^j a}^{2^j b} \frac{\varphi^{L\ or\ I\ or\ R}_k(x)}{x-2^j t}\,dx. \qquad (68)$$

Evaluation of integrals in (68) whenever the point t is dyadic and the point of singularity $2^j t$ falls beyond the supports of truncated scale function $\varphi^{L\,or\,R}_k(x)$, has been discussed by Kessler et el (2003). We just mention the formulae which will be used here. The values of $\omega^C_k[2^j t]$ for $k \in \{2^j t - \{2K-1\}, \ldots . 2^j t\}$ presented in Table 7, was calculated by Kessler et al (2003) by extending the limit of the integral in (68) to $(-\infty, \infty)$ using the properties of $\varphi^I_k(x)$.

Table-7 Numerical values of $\omega^C_{k'}$

k	w^C_{0k}	k	w^C_{0k}
−5	−0.23891482	0	1.51431442
−4	−0.30768589	1	0.55800637
−3	−0.30259405	2	0.35636165
−2	−1.75163320	3	0.26239622
−1	−0.17177891	4	0.20775723
		5	0.17198219

The evaluation of $\omega^C_k[2^j t]$ for other values of k are carried out with the help of the recurrence relation

$$\omega^C_k[2^j t] = \omega^C_{k'=k-2^j t}[0] = \sqrt{2}\ \sum h_l\ \omega^C_{2k'+l}(0) \qquad (69)$$

in conjunction with the asymptotic value of $\omega_{k'}^{C}[0]$ given by

$$\omega_{k'}^{C}[0] \approx \frac{1}{k' + \langle x \rangle} \qquad for\ k >> 1.$$

Numerical values of $\omega_k^C[2^j t]$ whenever $2^j a - (2K - 2) \leq k \leq 2^j a - 1$ and $2^j b - (2K - 2) \leq k \leq 2^j b - 1$ are performed by summing the series

$$\omega_k^C[2^j t] \approx \frac{1}{k - 2^j t} \sum_{r=0}^{r_{Max}} \frac{(-1)^r}{\left(k - 2^j t\right)^r} \times$$

$$\langle x \rangle_{[2^j a - k, 2K-2]\ or\ [0, 2^j b - k]} \qquad (70)$$

according as $2^j a - (2K - 2) \leq k \leq 2^j a - 1$ or $2^j b - (2K - 2) \leq k \leq 2^j b - 1$.

Using the expansion (37) for $f(x) \in L^2[a,b]$ in combination with the formula (66)-(68), the integral of (65) can be written as

$$\int_a^b \frac{f(x)}{x - t} dx \approx 2^{\frac{j}{2}} \sum_{k = a2^j - (2K-2)}^{b2^j - 1} f_{j\,k}\, \omega_k^C(2^j t) \qquad (71)$$

where f_{jk}'s are raw image of the function $f(x)$ in the basis $\varphi_{jk}(x)$ determined by using formulae (41)-(43). If we denote

$$\Omega_{j\,l}^{CL}(t) = \sum_{k = a2^j - (2K-2)}^{a2^j - 1} (N^L)^{-1}_{k - a2^j,\, l - a2^j}\, \omega_{j\,k}^C(2^j t) \qquad (72)$$

and

$$\Omega_{j\,r}^{CR}(t) = \sum_{k = b2^j - (2K-2)}^{b2^j - 1} (N^R)^{-1}_{k - b2^j,\, r - b2^j}\, \omega_{j\,k}^C(2^j t), \qquad (73)$$

then the quadrature rule in (71) can be recast into

$$Q[f;t] = \sum_{l=a2^j-(2K-2)}^{a2^j-1} \Omega_{jl}^{CL}(t)\,\omega_{jl}^{L} f(\bar{x}_{jl}^{L}) + \sum_{i=a2^j}^{b2^j-(2K-1)} \omega_{ji}^{C}(2^j t)\omega_{ji}^{I} f(\bar{x}_{ji}^{I}) + \sum_{r=b2^j-(2K-2)}^{b2^j-1} \Omega_{jr}^{CR}(t)\omega_{jr}^{R} f(\bar{x}_{jr}^{R}). \qquad (74)$$

To verify the efficiency of the formulae derived here we have computed approximate value of

$$\int_{-1}^{1} \frac{\boldsymbol{sin^{-1}x}}{\boldsymbol{x}}\boldsymbol{dx}$$

at several resolution j and the values of Legendre function of second kind $Q_3(x)$ from its integral representation

$$Q_3(x) = -\frac{1}{2}\int_{-1}^{1} \frac{P_3(t)}{t-x}\,dt$$

for several values of x at fixed resolution $j = 5$
by using (71) or (74). The relative errors of the approximate values are presented in Tables 8 and 9 and found to be reliable to apply these for the approximate evaluation of other CPV integrals.

Table-8 Relative error in $I^C = \int_{-1}^{1} \frac{sin^{-1}x}{x}\,dx$ in different j

j	3	5	7
I^C	7.2×10^{-5}	1.5×10^{-5}	2.1×10^{-6}

Table 9: Relative error in the evaluation of $Q_3(x)$ from its integral representation using (71) at resolution $j = 5$

x	$-\frac{3}{4}$	$-\frac{1}{2}$	$-\frac{1}{4}$
Rel.Error	2.7×10^{-5}	3.3×10^{-5}	1.7×10^{-6}
0	$\frac{1}{4}$	$\frac{1}{2}$	$\frac{3}{4}$
9.9×10^{-6}	3.0×10^{-5}	1.1×10^{-4}	4.9×10^{-5}

3.4 Composite quadrature formula for integrals having Cauchy and weak singularity

During the last few decades the numerical evaluation of a combination of weakly singular and Cauchy singular integrals became one of the important problems in numerical analysis and computational mathematics. For example, it is well known that the singular integral equation of first kind with Cauchy kernel

$$\int_{-1}^{1} \frac{f(t)}{t-x} dt = g(x) \qquad -1 < x < 1 \qquad (75)$$

where the integral is in the sense of CPV, has four kinds of solutions:

$$1.\ f(x) = \frac{A_0}{\sqrt{1-x^2}} + \frac{1}{\pi\sqrt{1-x^2}} \int_{-1}^{1} \frac{\sqrt{1-x^2}\, g(t)}{t-x}\, dt, \qquad (76a)$$

A_0 being an arbitrary constant,

$$2.\ f(x) = \frac{1}{\pi^2}\sqrt{\frac{1-x}{1+x}} \int_{-1}^{1} \sqrt{\frac{1+t}{1-t}} \frac{g(t)}{t-x}\, dt, \qquad (76b)$$

$$3.\ f(x) = \frac{1}{\pi^2}\sqrt{\frac{1+x}{1-x}} \int_{-1}^{1} \sqrt{\frac{1-t}{1+t}} \frac{g(t)}{t-x}\, dt, \qquad (76c)$$

$$4.\ f(x) = \frac{1}{\pi^2}\sqrt{1-x^2} \int_{-1}^{1} \frac{1}{\sqrt{1-t^2}} \frac{g(t)}{t-x}\, dt \qquad (76d)$$

subject to the condition that

$$\int_{-1}^{1} \frac{g(t)}{\sqrt{1-t^2}}\, dt = 0. \qquad (76e)$$

From the outward appearance of the integrals in (76a-e) it appears that although the integrals involved in (76a) and (76e) can be evaluated numerically by using the scale function based raw image dependent quadrature formula (71) and (74) respectively, integrals involved in other solutions (76b-d) remain intractable due to presence of multiple singularities of different types within the limits of integration. It is thus desirable to develop quadrature rule that may be called composite quadrature rule which can estimate singular integrals with multiple singularities with same order of accuracy as has been achieved in case of single singular cases.

So, we consider the integral

$$I[\mu,\ \nu;\ x] = \int_a^b \frac{1}{(t-a)^{\mu}\,(b-t)^{\nu}} \frac{g(t)}{t-x}\,dt$$

$$-a < x < b. \qquad (77)$$

We hypothetically divide the range $\Lambda = \{2^j a - (2K-2), \cdots\cdots, 2^j b - 1\}$ of raw images for regular part of the integrand into three parts $\Lambda_I = \{2^j a - (2K-2), \cdots\cdots, 2^j(c-\delta) - 1\}, \Lambda_C = \{2^j(c-\delta), \cdots\cdots, 2^j(c+\delta) - K\}$ and, $\Lambda_R = \{2^j(c+\delta) - K + 1, \cdots\cdots, 2^j b - 1\}$ with a suitable choice for $\delta > 0$, and treat

$$g_b(t,x) = \frac{g(t)}{(b-t)^{\nu}(t-x)}, \qquad (78a)$$

$$g_c(t,x) = \frac{g(t)}{(b-t)^{\nu}(t-a)^{\mu}}, \qquad (78b)$$

$$g_a(t,x) = \frac{g(t)}{(t-a)^{\nu}(t-x)} \qquad (78c)$$

as regular functions within the support of scale functions spanned by the respective index sets Λ_L, Λ_C and Λ_R . Then using the quadrature formulae for weakly and Cauchy singular integrals (62) and (71) with the raw images for g_b, g_c, g_a, the composite quadrature formula for the integral in (77) can be found as

$$I[\mu,\ \nu;\ x] \equiv Q[\mu,\ \nu;\ x]$$

$$= \sum_{k=a2^j-(2K-2)}^{(c-\delta)2^j-1} g_{b;\,j\,k}\,\omega_{j\,k}^{W\,L} +$$

$$\sum_{k=(c-\delta)2^j}^{(c+\delta)2^j-K} g_{c;\,j\,k}\,\omega_{k-2^j x}^{C} +$$

$$\sum_{k=(c+\delta)\,2^j-K+1}^{b2^j-1} g_{a;j\,k}\,\omega_{j\,k}^{W\,R}. \qquad (79)$$

We now compute the integral appearing in the fourth kind solution (76d) of Cauchy singular integral equation of first kind (75) for

$$g(t) = t^n, n = 0, 1, \ldots 4$$

and for $x = \pm\frac{3}{4}, \pm\frac{1}{2}, \pm\frac{1}{4}, 0.$

For evaluation of the integral

$\int_{-1}^{1} \frac{t^n}{\sqrt{1-t^2}} \frac{dt}{x-t}$ at $x = \pm\frac{1}{4}, 0$

we have partitioned the domain of integration into $[-1,-\delta] \cup [-\delta,\delta] \cup [\delta,1]$ with $\delta = \frac{1}{2}$ at the resolution $j = 5$. But for the evaluation of integrals for $x = \pm\frac{1}{2}$ 2 or $\pm\frac{3}{4}$, one needs to adjust both and the resolution j to $\frac{1}{4}, \frac{1}{8}$ and 6,7 respectively so that the condition

$j \geq \frac{4K-2}{(\text{upper limit}-\text{lower limit})}$ for each component

of the partition $[-1,-\delta]$, $[-\delta,\delta]$, and $[\delta,1]$ is satisfied. The approximate numerical values of this integral evaluated by our quadrature rule have been compared with the numerical values obtained from the exact expressions

$$\int_{-1}^{1} \frac{t^n}{\sqrt{1-t^2}(x-t)}\,dt = \begin{cases} 0 & \text{if } n = 0 \\ \pi & \text{if } n = 1 \\ \pi x & \text{if } n = 2 \\ \pi(x^2+\frac{1}{2}) & \text{if } n = 3 \\ \pi x(x^2+\frac{1}{2}) & \text{if } n = 4. \end{cases}$$

The absolute errors of our approximate values are presented partially in Table 10 and found to be $O(10^{-5})$ at the minimum resolution j.

Table-10 Relative Error

	$\delta=\frac{1}{2}$ $j=5$	$\delta=\frac{1}{2}$ $j=5$	$\delta=\frac{1}{4}$ $j=6$	$\delta=\frac{1}{8}$ $j=7$
X n	0	$\frac{1}{4}$	$\frac{1}{2}$	$\frac{3}{4}$
0	4.6×10^{-5}	4.9×10^{-5}	2.6×10^{-4}	4.5×10^{-4}
1	3.1×10^{-6}	1.2×10^{-5}	1.4×10^{-4}	3.6×10^{-4}
2	3.2×10^{-6}	5.9×10^{-6}	8.1×10^{-5}	2.9×10^{-4}
3	3.7×10^{-6}	8.2×10^{-6}	5.2×10^{-5}	2.5×10^{-4}
4	5.2×10^{-5}	5.7×10^{-5}	4.3×10^{-5}	2.2×10^{-4}

3.4 Observations

We have presented here the Daubechies scale function based quadrature rules for numerical

evaluation of definite integrals involving regular, weakly singular, Cauchy singular integrands and even a combination of them. Each formula consist of sum of product of some weight and the value of the regular part of the integrand evaluated at the nodes. Weights and nodes involved in the formulae are the moments of the interior and boundary scale functions. The efficiency of the quadrature rules derived here has been tested by comparing numerical results obtained by present formula and by other available methods for some examples for each case. An estimate of the bound of error in the quadrature formula for regular integral has been obtained. It appears that order of accuracy in the numerical evaluation of raw images for $f \in L^2[a,b]$ by one-point quadrature rule proposed here is good enough since it is comparable to the error in Daubechies-K scale function based multiresolution approximation of any L^2 function in approximation space($O(\frac{1}{(2^j)^{K-1}})$ at the resolution). One may, thus rely on the Daubechies scale function based formulae (45), (62), (71) and (79) for the approximate evaluation of regular or singular (upto Abel and Cauchy singularity) definite integrals with a desired order of accuracy at the appropriate resolution *j*. Formula for numerical evaluation of definite integral with logarithmic singularity can also be obtained in a similar way. This investigation further confirms that orthogonality is not a significant issue for the bases of approximation space for $L^2[a,b]$ as pointed out by Jia et al [?] in their studies of compactly supported wavelet bases for Sobolev spaces. It is expected that the idea of one-point quadrature rule for the evaluation of raw image corresponding to interior or boundary Daubechies scale function can be utilized for approximating numerical values of Cauchy singular integral or hypersingular integrals with singularty at one edge of the integration limit or finding numerical solution of singular integral equations. Some work in this direction has already been carried out.

Solution of second kind integral equation with Cauchy type kernel using Daubechies scale function, Panja, M. M. and Mandal, B. N., *J. Comput. Appl. Math* **241** (2013) 130-142

References

1. *A. Kunoth, Wavelet methods-elliptic boundary value problems and control problems,Teubner Verlag, 2001.*

2. *A. Cohen, Numerucal* analysis of wavelet methods in Studies in Mathematics and its applications, Vol. 32, Elsevier, 2003.

3. F. Keinert, Wavelets and MultiWavelets, Studies in Advances in Mathematics, Chapman & Hall/CRC , 2004.

4. S. Ebromovich, Multiwavelets and signal denoising, Sankhya, Ser. A 63 (2001) 367-393.

5. K. P. Soman, K. I. Ramachandran, N. G. Reshmi, Insight into wavelets: From theory to practice, PHI Learning Pvt. Ltd. (3rd. Ed.) 2010.

6. H L Resnikoff, Raymond O Wells, Jr. Wavelet Analysis, The scalable Structure of information, Springer India, 2004.

7. I. Daubechies, Orthonormal bases of compactly supported wavelets, Comm. on Pure. And Appl. Math. 41(1988) 909-996; Ten Lectures on Wavelets, SIAM, Philadelphia, PA, 1992.

8 . Meyer, Ondelettes sur I'intervealle, Rev. Mat. Iberoam.7, 115-133(1991).

9. J. C. Goswami and A. K. Chan, Fundamentals of wavelets: Theory, Algorithms, and Applications (2nd Ed.) Wiley, 2011, $10.4, pp. 312.

10. B. M. Kessler, G. L. Payne and W. W. Polyzou , Scattering calculation with wavelets, Few-Body system 33, 1-26(2003).

11. Panja, M. M. and Mandal, B. N. A note on one-point quadrature formula for Daubechies scale function with partial support, *Appl. Math. and Comput*. 218 (2011) 4147-4151.

12. Panja, M. M. and Mandal, B. N., Solution of second kind integral equation with Cauchy type kernel using Daubechies scale function, Panja, *J. Comput. Appl. Math* 241 (2013) 130-142

Papers on application of wavelets prepared by B N Mandal and associates

1. Numerical solution of an integral equation arising in the problem of cruciform crack, Bhattacharya, Subhra and Mandal, B. N., *Int. J. Appl. Math. & Mech*. **6** (2010) 70 – 77

2. A note on one-point quadrature formula for Daubechies scale function with partial support, Panja, M. M. and Mandal, B. N. *Appl. Math. and Comput*. 218 (2011) 4147-4151.

3. Evaluation of singular integrals using Daubechies scale functions, Panja, M.M. and Mandal, B. N. *Advances in Comput Math & its Applic* 1 (2012) 64-75.

4. Numerical solution of linear Fredholm and Volterra integral equations of the second kind by using Quadratic Legendre multi-wavelets, Singh, Rajeev Kr., Pathak, Ashish, and Mandal, B. N. , *J. Adv. Res. Sci. Comput* **4** no. 3 (2012) 49-58.

5. Solution of second kind integral equation with Cauchy type kernel using Daubechies scale function, Panja, M. M. and Mandal, B. N., *J. Comput. Appl. Math* 241 (2013) 130-142.
6. Daubechies scale function based quadrature rules for singular and hypersingular integralts with variable singularities, Panja, M. M. and Mandal, B. N., *Investigations in Mathematical Sciences* 3 no. 1 (2013) 155-176.

7. Numerical solution of linear Fredholm and Volterra integral equation of second kind by using Gegenbauer wavelet, Singh, R. K. and Mandal, B. N., *J. Adv.*

Res. In Scientific Computing **5** no. 3 (2013) 43- 53.

8. Numerical solution of linear Fredholm and Volterra integral equation of second kind by using Gegenbauer wavelet, Singh, R. K. and Mandal, B. N., *J. Adv. Res. In Scientific Computing* **5** no. 3 (2013) 43-53.

9. Numerical solution of linear Fredholm and Volterra integral equations of second kind using cubic Legendre multi-wavelets, Singh, R. K. and Mandal, B. N., *J. Adv. Res. Scientific Computing*, Vol. 6 no. 1 (2014) 25-35.

10. Numerical solution of Abel integral equations using Legendre multi-wavelets, Rajeev Kumar Singh , B. N.Mandal, *Int J Appl Math and Eng. Sci.,Vol.* 8 (2014)83-92.
11. Gauss-type quadrature rule with complex nodes and weights for integrals involving Daubechies scale functions and wavelets, Panja, M M and Mandal, B N., *J. Comput. Appl. Math* 290 (2015) 609-632.

12. Numerical solution of an integral equation arising in the problem of cruciform crack by using linear Legendre multiwavelets, Rajeev Kr Singh and B N Mandal, *J Adv Res Sci Comput* **7** issue 4 (2015) 16-25.

13. Multiscale approximation of the solution of weakly singular second kind Fredholm integral equation in Legendre Multiwavelet basis, Paul, S., Panja, M M and Mandal, B N, *J. Comput. Appl. Math* 300 (2016) 275–289.

14. Computing eigenelements of Sturm-Liouville problems by using Daubechies wavelets, by M. M. Panja, M.M Saha,U. Basu, D.Datta and B. N. Mandal, *Indian Journal of Pure and Applied Mathematics* (2016)

15. Wavelet based numerical solution of second kind hypersingular integral equation, Swaraj Paul, M M Panja,and B N Mandal, *Appl Math Sciences* (2016)

16. Use of Legendre multiwavelets in solving second kind singular integral equations with Cauchy type kernel" Swaraj Paul , M. M. Panja and B. N. Mandal, *Investigations in Mathematical Sciences* (2016)

The Mathematical Story in the Theory of Relativity

Prof. Subenoy Chakraborty

The aim of this lecture is to establish both special and general theory of relativity as geometric theories. According to Einstein, space and time should be on the same footing and we have four dimensional space-time. We start with Euclide's axiom that distance between two points in space is invariant and extend it to four dimensional space-time for two neighbouring points then we have

$$dl_4^2 = dx_1^2 + dx_2^2 + dx_3^2 + \lambda^2 dt^2 \tag{1}$$

to be an invariant quantity. Here, a factor λ having dimension of velocity is introduced on dimensional ground. Although space and time are on the same status in (1) but still time should have a separate identity due to (*i*) there is space reversibility *i.e.* $x_i \rightarrow -x_i$ but time can move only in the future direction, (*ii*) from the point of view of mechanics one should have an identification of time co-ordinate from eq. (1) after co-ordinate transformation. For this requirement, a simplest modification to equation (1) can be chosen as

$$ds^2 = dx_1^2 + dx_2^2 + dx_3^2 - \lambda^2 dt^2 . \tag{2}$$

Here *ds* is termed as space-time interval and it is claimed that it should be invariant under space-time co-ordinate transformation. For simplicity, we shall consider linear transformations which make the above space-time interval to be invariant. Interestingly, it is found that such a linear transformation is nothing but the Lorentz transformation with λ being the absolute velocity. Hence λ can be identified as the velocity of light. Further, from the invariance of ds^2 for two inertial frames *S* and *S*′ and using the Lorentz transformation between S and S′ one obtains the velocity identity as

$$\sqrt{1-\frac{u^2}{\lambda^2}}\sqrt{1-\frac{v^2}{\lambda^2}} = \sqrt{1-\frac{u'^2}{\lambda^2}}\left(1-\frac{u_x v}{\lambda^2}\right) \tag{3}$$

where *u*, *u*′ are the velocities of a particle in *S*- and *S*′- frame respectively and *v* is the relative velocity between the two frames of references. In particular if *u* and *v* are in the same direction then one obtains the law of composition of velocity as

$$u' = \frac{u-v}{1-\frac{uv}{\lambda^2}} \quad i.e. \quad u = \frac{u'+v}{1+\frac{u'v}{\lambda^2}} \tag{4}$$

or in other words we write

$$u = u' \oplus v\,.$$

The set of all Lorentz transformations having relative velocity in the same direction form a group with the above binary composition (known as Lorentz group). Thus by a simple modification of Euclide's axiom for a separate identification of time, we switch over from Newtonian theory to Einstein's special theory of relativity and also the algebraic structure has been changed. We shall now examine the geometric structure of the so constructed four dimensional space-time.

Similar to the space-time interval, the quadratic form $D^2 = x_1^2 + x_2^2 + x_3^2 - \lambda^2 t^2$ is invariant under Lorentz transformation (LT). Due to indefiniteness in sign, D^2 may have values +ve, −ve or zero. We shall first examine the situation $D^2 = 0$. In four dimensional space-time it represents a cone having axis along the time direction. Thus, for points inside the cone we have $D^2 < 0$ while $D^2 > 0$ for points outside the cone. Also it is easy to see that events occurring inside the cone have velocity less than the absolute velocity, the velocity will be greater than λ for events occurring outside the cone and the events occur with absolute velocity on the surface of the cone. This cone in special theory of relativity is termed as null cone or light cone. All natural physical events occur inside the light cone and outside the cone is physically inadmissible. Events occurring inside the cone are termed as time-like events while events outside the cone are known as space-like events and events on the surface of the cone are called null or light-like events. Thus the whole four dimensional space-time is divided into two regions having a common boundary as the surface of the cone. So the geometric structure of the space-time is no longer Euclidean, rather pseudo-Euclidean or Minkowskian in nature.

Now we shall discuss the geometric aspect of Einstein's general theory of relativity (GTR). The natural question that arises in Einstein's GTR is how curved geometry appears in the gravity theory ? We shall show that Einstein's equivalence principle leads to geometry of curved space- time. According to Einstein, the inertial mass and the gravitational mass are equivalent (weak equivalence principle) and it is verified experimentally. So the equation of motion of a particle moving in a gravitational field can be written as

$$m_i \frac{d^2 \vec{r}}{dt^2} = m_g \vec{g}\,.$$

As $m_i = m_g$ (weak equivalence principle) so we have

$$\frac{d^2\vec{r}}{dt^2} = \vec{g}\,.$$

If we now transform to a non-inertial frame described as

$$\vec{r'} = \vec{r} - \frac{1}{2}\vec{g}t^2$$

then we have

$$\frac{d^2\vec{r'}}{dt^2} = 0\,,$$

which shows that there is no gravitational force in the non-inertial primed system. Thus we can say that the given gravitational force and the accelerated non-inertial frame are equivalent and is known as strong equivalence principle.

Let $\{x_i\}$ be an inertial frame of reference and so we have the Minkowskian line element

$$ds^2 = \eta ij dx^i dx^j \quad , \quad \eta_{ij} = \mathrm{diag}(-1,+1,+1,+1)\,.$$

Suppose $\{y^\alpha\}$ be a non-inertial frame of reference and we write

$$ds^2 = g_{\alpha\beta} dy^\alpha dy^\beta\,.$$

As in the Minkowskian space-time there is no gravitational force so we have

$$\frac{d^2x^i}{d\tau^2} = 0\,,$$

$$\begin{aligned}
\text{Now,}\quad \frac{dx^i}{d\tau} &= \frac{\partial x^i}{\partial y^\alpha}\cdot\frac{dy^\alpha}{d\tau} \\
\Rightarrow\quad \frac{d^2x^i}{d\tau^2} &= \frac{\partial x^i}{\partial y^\alpha}\frac{d^2y^\alpha}{d\tau^2} + \frac{\partial^2 x^i}{\partial y^\alpha \partial y^\beta}\frac{dy^\alpha}{d\tau}\frac{dy^\beta}{d\tau} = 0 \\
\Rightarrow\quad \frac{d^2y^\alpha}{d\tau^2} &= -\Gamma^\alpha_{\mu\nu}\frac{dy^\mu}{d\tau}\frac{dy^\nu}{d\tau} \qquad (5) \\
\text{with}\quad \Gamma^\alpha_{\mu\nu} &= \frac{\partial^2 x^i}{\partial y^\mu \partial y^\nu}\cdot\frac{\partial y^\alpha}{\partial x^i}\,. \qquad (6)
\end{aligned}$$

Due to invariance of ds^2 we have

$$\begin{aligned} g_{\alpha\beta} &= \eta_{ij}\frac{\partial x^i}{\partial y^\alpha}\frac{\partial x^i}{\partial y^\beta} \\ \Rightarrow \quad \frac{\partial g_{\alpha\beta}}{\partial y^\lambda} &= \eta_{ij}\frac{\partial^2 x^i}{\partial y^\alpha \partial y^\lambda}\cdot\frac{\partial x^i}{\partial y^\beta} + \eta_{ij}\frac{\partial x^i}{\partial y^\alpha}\cdot\frac{\partial^2 x^i}{\partial y^\beta \partial y^\lambda} \\ &= g_{\beta\delta}\Gamma^\delta_{\alpha\lambda} + g_{\alpha\delta}\Gamma^\delta_{\beta\lambda} \\ \Rightarrow \quad \Gamma_{\lambda\mu\nu} &= \Gamma^\delta_{\lambda\mu}g_{\delta\nu} = \frac{1}{2}\left(\frac{\partial g_{\lambda\nu}}{\partial x^\mu} + \frac{\partial g_{\mu\nu}}{\partial x^\lambda} - \frac{\partial g_{\lambda\mu}}{\partial x^\nu}\right). \end{aligned} \tag{7}$$

These are the usual christoffel symbols. We can interpret eq. (5) as the geodesic equation in the non-inertial frame. Also in analogy to Newtonian theory $\Gamma^\lambda_{\mu\nu}$ is interpreted as the force term and the metric tensor components $g_{\mu\nu}$ represent the potential term.

Using the christoffel symbols we can define the covariant derivative and from the non-commutativity of the second order covariant derivative one can define the usual curvature tensor.

Thus starting from the equivalence principle we are able to show that the four dimensional space- time geometry is a curved geometry and is a Riemannian geometry with Lorentzian metric. Then following Einstein's logical arguments one arrives the Einstein's gravitational field equations

$$R_{\mu\nu} - \frac{1}{2}Rg_{\mu\nu} = -\frac{8\pi G}{c^4}T_{\mu\nu}\,.$$

In four dimensional space-time there are ten field equations which are not all independent – six equations are independent and four equations are the constraint equations.

Nonlinear oscillations in a finite temperature plasma

Nikhil Chakrabarti
Saha Institute of Nuclear Physics, 1/AF Bidhannagar Kolkata-700064, India

The nonlinear collective dynamics of one-dimensional finite temperature plasma is investigated using Lagrangian variables. An exact non-stationary nonlinear solution with a nontrivial space and time dependence is obtained. The results demonstrate that the formation of nonlinear localized solitary wave-like density structures when nonlinearity is being balanced by the wave dispersion. Solution predicts the catastrophic density collapse if nonlinearity overpower the dispersion.

I. INTRODUCTION

Perhaps, oscillation is the physical fact which was introduced in our early school days and still we continue to fetch a new direction in this area. Investigation of oscillations and waves and their nonlinear character in a plasma is a very fertile area for fundamental research. Specially the nonlinear exact solutions and their applications in a complex plasma media is almost a virgin territory. Electrostatic nonlinear oscillations and waves in plasmas are of fundamental importance due to their applications in laboratory and astrophysical situation. Starting from the earlier works [1, 2], studies on nonlinear oscillations and/or waves in plasmas have been an important topic of increasing interest among various researchers, [3–9] even in present days[10]. This interest is due the direct applications of these waves in plasma heating, [11] particle acceleration, [12] etc. Although the problem of nonlinear electron oscillations in a cold plasma has been investigated extensively, very little work has been reported with respect to the dynamics of a warm electron plasma.

For warm plasma, a pressure gradient term appears in the governing equations of the cold plasma oscillations and thus makes difficult to analyze the equations.[7] We have learned from the cold plasma results that nonlinear evolution of plasma oscillations very much depends on initial conditions. Depending on initial conditions coherent oscillations of field variables or singularity in density occur at a finite time. [4] In this work, we have investigated the effect of temperature on the space-time evolution of non-relativistic electron plasma waves. We have assumed a slow variation of plasma wave compared to equilibration time, so the temperature is taken to be constant throughout our analysis. For the sake of simplicity, we consider only the *electrostatic* mode without any magnetic field. This is a simplified model where the electron plasma oscillations are investigated homogeneous and unmagnetized plasma with finite temperature to elucidate its nonlinear character.

II. BASIC EQUATIONS

In order to obtain the mathematical tools for spatiotemporal evolution of large-amplitude electron oscillations in a finite temperature plasma, we use fluid equations supplemented by - Maxwell's equations for the electromagnetic field. In one spatial dimension namely (x), the basic equations are the continuity equation and the momentum equation of electron fluid

$$\left(\frac{\partial}{\partial t}+v_x\frac{\partial}{\partial x}\right)n=-n\frac{\partial v_x}{\partial x}, \tag{1}$$

$$\left(\frac{\partial}{\partial t}+v_x\frac{\partial}{\partial x}\right)v_x=-\frac{eE}{m}-\frac{v_{th}^2}{n}\frac{\partial n}{\partial x}. \tag{2}$$

Where n, v_x, $-e$, m, and $v_{th}(=\sqrt{T/m})$ denotes the density, x component of fluid velocity, charge, mass, and thermal velocity of electrons, respectively. Here T is the finite electron temperature, the wave electric field is $\mathbf{E}=E\hat{e}_x$, where $\hat{e}_x$ is the unit vector along the x direction.

As mentioned before above two equations are supplemented by the electric field evolution equation

$$\left(\frac{\partial}{\partial t}+v_x\frac{\partial}{\partial x}\right)E=4\pi en_0v_x. \tag{3}$$

It is to be noticed here that to derive Eq. (3), we have combined Poisson's equation

$$\frac{\partial E}{\partial x}=4\pi e(n_0-n)$$

and the x component of $\nabla\times\mathbf{B}$ equation, viz.,

$$0=-4\pi env_x+\frac{\partial E}{\partial t}.$$

We have also assumed that ions are immobile and they form a fixed charged neutralizing background with constant ion density n_0.

III. NONLINEAR ANALYSIS WITH LAGRANGIAN TRANSFORMATION TECHNIQUE

Next, we present an exact solution of Eqs. (1) - (3) by using the Lagrangian variables method [4, 13]. In solving these nonlinear equations, we transform from the Eulerian variables (x,t) to Lagrangian variables (ξ,τ) (such that $\xi=x$ at $t=0$), where

$$\xi\equiv x-\int_0^\tau v_x(\xi,\tau')d\tau' \qquad \tau\equiv t \tag{4}$$

so that ξ is a function of both x and t, but ξ and τ are treated as independent variables. In terms of these new variables, the convective derivative

$$\left(\frac{\partial}{\partial t}+v_x\frac{\partial}{\partial x}\equiv\frac{\partial}{\partial\tau}\right)$$

becomes partial time derivative. Thus, we obtain from Eq. (1)

$$n(\xi,\tau)=n(\xi,0)\left[1+\int_0^\tau d\tau'\,\frac{\partial}{\partial\xi}v_x(\xi,\tau')\right]^{-1}, \quad (5)$$

where $n(\xi,0)$ represents the initial ($\tau=0$) density distribution in space. From this relation and Eq. (4) one can write

$$\frac{n(\xi,\tau)}{n(\xi,0)}=\frac{\partial\xi}{\partial x}. \quad (6)$$

In these new variables, the fluid equations become

$$\frac{\partial}{\partial\tau}\left(\frac{1}{n}\right)=\frac{1}{n(\xi,0)}\frac{\partial v_x}{\partial\xi}, \quad (7)$$

$$\frac{\partial v_x}{\partial\tau}=-\frac{eE}{m}-\frac{v_{th}^2}{n(\xi,0)}\frac{\partial n}{\partial\xi}, \quad (8)$$

and

$$\frac{\partial E}{\partial\tau}=4\pi e n_0 v_x. \quad (9)$$

Combining Eqs. (8) and (9), we obtain the following equation

$$\left(\frac{\partial^2}{\partial\tau^2}+\omega_p^2\right)v_x=-\frac{v_{th}^2}{n(\xi,0)}\frac{\partial}{\partial\tau}\left(\frac{\partial n}{\partial\xi}\right), \quad (10)$$

where $\omega_p=\sqrt{4\pi e^2 n_0/m}$ is the typical plasma oscillation frequency of electron fluid. This equation (10) together with the equation (7) constitute a complete set to determine the dynamics of finite temperature electron plasma oscillation.

Before obtaining nonlinear solutions of these equations [Eqs. (7) and (10)], we linearize these equations by writing $n/n(\xi,0)\equiv\hat{n}=1+\tilde{n}$ and $v_x=0+\tilde{v}$ we then have

$$\frac{\partial\tilde{n}}{\partial\tau}=-\frac{\partial\tilde{v}}{\partial x}, \quad \text{and} \quad \left(\frac{\partial^2}{\partial\tau^2}+\omega_p^2\right)\tilde{v}=-v_{th}^2\frac{\partial}{\partial\tau}\left(\frac{\partial\tilde{n}}{\partial x}\right).$$

Supposing that all perturbed variables are proportional to $\exp(-i\omega\tau+ikx)$, where ω and k are the frequency and the wave number, respectively, we finally have the usual dispersion relation of waves in thermal plasma[4]: $\omega^2=\omega_p^2+k^2v_{th}^2$. This dispersion relation indicates that the electron plasma oscillation is modified by the finite temperature. This wave is dispersive as the group velocity, calculated from the above dispersion relation, comes out to be finite and function of k.

IV. ANALYTICAL SOLUTION AND NUMERICAL SIMULATION

To find the nonlinear solutions of Eqs. (7) and (10), we introduce the following normalization: $\hat{\tau}=\tau\omega_p$, $\hat{\xi}=\omega_p\xi/v_{th}$, and $\hat{v}=v_x/v_{th}$. Then the above Eqs. (7) and (10) can be recast in the following normalized form:

$$\frac{\partial}{\partial\hat{\tau}}\left(\frac{1}{\hat{n}}\right)=\frac{1}{\hat{n}(\hat{\xi},0)}\frac{\partial\hat{v}}{\partial\hat{\xi}}, \quad (11)$$

$$\left(\frac{\partial^2}{\partial\hat{\tau}^2}+1\right)\hat{v}=-\frac{1}{\hat{n}(\hat{\xi},0)}\frac{\partial}{\partial\hat{\tau}}\left(\frac{\partial\hat{n}}{\partial\hat{\xi}}\right), \quad (12)$$

Hereafter we remove all hat for simplicity of notations but all variables are understood as a normalized variables. Let us seek nonlinear solutions of Eqs. (11) and (12) by introducing the method of separation of variables. Accordingly, we propose the solutions of the form $n(\xi,\tau)=\chi(\xi)\phi(\tau)$ and $v(\xi,\tau)=V(\xi)\psi(\tau)$. Inserting these into Eqs.(11) and (12) and then separating space and time variable equations, we obtain

$$\left(\frac{1}{\frac{d\phi}{d\tau}}\right)\left(\frac{d^2}{d\tau^2}+1\right)\psi(\tau)=-\frac{1}{\chi(\xi)V(\xi)}\frac{d\chi}{d\xi}=\lambda_1, \quad (13)$$

and

$$\frac{1}{\psi}\frac{d}{d\tau}\left(\frac{1}{\phi}\right)=\frac{dV}{d\xi}=\lambda_2, \quad (14)$$

where $n(\xi,0)=\chi(\xi)\phi(0)$, $v(\xi,0)=V(\xi)\psi(0)$ and λ_1,λ_2 are the separation constants. Here $\psi(0)=\phi(0)=1$ as we are working with the normalized variables and also without loss of generality we can use $\phi(0)=\chi(0)=1$. Solving separately for spatial and temporal equations, one obtains a complete solution. Note here that the above four equations can be reduced to the following two equations:

$$\frac{d}{d\tau}\left(\frac{d^2}{d\tau^2}+1\right)\left(\frac{1}{\phi}\right)=\lambda\frac{d\phi}{d\tau}, \quad (15)$$

and

$$\frac{d^2\ln\chi}{d\xi^2}=-\lambda, \quad (16)$$

where $\lambda(=\lambda_1\lambda_2)$ is a separation constant to be determined later from the normalization condition. We readily obtain a solution of Eq. (16) in the form

$$\chi=e^{-\lambda\xi^2/2},$$

where we have used the boundary condition: $\chi=1$, $d\chi/d\xi=0$ at $\xi=0$. Finally using density conservation $\int_{-\infty}^{\infty}\chi(\xi,0)d\xi=1$, we obtain the separation constant $\lambda=2\pi$. With this value the spatial solution become

$$\chi=e^{-\pi\xi^2}. \quad (17)$$

In order to get a complete solution, we have to obtain a solution for the temporal part of Eq.(15). It should be noted that in a typical laboratory experiment, the fluid element always acquires an extra acceleration due to the trapping potential and therefore to solve the Eq. (15), we use the initial conditions at $\tau = 0$, $\phi = 1$, $d\phi/d\tau = 0$, and $d^2\phi/d\tau^2 = \alpha$ (constant). The second derivative of ϕ is the first time derivative of velocity amplitude which follows from Eq. (16). Physically this constant might be regarded as the initial wave acceleration depends on the experimental parameters (laser and field strength related parameters) and acts as source of energy so that it is related to the nonlinear strength of the wave. The temporal equation (15) now becomes

$$\left(\frac{d^2}{d\tau^2} + 1\right)\left(\frac{1}{\phi}\right) = \lambda\phi + \beta, \tag{18}$$

with β as the integration constant and is found to be $\beta = 1 - \lambda - \alpha$ due to the above specified initial conditions. Integrating Eq. (18) and applying the same initial condition, we obtain the following first order ordinary nonlinear differential equation

$$\frac{d\Phi}{d\tau} = \pm\sqrt{1 - \Phi^2 + 2\lambda \ln\Phi - 2\beta(1-\Phi)}, \tag{19}$$

where $\Phi = 1/\phi$ and $\pm$ sign indicate the decaying and growing branch of density amplitude ϕ. Since we are interested in the nonlinear solution we only consider growing branch corresponding to the negative sign in the right hand side of equation(19). First we have integrate this equation numerically for $\phi(\tau)$ using MATLAB to obtain the time dependent part of the density. The solution for density is given in figure below for a typical value of α. The time variation of the density amplitude shows nonlinear behavior as expected. To write the complete solution, we also need to convert the Lagrangian variables to Eulerian and is done by means of the Eq. (6), which is given by $\xi = x\phi$. Therefore, the density in terms of original (x, t) variables becomes,

$$n(x,t) = \phi(t)e^{-\pi x^2\phi^2(t)}, \tag{20}$$

where, $\phi(t)$ has to be determined from Eq.(19). The speciality of this newly found solution is that both the amplitude ($\sim \phi(t)$) and the dispersion ($\sim \phi(t)^{-2}/2\pi$) has a functional dependence on time. So this solution can easily capture the singularity that might occur due to the intrinsic nonlinearities of the physical system in course of time. The mean electron velocity of the plasma fluid can easily be obtained by a $V(\xi)$ multiplied by $\psi(\tau)$, which in terms of the original (x, t) variables becomes,

$$v(x,t) = x\phi(t)\frac{d}{dt}\left(\frac{1}{\phi(t)}\right). \tag{21}$$

We emphasize that the obtained expression of density and velocity given in Eqs. (20) and (21) are the complete solution of full nonlinear system of our governing

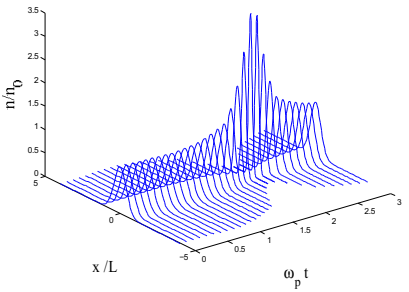

FIG. 1: In the above left side figure shows the normalized density solution for $\alpha = 3\pi$. The figure shows that a coherent structure is formed and increased in amplitude in time due to nonlinearity. The maximum amplitude $n/n_0 = 3.5$ attained at $\omega_p t = 2.1$. When dispersion overpower the nonlinearity amplitude decreases.

equations. We have pictorially represented the density solution in space and time for different values of nonlinearity parameters α as shown in Fig.(1) and (2). Initially at $\tau = 0$, the spatial profile is Gaussian like nature and evolves in time. The figure (1)shows that a coherent structure is formed and increased in amplitude in time due to nonlinearity. The maximum amplitude $n/n_0 = 3.5$ attained at $\omega_p t = 2.1$. The parameter α in these solutions controls the amplitude of the density. When nonlinearity feeds energy in the long scale wave amplitude of the wave increases and spatial scale become narrower and at scale v_{th}/ω_p, the dispersive effects are operative and it overpower the nonlinearity. As a result the amplitude decreases and solution spread in space as indicated in figure (1). Later, the analytical solution for sufficiently large amplitude wave clearly demonstrate this phenomena observed by the numerical simulation.

On the other hand, for large value of nonlinearity a density steepening occurs as a result singularity arise as time progresses and eventually density collapse occur in time when dispersion fail to prevent the nonlinear convection. At the very close to the collapse point the density becomes stronger peaked and narrower and form $\delta-$function like structure as shown in the Fig. (2).

We further try to find the root of the density collapse in time by analyzing Eq. (19) in the sufficiently large amplitude limit i.e. for $\phi \gg 1$ (or $\Phi \ll 1$). In this situation we can approximate $\ln\Phi \approx (\Phi - 1) - (\Phi - 1)^2/2 + \cdots$. Substituting in Eq. (19) integrating and using the initial condition as before, we finally obtain

$$\phi(\tau) \approx \left[1 - \frac{2\alpha}{1+\lambda}\sin^2\left(\frac{\sqrt{1+\lambda}}{2}\,\tau\right)\right]^{-1} \tag{22}$$

With this $\phi(t)$ the total expression of density can be writ-

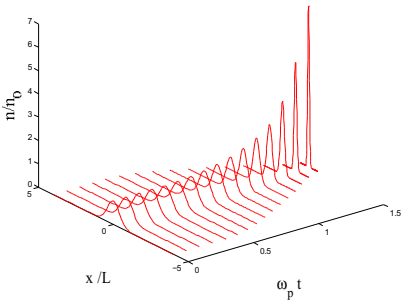

FIG. 2: In the above left side figure shows the normalized density solution for $\alpha = 4\pi$. The figure shows that a density singularity arises increased in amplitude in time due to nonlinearity. The maximum amplitude $n/n_0 = 7$ attained much earlier time at $\omega_p t = 1.5$. In this situation space scale become narrower and dispersive effect can not balance the nonlinearity eventually density collapse.

ten as is

$$n(x,t) \approx \frac{n_0}{\left[1 - \frac{2\alpha}{1+\lambda}\sin^2\left(\frac{\sqrt{1+\lambda}}{2}\,\tau\right)\right]} \exp\left[-\pi\xi^2\right], \quad (23)$$

where

$$\xi \approx \frac{x}{\left[1 - \frac{2\alpha}{1+\lambda}\sin^2\left(\frac{\sqrt{1+\lambda}}{2}\,\tau\right)\right]}. \quad (24)$$

This relation between ξ and x clearly shows that the relation is linear in space but strongly nonlinear in time. It is evident that as time increases for fixed ξ, x decreases. The spatial width of the solution decreases and amplitude increases which is evident from the figures. With the $\phi(t)$ given in En. (22), the mean electron velocity $v(\xi,\tau)$ is found to be

$$v(x,t) \approx -\frac{\alpha\, x\, \sin 2\left(\frac{\sqrt{1+\lambda}}{2}\tau\right)}{\sqrt{1+\lambda}\left[1 - \frac{2\alpha}{1+\lambda}\sin^2\left(\frac{\sqrt{1+\lambda}}{2}\,\tau\right)\right]}, \quad (25)$$

Thus the Eq. (23) represent the exact non-stationary solution of Eq. (11) and (12).

V. CONCLUSIONS

In this work, we have used Lagrangian fluid description to study the nonlinear collective dynamics of large amplitude oscillations in a one-dimensional electron plasma. We have formulated and solved the full set of fluid equations both analytically using the Lagrangian variable technique and numerically using MATLAB. In the limit of strong nonlinearity ($\alpha \sim 4\pi$), the evolution of the density is strongly time-dependent, becoming singular in finite time. This leads to a catastrophic density collapse in a warm plasma. We have found an approximate analytical expression for the singularity in the temporal solution. To characterize the obtained solution if we ignore the thermal effect then Eqs. (11) and (12) are decoupled Eq. (12) become linear in Lagrangian frame. The solution is just oscillations with frequency ω_p. Therefore initially ($t = 0$) we can take arbitrary density/ velocity perturbation with an arbitrary spatial scale. For finite temperature effect this is not possible. If one look at the linear wave frequency i.e. $\omega^2 = \omega_p^2(1 + k^2l^2)$ where $l = v_{th}/\omega_p$, which gives an unique value of k for a given ω. Therefore only one mode can excited. This feature is capture by our separation of variable method where spatial form is determined from equation not initially shaped arbitrarily. By taking this theoretical approach, with the subsequent observations in experiment a coherent structure formation and subsequent destruction by singularity formation could be studied to provide a new avenue for investigating the behavior of interacting thermal plasma.

VI. ACKNOWLEDGEMENT

I would like to acknowledge Prof. Samiran Ghosh, Dr. Sudip Garai, Dr. Anwesa Sarkar, Dr. Manjistha Dutta and Dr. Chandan Maity for their contributions.

[1] A. I. Akhiezer and R. V. Polovin, Sov. Phys. JETP **3**, 696 (1956).
[2] J. M. Dawson, Phys. Rev. **113**, 383 (1959).
[3] G. Kalman, Ann. Phys. **10**, 1 (1960).
[4] R. C. Davidson and P. P. Schram, Nucl. Fusion **8**, 183 (1968).
[5] T. P. Coffey, Phys. Fluids **14**, 1402 (1971).
[6] R. C. Davidson, *Methods in Nonlinear Plasma Theory* (Academic, New York) (1972).
[7] E. Infeld and G. Rowlands, Phys. Rev. Lett. **58**, 2063 (1987).
[8] S. Sengupta, V. Saxena, P. K. Kaw, A. Sen, and A. Das, Phys. Rev. E **79**, 026404 (2009).
[9] T. Coffey, Phys. Plasmas **17**, 052303 (2010).
[10] A. Sarkar, C. Maity, and N. Chakrabarti, Physics of Plasmas. **20**, 122303 (2013).
[11] P. Koch and J. Albritton, Phys. Rev. Lett. **32**, 1420 (1974).
[12] T. Tajima and J. M. Dawson, Phys. Rev. Lett. **43**, 267 (1979).
[13] N. Chakrabarti, C. Maity, and H. Schamel, Phys. Rev. Lett. **106**, 145003 (2011).

Irregular flow of blood through a narrow arterial tube in presence of overlapping stenosis

By

Dr.Arun Kumar Maiti

Assistant Professor in Mathematics,

Shyampur Siddheswari Mahavidyalaya

Ajodhya, Howrah-711312

Email: dr.arun.maiti@gmail.com

Abstract:

The aim of the present study is to investigate the nature of blood flow through an arterial tube under overlapping stenotic condition. The expressions forFlux and resistance to flow with different stenosis height have been studied here by considering the blood as pseudo plastic power law type non-Newtonian fluid. The numerical results for various parameters are shown graphically and discussed.

Key Words: Overlapping Stenosis, flux, resistance to flow, power law fluid.

Introduction:

Blood flow related problems are quite different from all other fluid flow problems due to its unusual fluid properties, rhythmic action of heart valves and high Reynolds number of blood.So actual mathematical model of blood flow problems is unknown to us. Many Mathematicians have investigated some mathematical models to study the blood flow characteristics by considering the blood as Newtonian fluid under stenosed condition (Young [1], Lee and Fung [2], Shukla et. al [3]). But since blood consists of formed elements like red cells, white cells and platelets in an aqueous solution, blood behaves like a non-Newtonian fluid under certain conditions. So it is more appropriate to consider the blood as non-Newtonian fluid when it present as a mathematical model.

Blood flow characteristics can be altered significantly by the arterial diseases such as aneurysm and stenosis. Stenosis is a serious cardiovascular disease. Stenosis is formed by the deposition of fatty substances like fats/cholesterol in the lumen of the artery. If stenosis is formed, bore of the artery becomes narrow and so normal blood flow is disturbed abnormally whose consequences cause several diseases like stroke, hypertension, brain haemorrhage etc. some researchers have presented two layered mathematical models to study the haematocrit effects on blood flow (Mazumdar et. al. [4], Sanyal and Maiti [5], Sanyal and Sarkar [6]).

Few medical researchers have analysed mathematical models to discuss the effect of stenosis on blood flow by considering blood as various types of non-Newtonian fluid such as power law fluid, Herschel bulkley fluid, Casson fluid and Bingham-plastic type fluid (Richard et. al [7], Tu et. al [8], Siddiqui et. al [9], Biswas et. al. [10] and Kumar et. al. [11]. They have considered the effect of single stenosis. But since stenosis may have developed in series or in overlapping form, many researchers have studied the effect of overlapping stenosis on blood flow through an arterial tube by consider blood as non-Newtonian fluid (Chakraborty et. al. [12], Layek et. al. [13] and Srivastava et. al. [14]).

In the present analysis I have considered a mathematical model to study the non-Newtonian behaviour of blood in presence of overlapping arterial stenosis by considering blood as pseudo-plastic power law type fluid.

Mathematical Formulation:

Let us consider the steady flow of blood through an inelastic constricted arterial tube which is axially symmetric but radially non-symmetric.

The geometry of stenosis can be taken as [13]

$$h = \frac{R(z)}{R_0}$$

$$= 1 - \frac{3\delta}{2R_0 L_0^4}[11(z-d)L_0^3 - 47(z-d)^2 L_0^2 + 72(z-d)^3 L_0 - 36(z-d)^4],\ d \le z \le d + L_0$$

$$= 1, \text{ otherwise,} \qquad (1)$$

Where $R(z)$ is the radius of the tube in the stenotic region, R_0 is the radius of the tube outside the stenotic region, R_p is the radius in the plug flow region , L_0 is the length of the stenosis and d indicates its location, δ is the maximum height of the stenosis. Projection of stenosis at the two positions is denoted by z as $z = d + \frac{L_0}{6}$, $z = d + \frac{5L_0}{6}$. The critical height is taken as $\frac{3\delta}{4}$ at $z = d + \frac{L_0}{2}$ from the origin.

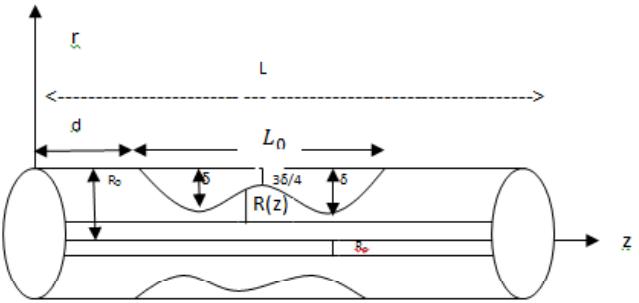

Fig.1: Geometry of a uniform tube of circular cross section with overlapping stenosis

The equation governing the flow is given by

$$-\frac{\partial p}{\partial z} = \frac{1}{r}\frac{\partial}{\partial r}(r\tau_{rz}), \qquad (2)$$

in which τ_{rz} represents the shear stress of blood for Bingham-plastic fluid and p is the pressure gradient.

The relationship between shear stress and shear rate is given by

$$\tau_{rz} = \mu(\frac{\partial u}{\partial r})^n \ , \tau_{rz} \geq \tau_0$$

$$\frac{\partial u}{\partial r} = 0 \qquad \tau_{rz} < \tau_0 \qquad (3)$$

Whereu standsfor the axial velocity of blood;τ_0, the yield stress and μ, the coefficient of viscosity of blood.

The boundary conditions are

$$\text{(i)}\tau_{rz} \text{ is finite at } r = 0$$

$$(ii) \ u = \text{at } r = h(z)$$

$$\text{(iii)}\frac{\partial u}{\partial r} = 0 \text{at} r = 0 \text{ if } \tau_{rz} < \tau_0 \qquad (4)$$

Solution:

Integrating (2) and using the boundary condition (i) of (4) we get

$$\tau_{rz} = \frac{Pr}{2}$$

For simplicity we take n = ½ in (3)

From (3) we get by using the boundary condition (ii) of (4)

$$u = \frac{P^2}{12\mu^2}(h^3 - r^3) \qquad (5)$$

Since $\frac{\partial u}{\partial r} = 0$ at $r = r_0$, the upper limit of the plug flow region is obtained as

$$r_0 = \frac{2\tau_0}{P}$$

The plug velocity u_p is given by

$$u_p = \frac{P^2}{12\mu^2}(h^3 - r_0^3) \qquad (6)$$

The volumetric flow rate i.e, the flux is given by

$$Q = 2\left[\int_0^{r_0} u_p r dr + \int_{r_0}^{h} ur dr\right]$$

$$= \frac{P^2 h^5}{12\mu^2}\left(1 - \frac{r_0^5}{h^5}\right) \qquad (7)$$

Thus

$$\frac{\partial p}{\partial z} = -P = \frac{-2\mu\sqrt{5Q}}{(h^5 - r_0^5)^{1/2}} \qquad (8)$$

The pressure drop Δp across the stenosis between z = 0 to z = L is obtained as

$$\Delta p = \int_0^L \frac{\partial p}{\partial z} dz$$

$$= -2\mu\sqrt{5Q}\int_0^L \frac{1}{(h^5 - r_0^5)^{1/2}} dz \qquad (9)$$

Introducing the following non-dimensional quantities we get

$$\bar{z} = \frac{z}{L}, \bar{\delta} = \frac{\delta}{R_0}, \bar{h}(z) = \frac{R(z)}{R_0}, \bar{Q} = \frac{Q}{\pi U R_0^2},$$

$$\bar{\tau_0} = \frac{\tau_0}{\mu U/R_0}, \overline{\tau_{rz}} = \frac{\tau_{rz}}{\mu U/R_0}, \bar{P} = \frac{P}{\mu UL/R_0^2}, \qquad (10)$$

in equation (9) we finally get (after dropping the bars)

$$\Delta p = \int_0^1 \frac{-2\mu\sqrt{5Q}}{(h^5 - r_0^5)^{1/2}} dz \qquad (11)$$

The resistance to flow λ is defined as

$$\lambda = \frac{\Delta p}{Q} = -\int_0^1 \frac{2\mu\sqrt{5Q}}{(h^5 - r_0^5)^{1/2} Q} dz \qquad (12)$$

The pressure drop in the absence of stenosis (h =1) is denoted by Δp_N and is obtained from (11) as

$$\Delta p_N = \int_0^1 \frac{-2\mu\sqrt{5Q}}{(1 - r_0^5)^{1/2}} dz \quad (13)$$

The resistance to flow in the absence of stenosis as

$$\lambda_N = \frac{\Delta p_N}{Q} = \int_0^1 \frac{-2\mu\sqrt{5Q}}{(1 - r_0^5)^{1/2} Q} dz$$

$$= \frac{-2\mu\sqrt{5Q}}{(1 - r_0^5)^{1/2} Q}$$

Hence the normalised resistance to flow $\bar{\lambda}$ is given by

$$\bar{\lambda} = \frac{\lambda}{\lambda_N} = (1 - r_0^5)^{1/2} \int_0^1 \frac{1}{(h^5 - r_0^5)^{1/2}} dz \qquad (14)$$

Results and discussions:

To illustrate the flow behaviour the results are shown graphically with the help of MATLAB-7.6.The numerical results are shown graphically and discussed for various values of the shape parameters.

Figures 2-4 represent variations of flux Q for the variation of stenosis length L_0, z and d with the variation of stenosis height δ. It is observed that Q decreases with the increase of ,$L_0$and$d$ for fixed values of the other parameters, but it increases when z increases as stenosis develops.

Figures 5-7 depict the variations of non -dimensional resistance to flow$\bar{\lambda}$ with the variations of stenosis height for different values ofL_0, d and z. It is found that as stenosis increases, resistance to flow $\bar{\lambda}$ increases with the increase of d but opposite phenomenon occurs when $L_0$and z increase.

Conclusions:

Blood flow characteristics mainly dependon flux and resistance to flow. It is clear that resistance to flow increases with the increase of stenosis height for which several cardiovascular diseases occur. So from clinical point of view this model may be helpful for further study of the medical researchers relating to blood flow problems.

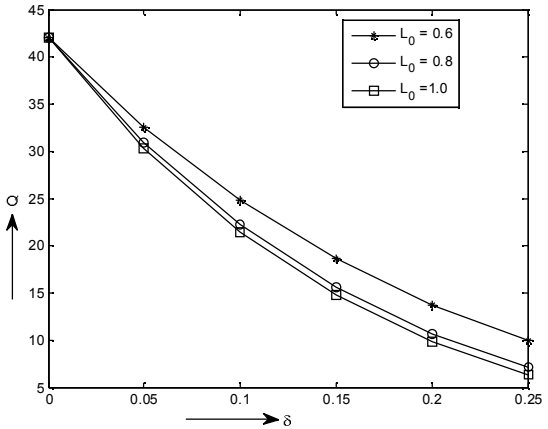

Figure -2

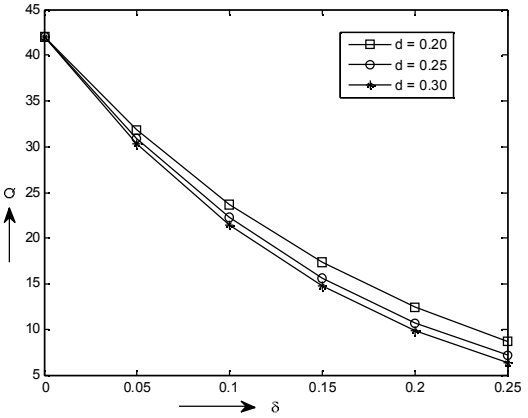

Figure -3

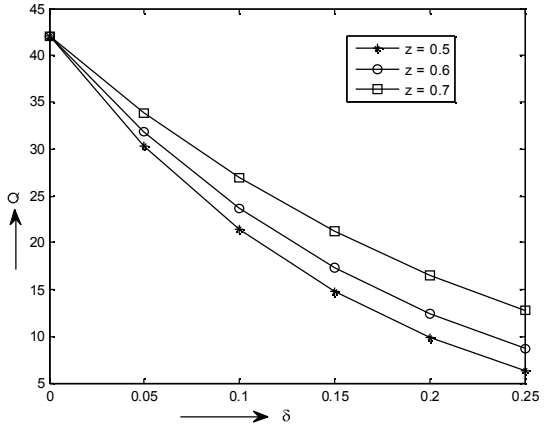

Figure – 4

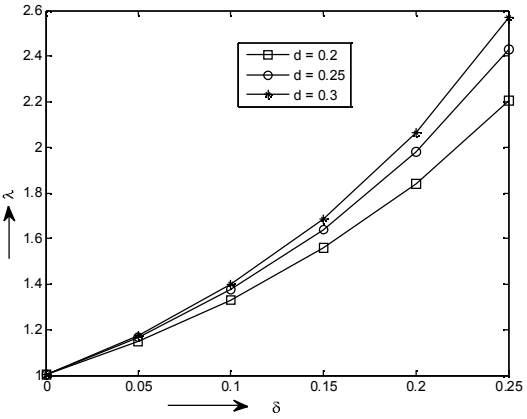

Figure – 5

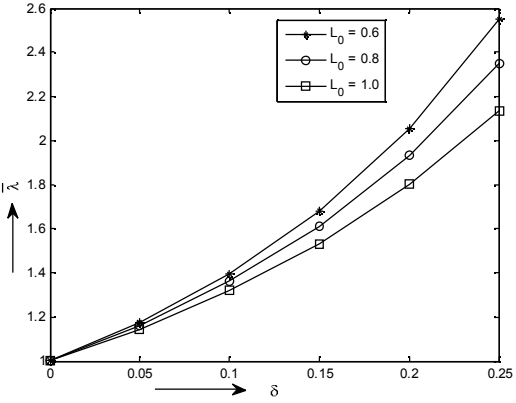

Figure – 6

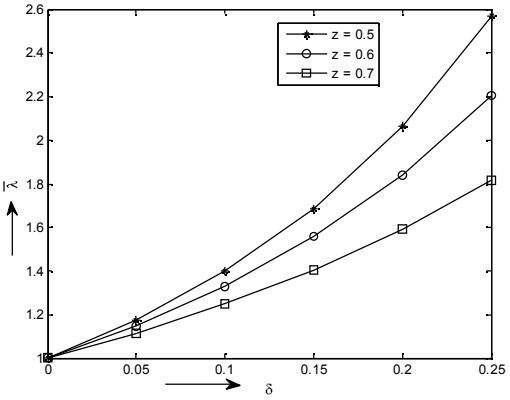

Figure – 7

References:

[1]. Young, D. F.: Effects of a time-dependency stenosis on flow through a tube, J. Engg.Ind., Trans ASME, Vol. 90, 248-254, (1968).

[2]. Lee, J. S. and Fung, Y. C.: Flow in locally constricted tubes and low Reynolds number, J. Appl. Mech., Trans ASME, Vol. 37, 9-16, (1970).

[3]. Shukla, J. B.., Parihar, R. S. and Rao, B. R. P.: Effects of stenosis on non-Newtonian flow through an artery with mild stenosis, Bull. Math.Biol., Vol. 42, 283-294, (1980).

[4]. Mazumdar, H. P., Habishyasi, U. N., Ghorai, S. and Roy, B. C. : On the consistency coefficient of a power- law flow of blood through narrow vessel, Engg. Trans. Polish Academy of Sciences, Institute of Fundamental Technological Research, Vol. 43, 373-382, (1995).

[5]. Sanyal, D. C. and Maiti, A. K. : On the consistency coefficient for Herschel Bulkley flow of blood through narrow arterial tube, ActacienciaIndica Vol. XXIIIM,(1), 57-64, (1997).

[6]. Maiti, A. K. and Sanyal, D. C. : Some characteristics of coefficient of viscosity for two layered power-law flow of blood through narrow vessel, Assam University Journal of Science and Technology, Vol. 8(II), 15-20, (2011).

[7]. Richard, L. K., Young, D. F.and Chalvin, N. R.: Wall vibrations induced by flow through simulated stenosis in Models and arteries, J. Biomech., Vol.10(431), (1977).

[8]. Tu, C. and Deville, M.: Pulsatile flow of non-Newtonian fluid through arterial stenosis, J. Biomech., Vol.29, 899-908, (1986).

[9]. Siddiqui, S. U., Verma, N. K. and Gupta, R.S.: A mathematical model for pulsatile flow of Herschel-Bulkley fluid through an stenosed arteries, Journal of science and technology, vol. 4(5), 49-66,(2010).

[10]. Biswas, D. and Laskar, R. B. : Steady flow of blood through a stenosed artery: A non-Newtonian fluid model, Assam University Journal of Sci and Tech. vol. 7(11), 144-153, (2011),

[11].Kumar, S. and Diwakar, C. : A Mathematical model of power-law fluid with an application of blood flow through an artery with stenosis, Advances in Applied Mathematical Biosciences vol. 4(2), 51-61, (2013).

[12]. Chakravarthy, S., Mandal, T. K.: Mathematical modelling of blood flow through an overlapping stenosis, Math. Compute. Model., Vol. 19,59-73, (1994).

[13].Layek, G. C. and Glora, R. S. R. : Unsteady viscous flow with various viscosity in a vascular tube with an overlapping constriction, Int. J. Engg. Sci. Vol. 47, 649-659, (2009).

[14]. Srivastava, V. P. and Rastogi, R. : Effects of haematocrit on impedance and shear stress during stenosed artery Catheterization, Applications and Applied Mathematics, Vol.4, 98-113, (2009).

A Probabilistic Approach to Analyze the Extinction Vulnerability of Prey and Predator

Bapi Saha *

September 10, 2016

Abstract

In this chapter discrete time Markov chain process is used in prey predator model. Here we have developed a method to find the probability of reaching the $(0, 0)$ before reaching any interior equilibrium. To validate the result we took two types of growth model of prey species, viz. θ-logistic and logistic. Here we have shown the effect of different parameters on that probability. We have also evaluated the stationary distribution for the dynamical system.

Keywords Predator Prey Model, Diffusion Process, Theta Logistic Model, Extinction, Stochastic Stability

*Government College of Engineering & Textile Technology, 1 Barrack Square, Berhampore, Email: bapi.math@gmail.com

1 Introduction

One of the major challenges in ecology is to predict the patterns in the risk of extinction of species from their demographic history and find the physical or behavioral features showing such patterns. Different demographic characteristics across wide range of taxa are extremely useful in identifying the "extinction vortices" [16] which describe the extinction pattern. Stochastic population models serve as fundamental mathematical framework in modern ecological theory and applied in various interdisciplinary research areas including population ecology [21], epidemiology [22], conservation biology [26] and many others. For example, discrete and continuous time Markov chain models and stochastic differential equation models are useful in many areas of population biology. In general the Kolmogorov differential equations (often termed as Master equation [7]) are developed to compute the transition probability distributions when the rates of different possible transitions are provided (e.g. birth and death rates). The equilibrium distribution may be obtained for large time by taking time sufficiently large.

The predator prey models governed by deterministic differential or difference equations play a crucial role in quantitative studies of the dynamics of natural populations. The dynamical characteristics of the systems, viz. stability of equilibrium points, stability of limit cycles etc. can be predicted uniquely in the deterministic set up. However, while applying these models in natural populations, it is more realistic to consider the stochastic dynamics of the system, where the randomness is generated either from variation among individual growth rates or due to environmental fluctuations. In such cases, the characteristics of the deterministic models are replaced by the probability statements. For example, in stochastic version of the logistic model, the equilibrium point is replaced by the equilibrium distribution, which is represented by the cloud points around the equilibrium point rather than a fixed value [31]. The main difference is that, in logistic growth, the carrying capacity is the only stable point, hence the population never reaches zero for positive value of intrinsic growth rate, whereas, in stochastic environment there is always a positive probability associated with the extinction of the population and thus making the stochastic model framework more appealing in real life scenarios [40, 42].

The interest in the stability of predator-prey system has long been a well discussed issue since the theoretical work of Lotka [27], Volterra [48] and the experimental work of [15]. Several studies have already been carried out on both deterministic and stochastic set up of predator prey dynamics. The probability of reaching to the stable interior equilibrium point is also important. Because once the

population size reaches stable point it remains there irrespective of time. Given a population size of prey and predator what amount of risk of extinction both the interacting population face, is an important aspect of population dynamics. Here the risk of extinction is quantified as the probability of reaching the extinction equilibrium, before reaching stable states [23, 44]. Recently [44] used the stochastic differential equation model including demographic stochasticity and predicted the time to extinction and probability of extinction for the Atlantic Herring populations. They have used the mean time to extinction from the distribution of the sojourn time that, the amount of time spent by the species at each population size given an initial abundance [20].

To incorporate the randomness in dynamical system mainly three types of stochastic models are used and they are discrete time Markov chain (DTMC) model, continuous time Markov chain (CTMC) model and stochastic differential equation (SDE) model. The DTMC models have already been applied to describe the stochastic dynamics of single species populations [4, 44]. In this chapter, rather than using diffusion approximation, we shall use the continuous time Markov chain model (CTMC) to predict the different extinction measures viz. expected extinction time and the probability of extinction given a starting population size. We shall also discuss the interplay between the deterministic and corresponding stochastic analogue of the predator prey system. The CTMC model is a popular stochastic modeling technique to answer various questions in ecology, invasion biology, species coexistence of single or multiple species [5]. We are interested to derive the persistence time of prey and predator separately. [3] has used the similar method in order to derive the persistence time for both of the populations.

In this chapter we have used DTMC process in prey-predator dynamical system to obtain the joint probability distribution of prey and predator and mean persistence time of the same. We have also developed a method to find the probability of reaching to the extinction before reaching to interior equilibrium. The stationary distribution is evaluated.

2 Background

We start our discussion in this section with a general predator prey system, where the different ecological mechanisms such as predation, death, birth etc. are modeled by general functions and eventually we shall show applications with specific examples with stipulated biological scenario. The approach will be applicable to populations of the same species or to populations of different species. Populations of the prey or predator species may differ, for example, by geographic location

or by interaction status of them. Consider the following prey-predator dynamical system,

$$\begin{aligned} \frac{\mathrm{d}x(t)}{\mathrm{d}t} &= b_1(x(t)) - d_1(x(t)) - g(x(t), y(t)) \\ \frac{\mathrm{d}y(t)}{\mathrm{d}t} &= \alpha g(x(t), y(t)) - d_2(y(t)) \end{aligned} \tag{1}$$

where $x(t)$, $y(t)$ denote the population densities of the prey and predator at time t respectively; $b_1(x)$ is the birth rate of the prey species; $d_i(.)(i = 1, 2)$ are the death rates (natural) of the prey and predator populations respectively. The initial conditions are being non-negative, $x(0) \geq 0, y(0) \geq 0$. The birth and death rates may be density dependent or density independent, described by the biological background of the two interacting species. The function $g(x, y)$ denotes the inter-specific interaction between the prey and predators, known as predator's functional response. α is the conversion efficiency of ingested prey into new predators and assumed to lie between 0 and 1.

The stochastic formulation of the single species dynamics in absence of predators are studied by several authors. Density dependent growth models, often mimicked by logistic and generalized logistic law of population dynamics have been elaborated in the above cited literatures. In absence of predators, model (1) reduces to a single species model with birth and death rates $b_1(x)$ and $d_1(x)$ respectively. Various stochastic formulations of the logistic model have been studied in the literature [28, 30, 29, 33, 34]. In general, there are infinitely many choices of functions available for birth and death rates for different choices of parameters. The choices of the functions are mainly driven by the collected data on the species under investigation [9]. In addition, while studying real populations, there is generally other information also available such as, life expectancy (hence the estimate of intrinsic growth rate). For example, in modeling the muskrat population dynamics in Netherlands, [30] used the estimate of average life expectancy to obtain the estimates of intrinsic rate parameters, that help them to uniquely chose the value of the rate parameters.

Model (1) serves as the deterministic skeleton in formulating analogous stochastic models that account for the variability in births, deaths, transmission and recovery. We derive a Continuous Time Markov Chain model (CTMC), where time is continuous but the random variables for the states are discrete. We shall represent eqn. (1) as a two dimensional birth-death process. In the stochastic formulation we assume $X(t)$ and $Y(t)$ are two discrete random variables representing the number of prey and predator populations respectively taking values in the state space $\{(x, y) : x = 0, 1, \ldots M; y = 0, 1, \ldots N\}$ where M and N are the maximum sustainable population size of prey and predator population respectively. Let the time step Δt be sufficiently small such that there can be a change in the population size of at most one, i. e. $\Delta X(t) = X(t + \Delta t) - X(t) \in \{-1, 0, 1\}$

and $\Delta Y(t) = Y(t+\Delta t) - Y(t) \in \{-1, 0, 1\}$. Thus the change in population size $\Delta X(t)$ and $\Delta Y(t)$ neglects multiple births, deaths, or transformations in time Δt which have probabilities of order $(\Delta t)^2$. The infinitesimal probabilities of the birth death formulation of model (1) is depicted in Table 2. For example, $(\Delta X(t), \Delta Y(t)) = (1, 0)$ denotes event of the birth of a prey and no change in predator abundance in time Δt, whose probability is equal to the product of the probabilities of one birth of prey $(b_1(x)\Delta t)$ and no death of predator $((1 - d_2(y)\Delta t))$. Similarly probabilities of the other events are defined.

Event	Transition	Transition probability
Prey birth and no birth or death of predator	$(x, y) \longrightarrow (x+1, y)$	$b_1(x)\Delta t(1 - d_2(y)\Delta t)$
One death of prey due to predation	$(x, y) \longrightarrow (x-1, y+1)$	$\alpha g(x, y)\Delta t$
No birth or death of prey and one death of predator	$(x, y) \longrightarrow (x, y-1)$	$d_2(y)\Delta t(1 - b_1(x)\Delta t)$
Death of one prey due to intra-species competition or predation and no birth or death of predator	$(x, y) \longrightarrow (x-1, y)$	$d_1(x)\Delta t + (1-\alpha)g(x, y)\Delta t$
No birth or death of either population	$(x, y) \longrightarrow (x, y)$	$1 - [b_1(x) + \alpha g(x, y) + d_2(y)$ $+d_1(x) + (1-\alpha)g(x, y)]\Delta t$

Table 1: Possible changes in the predator-prey densities with the corresponding probabilities

The transition probabilities defined in Table 2 which describes a continuous time Markov chain model for the random variables $X(t)$ and $Y(t)$ [20, 1, 5]. Note that, here the randomness in population growth rate is due to demographic stochasticity which is the chance variation in the number of individual births and deaths and usually modeled by using birth and death process. So in the CTMC, demographic stochasticity is the main source of variation affecting the population dynamics which becomes particularly important at low population sizes [10]. So the above model

does not depict the random variations in the environmental conditions although the environmental fluctuation has significant effect on the population dynamics, for example, effecting the survival and reproduction rates [25].

3 Derivation of joint probability distribution

In this section we will derive the joint probability distribution of prey and predator using the transition probabilities given in Table 2. The state of the system at time t can be characterized by the probability $p_{xy}(t)$ of having x individuals of prey and y individuals of predator, where (x, y) takes values in $\{0, 1, \ldots, M\} \times \{0, 1, \ldots, N\}$, in notation, $p_{xy}(t) = \mathbb{P}\{X(t) = x, Y(t) = y\}$. The probability of having the same number of individuals of both species at time $t+\Delta t$ can be obtained from the following equation.

$$\begin{aligned} p_{xy}(t+\Delta t) &= p_{x-1,y}(t)b_1(x-1)\Delta t + p_{x+1,y-1}(t)\alpha g(x+1,y-1)\Delta t + p_{x+1,y}(t) \\ &\quad [d_1(x+1) + (1-\alpha)g(x+1,y)]\,\Delta t + p_{x,y+1}(t)d_2(y+1)\Delta t + \\ &\quad [1 - (b_1(x) + g(x,y) + d_1(x) + d_2(y))\,\Delta t]p_{xy}(t) \\ &\quad \text{where} \quad 0 < x < M, 0 < y < N. \end{aligned}$$

In addition we will have the following cases

1. $p_{0y}(t+\Delta t) = p_{1,y-1}(t)\alpha g(1,y-1)\Delta t + p_{1y}(t)(d_1(1)+(1-\alpha)g(1,y))\Delta t + p_{0,y+1}(t)d_2(y+1)\Delta t + [1 - (b_1(0) + g(0,y) + d_1(0) + d_2(y))\Delta t]p_{0y}(t);\ 0 < y < N$

2. $p_{x0}(t+\Delta t) = p_{x-1,0}(t)b_1(x-1)\Delta t + p_{x1}(t)d_2(1)\Delta t + p_{x+1,0}[d_1(x+1) + (1-\alpha)g(x+1,0)]\Delta t + [1 - (b_1(x) + g(x,0) + d_1(x) + d_2(0))\Delta t]p_{x0}(t);\ 0 < x < M$

3. $p_{M0}(t+\Delta t) = p_{M-1,0}(t)b_1(M-1)\Delta t + p_{M1}(t)d_2(1)\Delta t + [1 - (b_1(M) + d_1(M))\Delta t]p_{M0}(t)$

4. $p_{0N}(t+\Delta t) = p_{1,N-1}(t)\alpha g(1,N-1)\Delta t + p_{1N}(t)(d_1(1)+(1-\alpha)g(1,N))\Delta t + (1-d_2(N)\Delta t)p_{0N}(t)$

5. $p_{MN}(t+\Delta t) = p_{M-1,Ns}(t)b_1(M-1)\Delta t + [1 - (b_1(M) + g(M,N) + d_1(M) + d_2(N))\Delta t]p_{MN}(t)$

6. $p_{00}(t+\Delta t) = p_{10}(t)d_1(1)\Delta t + p_{01}(t)d_2(1)\Delta t + p_{00}(t)$

7. $p_{My}(t+\Delta t) = p_{M-1,y}(t)b_1(M-1)\Delta t + [1 - (b_1(M) + g(M,y) + d_1(M) + d_2(y))\Delta t]p_{My}(t) + p_{M,y+1}(t)d_2(y+1)\Delta t;\ 0 < y < N;$

8. $p_{xN}(t+\Delta t) = p_{x-1,N}(t)b_1(x-1)\Delta t + p_{x+1,N-1}(t)\alpha g(x+1,N-1)\Delta t + p_{x+1,N}(t)[d_1(x+1) + (1-\alpha)g(x+1,N)]\Delta t + [1-(b_1(x)+g(x,N)+d_1(x)+d_2(N))\Delta t]p_{xN}(t);\ 0 < x < M;$

This system of equations generates the probability distribution of the prey and predator populations at time $t+\Delta t$ which can be obtained using numerical methods.

3.1 Marginal distribution of prey

In this section we denote the marginal distribution of the prey and predator populations by $p_{x.}$ and $p_{.y}$ respectively. Let $p_{x.}(t) = \mathbb{P}\{X(t) = x\}$ and $p_x^{ji} = \mathbb{P}\{X(t+\Delta t) = j | X(t) = i\}$.

$$\begin{aligned}
p_x^{i+1,i}(\Delta t) &= \mathbb{P}\{X(t+\Delta t) = i+1 | X(t) = i\} \\
&= \frac{\mathbb{P}\{X(t+\Delta t) = i+1 \cap X(t) = i\}}{\mathbb{P}\{X(t) = i\}} \\
&= \frac{\sum_k \mathbb{P}\{X(t+\Delta t) = i+1 \cap X(t) = i \cap Y(t) = k\}}{\sum \mathbb{P}\{X(t) = i \cap Y(t) = k\}} \\
&= \frac{\sum_k \mathbb{P}\{X(t) = i \cap Y(t) = k\}\,\mathbb{P}\{X(t+\Delta t) = i+1 | X(t) = i \cap Y(t) = k\}}{\sum \mathbb{P}\{X(t) = i \cap Y(t) = k\}} \\
&= \frac{\sum_k p_{ik} b_1(i)\Delta t}{\sum_k p_{ik}} \\
&= b_1(i)\Delta t
\end{aligned} \tag{2}$$

$$\begin{aligned}
p_x^{i-1,i}(\Delta t) &= \mathbb{P}\{X(t+\Delta t) = i-1 | X(t) = i\} \\
&= \frac{\mathbb{P}\{X(t+\Delta t) = i-1 \cap X(t) = i\}}{\mathbb{P}\{X(t) = i\}} \\
&= \frac{\sum_k \mathbb{P}\{X(t+\Delta t) = i-1 \cap X(t) = i \cap Y(t) = k\}}{\sum \mathbb{P}\{X(t) = i \cap Y(t) = k\}} \\
&= \frac{\sum_k \mathbb{P}\{X(t) = i \cap Y(t) = k\}\,\mathbb{P}\{X(t+\Delta t) = i-1 | X(t) = i \cap Y(t) = k\}}{\sum_k \mathbb{P}\{X(t) = i \cap Y(t) = k\}} \\
&= \frac{\sum_k p_{ik}\left(g(i,k) + d_1(i)\right)\Delta t}{\sum_k p_{ik}} \\
&= \left[\frac{\sum_k p_{ik} g(i,k)}{\sum_k p_{ik}} + d_1(i)\right]\Delta t
\end{aligned} \tag{3}$$

$$
\begin{aligned}
p_x^{ii}(\Delta t) &= \mathbb{P}\{X(t+\Delta t) = i | X(t) = i\} \\
&= \frac{\mathbb{P}\left\{X(t+\Delta t) = i \cap X(t) = i\right\}}{\mathbb{P}\{X(t) = i\}} \\
&= \frac{\sum_k \mathbb{P}\left\{X(t+\Delta t) = i \cap X(t) = i \cap Y(t) = k\right\}}{\sum \mathbb{P}\left\{X(t) = i \cap Y(t) = k\right\}} \\
&= \frac{\sum_k \mathbb{P}\{X(t) = i \cap Y(t) = k\} \mathbb{P}\left\{X(t+\Delta t) = i | X(t) = i \cap Y(t) = k\right\}}{\sum_k \mathbb{P}\left\{X(t) = i \cap Y(t) = k\right\}} \\
&= \frac{\sum_k p_{ik}\left(1 - (b_1(i) + g(i,k) + d_1(i))\,\Delta t\right)}{\sum_k p_{ik}} \\
&= \frac{\sum_k p_{ik}\left(1 - (b_1(i) + g(i,k) + d_1(i))\,\Delta t\right)}{\sum_k p_{ik}} \\
&= 1 - \left[b_1(i) + d_1(i) + \frac{\sum_k p_{ik} g(i,k)}{\sum_k p_{ik}}\right]\Delta t
\end{aligned} \tag{4}
$$

Hence we can write that,

$$
\begin{aligned}
p_x^{ji}(\Delta t) &= \lambda_1(i)\Delta t, \qquad i = j-1, j \in \{2, 3, \ldots, M\} \\
&= \lambda_2(i)\Delta t, \qquad i = j+1, j \in \{0, 1, \ldots, M-1\} \\
&= 1 - \lambda_3(i)\Delta t, \quad j = i, \qquad j \in \{0, 1, \ldots, M\} \\
&= 0 \qquad\qquad\qquad \text{otherwise}
\end{aligned} \tag{5}
$$

where

$$
\begin{aligned}
\lambda_1(i) &= b_1(i) \\
\lambda_2(i) &= d_1(i) + \frac{\sum_k p_{ik} g(i,k)}{\sum_k p_{ik}} \\
\lambda_3(i) &= b_1(i) + d_1(i) + \frac{\sum_k p_{ik} g(i,k)}{\sum_k p_{ik}}
\end{aligned} \tag{6}
$$

Then, $p_x.(t+\Delta t)$ satisfies the following difference equations,

$$
\begin{aligned}
p_x.(t+\Delta t) &= \lambda_1(x-1)\Delta t p_{x-1}.(t) + \lambda_2(x+1)\Delta t p_{x+1}.(t) + (1 - \lambda_3(x)\Delta t) p_x.(t) \\
p_0.(t+\Delta t) &= p_1.(t)\lambda_2(1)\Delta t + p_0.(t) \\
p_M.(t+\Delta t) &= \lambda_1(M-1)\Delta t p_{M-1}.(t) + (1 - \lambda_3(M)\Delta t) p_M.(t) \\
&\quad \text{where} \;\; x = 1, 2, \ldots, M-1
\end{aligned} \tag{7}
$$

The difference equations, project forward in time, can be expressed in matrix form as

$$
p_X(t+\Delta t) = P p_X(t), p_{x_0}(0) = 1
$$

where $p_X(t) = (p_0.(t), p_1.(t), \ldots, p_M.(t))^T$ and the matrix P is the one step transition matrix given by

$$P = \begin{pmatrix} 1 & \lambda_2(1)\Delta t & 0 & 0 & \ldots & 0 \\ 0 & 1-\lambda_3(1)\Delta t & \lambda_2(2)\Delta t & 0 & \ldots & 0 \\ 0 & \lambda_1(1)\Delta t & 1-\lambda_3(2)\Delta t & \lambda_2(3)\Delta t & \ldots & 0 \\ 0 & 0 & \lambda_1(2)\Delta t & 1-\lambda_3(3)\Delta t & \ldots & 0 \\ \vdots & \vdots & \vdots & \vdots & \vdots & \vdots \\ 0 & 0 & 0 & 0 & \ldots & \lambda_2(M)\Delta t \\ 0 & 0 & 0 & 0 & \ldots & 1-\lambda_3(M)\Delta t \end{pmatrix}$$

To ensure that P is a stochastic matrix (non-negative and column sum to 1) it is assumed that

$$\max_{x\in\{1,2,\ldots,M\}} \lambda_3(x)\Delta t \leq 1.$$

The equilibrium $(0, 0$ is the absorbing state, since, once the population reaches this state, the process stops. Thus, $p_{00}(\Delta t) = 1$. Eventually population extinction occur with probability 1 i.e $\lim_{t\longrightarrow\infty} p_0.(t) = 1$. Now as $\Delta t \longrightarrow 0$ the system of difference equations (7) reduces to

$$\begin{aligned} \frac{\mathrm{d}p_0.(t)}{\mathrm{d}t} &= p_1.(t)\lambda_2(1) \\ \frac{\mathrm{d}p_x.(t)}{\mathrm{d}t} &= \lambda_1(x-1)p_{x-1}.(t) + \lambda_2(x+1)p_{x+1}.(t) - \lambda_3(x)p_x.(t) \\ \frac{\mathrm{d}p_M.(t)}{\mathrm{d}t} &= \lambda_1(M-1)p_{M-1}.(t) - \lambda_3(M)p_M.(t) \end{aligned} \tag{8}$$

Following [35], a convenient notation for the system of equations (8) is given by

$$\frac{\mathrm{d}p}{\mathrm{d}t} = Ap$$

where A is given by

$$\begin{pmatrix} -\lambda_3(0) & \lambda_1(0) & 0 & \cdots & 0 \\ \lambda_2(1) & -\lambda_3(1) & \lambda_1(1) & \cdots & 0 \\ 0 & \lambda_2(2) & -\lambda_3(2) & \cdots & 0 \\ \vdots & \vdots & \vdots & \vdots & \vdots \\ 0 & 0 & 0 & \cdots & -\lambda_3(M) \end{pmatrix}$$

In absence of predators the above system of equations are well studied in the literature. For example, when the birth and death rates are governed by the logistic and power law logistic model, the associated equilibrium probability distributions are found in [28, 30]. In such cases, the analytical solutions of the differential equations can not be obtained, however, for small M, numerical

methods using Matlab or Mathematica [49] can be employed to solve the above systems of equations. [38] obtains a representation of the solution using Laplace transforms and continued fractions approximations. [2] studied the stochastic dynamics of the Allee effect in the context of invasion biology by suitable defining the birth and death process from the deterministic skeleton of the model depicting the Allee effect.

3.2 Marginal distribution of predator

We shall implement the same technique in order to find the marginal distribution of the predator populations, i.e.

$$p_y^{ji}(\Delta t) = \mathbb{P}\{Y(t+\Delta t) = j | Y(t) = i\}.$$

We have the following expressions for the marginal distributions of the predator.

$$\begin{aligned} p_y^{i+1,i}(\Delta t) &= \frac{\sum_k \mathbb{P}\{X(t)=k \cap Y(t)=i\}\mathbb{P}\{Y(t+\Delta t)=i+1 | X(t)=k \cap Y(t)=i\}}{\sum_k p_{ik}} \\ &= \frac{\sum_k p_{ki}\alpha g(k,i)\Delta t}{\sum_k p_{ik}} \\ &= \alpha\frac{\sum_k p_{ki} g(k,i)}{\sum_k p_{ki}})\Delta t \end{aligned}$$

$$\begin{aligned} p_y^{i-1,i}(\Delta t) &= \frac{\sum_k \mathbb{P}\{X(t)=k \cap Y(t)=i\}\mathbb{P}\{Y(t+\Delta t)=i-1 | X(t)=k \cap Y(t)=i\}}{\sum_k p_{ki}} \\ &= \frac{\sum_k p_{ki} d_2(i)\Delta t}{\sum_k p_{ki}} \\ &= d_2(i)\Delta t \end{aligned}$$

$$\begin{aligned} p_y^{ii}(\Delta t) &= \frac{\sum_k \mathbb{P}\{X(t)=k \cap Y(t)=i\}\mathbb{P}\{Y(t+\Delta t)=i | X(t)=k \cap Y(t)=i\}}{\sum_k p_{ki}} \\ &= \frac{\sum_k p_{ki}\left(1-(\alpha g(k,i)+d_3(i))\Delta t\right)}{\sum_k p_{ki}} \\ &= 1-\left[d_2(i)+\alpha\frac{\sum_k p_{ki} g(k,i)}{\sum_k p_{ki}}\right]\Delta t \end{aligned}$$

Therefore,

$$\begin{aligned} p_y^{ji}(\Delta t) &= \nu_1(i)\Delta t, && i=j-1, j\in\{1,2,\ldots,N\} \\ &= \nu_2(i)\Delta t, && i=j+1, j\in\{1,2,\ldots,N\} \\ &= 1-\nu_3(i)\Delta t, && j\in\{1,2,\ldots,N\} \\ &= 0 && \text{otherwise} \end{aligned}$$

where

$$\begin{aligned}\nu_1(i) &= \alpha\frac{\sum_k p_{ki}g(k,i)}{\sum_k p_{ki}}\\ \nu_2(i) &= d_2(i)\\ \nu_3(i) &= d_2(i)+\alpha\frac{\sum_k p_{ki}g(k,i)}{\sum_k p_{ki}}\end{aligned}$$

Then, $p_{\cdot y}(t+\Delta t)$ satisfies the following difference equations,

$$\begin{aligned}p_{\cdot y}(t+\Delta t) &= \nu_1(y-1)\Delta t p_{\cdot y-1}(t)+\nu_2(y+1)\Delta t p_{\cdot y+1}(t)+(1-\nu_3(y)\Delta t)p_{\cdot y}(t)\\ p_{\cdot 0}(t+\Delta t) &= p_{\cdot 1}(t)\nu_2(1)\Delta t+p_{\cdot 0}(t)\\ p_{\cdot N}(t+\Delta t) &= \nu_1(N-1)\Delta t p_{\cdot N-1}(t)+(1-\nu_3(N)\Delta t)p_{\cdot N}(t)\\ &\quad \text{where}\ \ y=1,2,\ldots,N-1\end{aligned} \tag{9}$$

The difference equations project forward in time and can be expressed in matrix form as

$$p_Y(t+\Delta t)=Pp_Y(t), p_{y_0}(0)=1$$

where $p_Y(t)=(p_{\cdot 0}(t),p_{\cdot 1}(t),\ldots,p_{\cdot N}(t))^T$ and the matrix P is the one step transition probability matrix given by

$$P=\begin{pmatrix}1 & \nu_2(1)\Delta t & 0 & 0 & \ldots & 0\\ 0 & 1-\nu_3(1)\Delta t & \nu_2(2)\Delta t & 0 & \ldots & 0\\ 0 & \nu_1(1)\Delta t & 1-\nu_3(2)\Delta t & \nu_2(3)\Delta t & \ldots & 0\\ 0 & 0 & \nu_1(2)\Delta t & 1-\nu_3(3)\Delta t & \ldots & 0\\ \vdots & \vdots & \vdots & \vdots & \vdots & \vdots\\ 0 & 0 & 0 & 0 & \ldots & \nu_2(N)\Delta t\\ 0 & 0 & 0 & 0 & \ldots & 1-\nu_3(N)\Delta t\end{pmatrix}$$

To ensure that P is a stochastic matrix (non-negative and column sum to 1) it is assumed that

$$\max_{y\in\{1,2,\ldots,N\}}\nu_3(y)\Delta t\leq 1.$$

In this case also $(0,0)$ is the absorbing state and hence $p_{00}(\Delta t)=1$. and eventually population extinction occur with probability 1 i.e $\lim_{t\longrightarrow\infty}p_0(t)=1$. Taking $\Delta t\longrightarrow 0$ the system of difference equations (9) reduces to

$$\begin{aligned}
\frac{\mathrm{d}p_{\cdot 0}(t)}{\mathrm{d}t} &= p_{\cdot 1}(t)\mu_2(1) \\
\frac{\mathrm{d}p_{\cdot y}(t)}{\mathrm{d}t} &= \mu_1(y-1)p_{\cdot y-1}(t) + \mu_2(y+1)p_{\cdot y+1}(t) - \mu_3(y)p_{\cdot y}(t) \\
\frac{\mathrm{d}p_{\cdot N}(t)}{\mathrm{d}t} &= \mu_1(N-1)p_{\cdot N-1}(t) - \mu_3(N)p_{\cdot N}(t)
\end{aligned} \tag{10}$$

4 Derivation of difference equation for persistence time of prey

The persistence time of the prey and predator populations may be defined as either the time when both the population numbers are zero or the time when the prey population size is zero. Let T be the random variable for the time until population extinction. It is to be noted that the distribution of T depends on the initial population size, and hence we shall denote this dependence by T_{x_0}. Let τ_{x_0} denote the expected time until extinction occur when initial population size is x_0 i.e. $\mathbb{E}(T_{x_0}) = \tau_{x_0}$. The mean persistence time for the DTMC model satisfies the following difference equations:

$$\tau_x = \lambda_1(x)\Delta t(\tau_{x+1} + \Delta t) + \lambda_2(x)\Delta t(\tau_{x-1} + \Delta t) + (1 - \lambda_3(x)\Delta t)(\tau_x + \Delta t) \tag{11}$$

where $x = 1, 2, \ldots M$. This difference equations can be simplified as

$$\lambda_2(x)\tau_{x-1} - \lambda_3(x)\tau_x + \lambda_1(x)\tau_{x+1} = -1 \tag{12}$$

Equation (12) can be written in the matrix form as $D\tau = -\mathbf{1}$, where $\mathbf{1} = (1, \ldots, 1)^T$ and

$$D = \begin{pmatrix}
-\lambda_3(1) & \lambda_1(1) & 0 & \ldots & 0 & 0 \\
\lambda_2(2) & -\lambda_3(2) & \lambda_1(2) & \ldots & 0 & 0 \\
\vdots & \vdots & \vdots & \vdots & \vdots & \vdots \\
0 & 0 & 0 & \ldots & \lambda_2(M) & -\lambda_3(M)
\end{pmatrix}$$

The solution for the mean persistence time is given by $\tau = D^{-1}\mathbf{1}$, where the inverse always exists. The matrix D is irreducibly diagonally dominant, hence nonsingular. The persistence time of predator can also be found using similar technique. The difference equation to evaluate the persistence time takes the form of a differential equation for continuous processes, where the stochastic growth equations are described by diffusion process. For example, in a single population dynamics

of population size N, the diffusion process is characterized by the infinitesimal mean $\mu(N)$ and infinitesimal variance $\sigma^2(N)$. Then, starting from a given initial population size $N = N_0$, the mean time to extinction, $T(N_0)$ is the solution of the equation

$$\frac{1}{2}\sigma^2(N_0)\frac{\mathrm{d}^2T}{\mathrm{d}N_0^2} + \mu(N_0)\frac{\mathrm{d}T}{\mathrm{d}N_0} = -1$$

with the boundary conditions $T(1) = 0$ and a reflecting boundary at the maximum population size K [24].

5 Simultaneous Extinction probability

In this section we derive the expression for the simultaneous extinction probability of prey and predator or the joint distribution of the probability of the extinction time of the prey and predator. Let $T_x(s)$ be the first passage time of the random variable X to the value s and $T_y(s)$ be the first passage time of the random variable Y to the point s. This is also known as persistent time or the first exit time in engineering literature. Thus the event $\{T_x(0) < T_x(M)\}$ represents the event that starting with population size x, prey goes to extinction before reaching its maximum population size M. We define

$$u(x,y) = \mathbb{P}\left\{T_x(0) < T_x(M), T_y(0) < T_y(N) | X(0) = x, Y(0) = y\right\} \tag{13}$$

Therefore

$$\begin{aligned} u(x,y) &= \Sigma_{\Delta x}\Sigma_{\Delta y}\mathbb{P}\left\{T_x(0) < T_x(M), T_y(0) < T_y(N)\right., \\ &\quad \left. X(0+\Delta t) = x + \Delta x, Y(0+\Delta t) = y + \Delta y | X(0) = x, Y(0) = y\right\} \end{aligned} \tag{14}$$

From [20], it can be shown that

$$u(x,y) = \mathbb{E}\left[u(X(\Delta t), Y(\Delta t)) | X(0) = x, Y(0) = y\right]$$

Now,

$$\begin{aligned} u(x+\Delta x, y+\Delta y) &= u(x,y) + \Delta x\frac{\partial u}{\partial x} + \Delta y\frac{\partial u}{\partial y} + \frac{1}{2}(\Delta x)^2\frac{\partial^2 u}{\partial x^2} + \Delta x\Delta y\frac{\partial^2 u}{\partial x \partial y} \\ &\quad + \frac{1}{2}\frac{\partial^2 u}{\partial y^2}(\Delta y)^2 \end{aligned}$$

Taking expectation in both sides

$$\begin{aligned} u(x,y) = u(x,y) \quad + \quad & \mathbb{E}(\Delta x)\frac{\partial u}{\partial x} + \mathbb{E}(\Delta y)\frac{\partial u}{\partial y} + \frac{1}{2}\mathbb{E}(\Delta x)^2\frac{\partial^2 u}{\partial x^2} \\ & + \mathbb{E}(\Delta x \Delta y)\frac{\partial^2 u}{\partial x \partial y} + \frac{1}{2}\frac{\partial^2 u}{\partial y^2}\mathbb{E}(\Delta y)^2 \end{aligned}$$

Using the equation (1), we obtain the following equation

$$\begin{aligned} 0 \quad = \quad & [b_1(x) - g(x,y) - d_1(x)]\frac{\partial u}{\partial x} + [\alpha g(x,y) - d_2(y)]\frac{\partial u}{\partial y} \\ & + \frac{1}{2}[b_1(x) + \alpha g(x,y) + d_1(x)]\frac{\partial^2 u}{\partial x^2} - \alpha g(x,y)\frac{\partial^2 u}{\partial x \partial y} \\ & + \frac{1}{2}[\alpha g(x,y) + d_2(y)]\frac{\partial^2 u}{\partial y^2} \end{aligned}$$

Now replacing the coefficients of $\frac{\partial u}{\partial x}$ and $\frac{\partial u}{\partial y}$ by $\frac{\mathrm{d}x}{\mathrm{d}t}$ and $\frac{\mathrm{d}y}{\mathrm{d}t}$ respectively, by virtue of the equation (1), and noting that, $\frac{\partial u}{\partial t} = \frac{\partial u}{\partial x}\frac{\mathrm{d}x}{\mathrm{d}t} + \frac{\partial u}{\partial y}\frac{\mathrm{d}y}{\mathrm{d}t}$, we obtain the following partial differential equation

$$\begin{aligned} 0 \quad = \quad & \frac{\partial u}{\partial t} + \frac{1}{2}[b_1(x) + \alpha g(x,y) + d_1(x)]\frac{\partial^2 u}{\partial x^2} - \alpha g(x,y)\frac{\partial^2 u}{\partial x \partial y} \\ & + \frac{1}{2}[\alpha g(x,y) + d_2(y)]\frac{\partial^2 u}{\partial y^2} \end{aligned}$$

Therefore the above expression can be written as

$$\begin{aligned} \frac{\partial u}{\partial t} \quad = \quad & -\frac{1}{2}\left[b_1(x) + \alpha g(x,y) + d_1(x)\right]\frac{\partial^2 u}{\partial x^2} + \alpha g(x,y)\frac{\partial^2 u}{\partial x \partial y} \\ & -\frac{1}{2}\left[\alpha g(x,y) + d_2(y)\right]\frac{\partial^2 u}{\partial y^2} \end{aligned} \tag{15}$$

To compute the first passage probabilities given the size of prey and predator, the above equation is solved numerically. The numerical scheme is depicted in the Appendix. We now proceed to develop appropriate boundary conditions for the above differential equation. We have,

$$u(x,y) = \mathbb{P}\left\{T_x(0) < T_x(M), T_y(0) < T_y(N) | X(0) = x, Y(0) = y\right\}$$

Therefore

$$\begin{aligned} u(0,y) \quad &= \quad \mathbb{P}\left\{T_x(0) < T_x(M), T_y(0) < T_y(N) | X(0) = 0, Y(0) = y\right\} \\ &= \quad g(0,y) = 1 \end{aligned} \tag{16}$$

$g(0,y) = 1$, because, from biological point of view, if there is no prey available in the system then predator will die out. From the basic model also it is clear that, predator survives only by predating

on the prey and no additional food source is available. Also,

$$\begin{aligned} u(x,0) &= \mathbb{P}\{T_x(0) < T_x(M), T_y(0) < T_y(N) | X(0) = x, Y(0) = 0\} \\ &= \mathbb{P}\{T_x(0) < T_x(M) | X(0) = x\} \\ &= f(x) \quad \text{say} \end{aligned} \tag{17}$$

The function $f(x)$ is given by

$$\begin{aligned} f(x) &= \frac{\int_x^M \exp[-\phi(u)]\mathrm{d}u}{\int_0^M \exp[-\phi(u)]\mathrm{d}u} \qquad \text{where} \\ \phi(u) &= 2\int \frac{b(u)-d(u)}{b(u)+d(u)}\mathrm{d}u \end{aligned}$$

Now

$$\begin{aligned} u(M,y) &= \mathbb{P}\{T_x(0) < T_x(M), T_y(0) < T_y(N) | X(0) = M, Y(0) = y\} \\ &= 0, \quad \text{because} \quad \mathbb{P}\{T_x(0) < T_x(M) | X(0) = M\} = 0 \end{aligned} \tag{18}$$

$$\begin{aligned} u(x,N) &= \mathbb{P}\{T_x(0) < T_x(M), T_y(0) < T_y(N) | X(0) = x, Y(0) = N\} \\ &= 0, \quad \text{because} \quad \mathbb{P}\{T_y(0) < T_y(N) | Y(0) = N\} = 0 \end{aligned} \tag{19}$$

6 Application to predator-prey models

6.1 Logistic growth Model

For illustration we first consider the logistic model for the prey growth process. The stochastic logistic model is a basic model, described by nonlinear birth and death rates, widely applied in ecology and epidemiological studies [40, 33]. The deterministic logistic growth model is depicted by the differential equation

$$\frac{1}{x(t)}\frac{\mathrm{d}x(t)}{\mathrm{d}t} = r_m\left(1 - \frac{x(t)}{K}\right) \tag{20}$$

with the initial condition $X(0) = x_0$. In the equation, r_m is the intrinsic growth rate and K is the carrying capacity of the environment. There exists a unique solution $x(t)$ with $\lim_{t\to\infty} x(t) = K$. The stochastic version of the logistic model was studied by many other authors and several approximation methods are available to study the behavior of the equilibrium distribution in terms of moments and cumulants of the stationary distribution [8, 28, 21, 39, 41]. It is common technique

to include demographic stochasticity in deterministic models, where the differential equation is decomposed into birth and death rates by suitably defining the birth and death functions $b_1(x)$ and $d_1(x)$ respectively. The different $b_1(x) - d_1(x)$ recovers the original differential equation. The quantities $b(x)_1\Delta t$ and $d(x)_1\Delta t$ are the probability of birth and death for a single individual, in a population of size x, in the time interval t to $t + \Delta t$. For example, [28, 39] considered the birth process as $b_1(x) = a_1x - c_1x^2$ and death process as $d_1(x) = a_2x + c_2x^2$ to describe stochastic logistic model, where a_i's and c_i's are defined as intrinsic growth rates. The model was studied by [29] to model the annual catch of an invasive maskrats in eleven Dutch provinces between 1968 to 1991, and the rapid colonization of Africanized honey bees of North and South America [28, 30]. Several authors have studied the stochastic analogue of the logistic model using CTMC, DTMC and diffusion processes (see [4] and other references therein).

To study the interactive dynamics of predator and prey, we consider the following system of equations for the predator prey model.

$$\begin{aligned} \frac{\mathrm{d}x(t)}{\mathrm{d}t} &= rx(t)\left(1 - \frac{x(t)}{K}\right) - \frac{ax(t)y(t)}{1 + ahx(t)} \\ \frac{\mathrm{d}y(t)}{\mathrm{d}t} &= \alpha\frac{ax(t)y(t)}{1 + ahx(t)} - dy(t) \end{aligned} \tag{21}$$

where $x(t)$ and $y(t)$ represents the prey and predator abundance at time t. We also assume that the prey with no predators grows logistically to its environmental capacity K, with an intrinsic birth rate constant r. The per capita rate at which predator $y(t)$ captures prey $x(t)$ is represented by the term $\frac{ax}{1+ahx}$ which gets labeled off to a at higher densities of the prey. The type II functional response is the simplest expression that takes into account the time taken for predators to locate and consume (handle) their prey. The type II functional response is classically associated with specialist predators [47]. $1/h$ is the maximum intake rate at which predator gets saturated [18]. α is the conversion efficiency and d is the natural mortality of the predator. Before going into the stochastic description of the system (21), we describe some basic dynamical properties of the system, that will help us to explain the system dynamics in different parameter spaces. This model was studied by many authors.

6.2 Theta logistic model

In most of the prey-predator systems the growth process of prey populations are assumed to follow the logistic growth process. The logistic model assumes a linear decline in the per capita growth rate with abundance (often called $r - n$ curve). Both theoretical and empirical work have shown

that, in general, for natural populations the $r-n$ curve is concave upward [45, 12]. After studying the laboratory fruit fly populations [17] were led to add a shape parameter θ heuristically to the growth term in logistic model, such that;

$$\frac{1}{x(t)}\frac{\mathrm{d}x(t)}{\mathrm{d}t} = r_m\left[1-\left(\frac{x(t)}{K}\right)^{\theta}\right] \tag{22}$$

which resulted in the theta-Ricker or theta-logistic model [17, 46]. The parameter θ reflects how abruptly growth slows as abundance interacts with resource availability [13, 45] and type of competition [19]. For concave ($\theta < 1$), nature of the growth response ideally characterizes a population unable to recover quickly from extrinsic perturbations. In case of a convex ($\theta > 1$) growth process the density feed back occurs mainly above some (relatively large) threshold abundance [12, 36], which generally happens in case of the population dynamics of large mammals [32, 36]. For this model we have to identify the birth rate $b_1(x)$ and death rate $d_1(x)$. In case of θ-logistic model many forms of birth rate and death rates are available [30]. Here we consider the form of $b_1(x)$ and $d_1(x)$ as follows,

$$b_1(x) = a_1x - c_1x^{\theta+1} \qquad \text{and} \qquad d_1(x) = a_2x + c_2x^{\theta+1}$$

respectively, called power law logistic model. The a_i are "intrinsic rate" and c_i are the "crowding coefficients". The birth rate and death rate for logistic model can be obtained from that of θ-logistic by putting $\theta = 1$.

In most of the cases we consider the idealized linear interactions which is basically a valid first order approximation of more general interaction. Due to unavoidable heterogeneity exact fit is not expected in testing the linear model with biological data [17]. In fact the study of seven Drosophila systems has confirmed the inadequacy of the Lotka-Volterra model [6]. The theta-logistic model was successfully used in a predator-prey interaction of the Serengeti wildebeest population to approximate the curvilinear density-dependent response. Different versions of the type II functional responses were utilized to study the evidence of group formation in the prey and predator [14]. We consider the following differential equation to describe the interactive predator-prey dynamics.

$$\begin{aligned}\frac{\mathrm{d}x(t)}{\mathrm{d}t} &= rx(t)\left[1-\left(\frac{x(t)}{K}\right)^{\theta}\right] - \frac{ax(t)y(t)}{1+ahx(t)}\\ \frac{\mathrm{d}y(t)}{\mathrm{d}t} &= \alpha\frac{ax(t)y(t)}{1+ahx(t)} - dy(t)\end{aligned} \tag{23}$$

6.3 Stability analysis of equilibrium

Equating $\frac{\mathrm{d}x(t)}{\mathrm{d}t} = 0$ and $\frac{\mathrm{d}y(t)}{\mathrm{d}t} = 0$ we get the interior equilibrium point as

$$\begin{aligned} x^* &= \frac{d}{a(\alpha - dh)} \\ y^* &= \frac{r\alpha}{a(\alpha - dh)}\left[1 - \left(\frac{x^*}{K}\right)^{\theta}\right] \end{aligned}$$

The jacobian matrix at (x^*, y^*) is given by

$$J = \begin{bmatrix} r\left(\frac{dh}{\alpha} - \left(\theta + \frac{dh}{\alpha}\right)\left(\frac{x^*}{K}\right)^{\theta}\right) & -\frac{d}{\alpha} \\ r(\alpha - dh)\left(1 - \left(\frac{x^*}{K}\right)^{\theta}\right) & 0 \end{bmatrix}$$

Now from Routh-Hurwitz's criteria the interior equilibrium will be stable if $\mathrm{tr}(J) < 0$ and $\det(J) > 0$. So in this case the interior equilibrium point will be locally asymptotically stable if

$$\left[\frac{dh}{\alpha} - \left(\theta + \frac{dh}{\alpha}\right)\left(\frac{x^*}{K}\right)^{\theta}\right] < 0 \tag{24}$$

which can be simplified to obtain

$$\left(\frac{dh}{\alpha\theta + dh}\right)^{\frac{1}{\theta}} < \frac{d}{ak(\alpha - dh)}$$

The other equilibrium points are $(K, 0)$ and $(0, 0)$. The jacobian matrix for $(0, 0)$ is

$$J\big|_{(0,0)} = \begin{bmatrix} r & 0 \\ 0 & -d \end{bmatrix}$$

Now for this $\det(J) = -rd < 0$. So $(0, 0)$ is always unstable. Again for boundary equilibrium $(K, 0)$ the jacobian matrix is

$$J\big|_{(K,0)} = \begin{bmatrix} -r\theta & -\frac{aK}{1+haK} \\ 0 & \frac{\alpha aK}{1+haK} - d \end{bmatrix}$$

It is easy to show that the boundary equilibrium point $(K, 0)$ will be stable if $\frac{\alpha aK}{1+haK} < d$. If we put $\theta = 1$, then the stability conditions for the equilibrium points of model (21) follows directly.

To study the stochastic dynamics, we have chosen the parameter values as $r = 1$, $K = 20$, $a = 1$, $H = 1$, $\theta = 0.8$ in eqn. (23). Figure 3 shows the stationary distribution of prey and predator populations. The effect of parameters θ, K and h on the probability of extinction. If the value of K is increased then the probability of extinction decreases. A similar changes in extinction probability is found with respect to the handling time as well.

We have evaluated the marginal stationary distribution following the method of [37] for different choices of the model parameters. It is observed from figure 1(a) that, as the carrying capacity of prey increases, probability of extinction decreases. This means that, the stability of the system increases under the stochastic set up, which is contrary to the conclusion obtained by [43] under the deterministic model set up. [43] showed that, there is a critical threshold for K at which the equilibrium becomes unstable through a Hopf bifurcation and stable limit cycle emerges. However, under the stochastic set up, the probability of extinction tends to diminish for very large K and does not generate such bifurcation phenomena. Nature of probability of extinction with varying θ is depicted in figure 1(c).

6.4 Quasi-stationary

An important aspect of the dynamical system is the quasi stationarity. If the deterministic rate equation has at least one stable fixed point,the system approaches a quasi stationary state with a time independent distribution; this is called the Quasi stationary Distribution [8, 35]. In case of single species model the quasi stationary distribution is obtained from the probability $p_c(n,t)$, that of finding n individuals at time t, conditioned on the fact that fact that extinction has not occurred yet:

$$p_c(n,t) = \frac{p(n,t)}{1-p(0,t)} \tag{25}$$

In the present analysis we obtain the quasi stationary distribution for marginal probability distribution. In case of prey population the quasi stationary distribution resembles normal distribution (Fig. 2(a)). When it comes to predator population the pdf of quasi stationary distribution sharply decline with increase in predator population (Fig. 2(b)).

6.5 Allee growth dynamics

We have studied the following Allee effect model in this manuscript.

$$\frac{dx}{dt} = rx(x-A)\left(1-\frac{x}{K}\right) - \frac{axy}{1+ahx} \tag{26}$$

$$\frac{dy}{dt} = \frac{\alpha axy}{1+ahx} - dy \tag{27}$$

where, $x(t)$ and $y(t)$ stands for population densities of prey and predator over time t. r is the intrinsic growth rate and the Allee effect is characterized by A. Allee effect is strong or weak that depends on where $A > 0$ or $A \leq 0$ respectively. There are several mathematical models

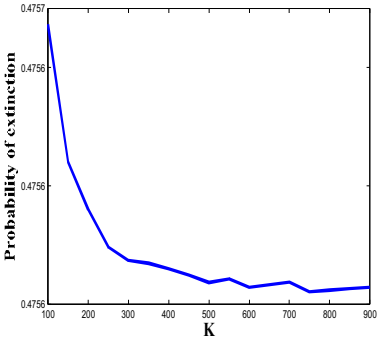

(a) Carrying capacity K vs probability of extinction.

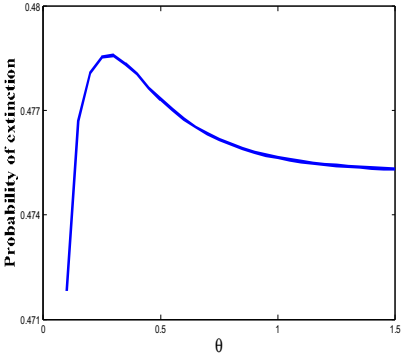

(b) θ vs probability of extinction.

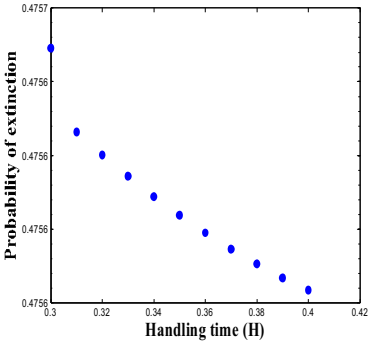

(c) handling time vs probability of extinction.

Figure 1: The parameters are $r = 0.5$, $\theta = 0.8$, $K = 20$,$d = 0.8$,$a = 0.1$,$\alpha = 0.5$, $H = 0.3$.

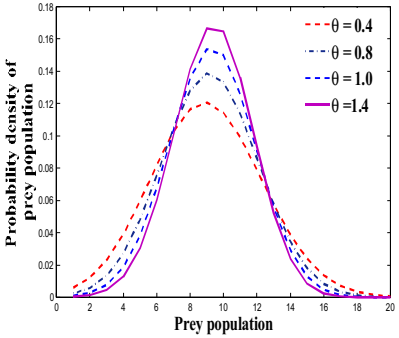

(a) The quasi-stationary probability distribution of prey population for different values of θ time.

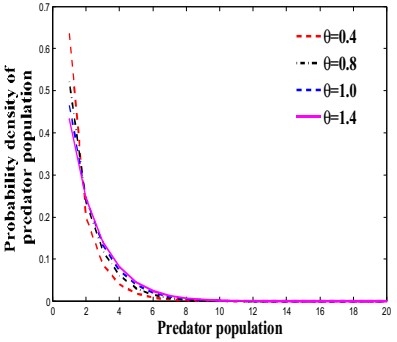

(b) The quasi-stationary probability distribution of predator for different values of θ time.

Figure 2: The parameters are $\alpha = 0.5$, $r = 1$, $\theta = 0.8$, $K = 20$,$d = 0.8$,$a = 0.1$, $H = 0.3$.

are available to describe Allee effect [10]. The other parameters are already explained in the previous sections. In the model with Allee effect, the stochastic effects increase the probability of extinction above the Allee threshold, but decrease the probability of extinction below the critical threshold [11] and the stationary distribution of the population abundance is characterizes by a bimodal distribution [44]. [2] studied how stochastic variability coupled with an Allee effect impact species invasion success in a multi-patch system. We first study the linear stability analysis of the equilibrium points to understand basic dynamical features of the deterministic model. Let, $f_1(x,y) = rx(x-A)\left(1-\frac{x}{K}\right) - \frac{axy}{1+ahx}$ and $f_2(x,y) = \frac{\alpha axy}{1+ahx} - dy$.

$$\begin{aligned}
\frac{\partial f_1}{\partial x} &= r(x-A)\left(1-\frac{x}{K}\right) + rx\left(1-\frac{x}{K}\right) - \frac{r}{K}x(x-A) - \frac{ay}{(1+ahx)^2} \\
\frac{\partial f_1}{\partial y} &= -\frac{ax}{1+ahx} \\
\frac{\partial f_2}{\partial x} &= \frac{\alpha ay}{(1+ahx)^2} \\
\frac{\partial f_2}{\partial y} &= \frac{\alpha ax}{1+ahx} - d
\end{aligned}$$

The equilibrium points of the system 26 is $(0,0)$, $(A,0)$, $(K,0)$ and the interior equilibrium is given by (x^*, y^*) where

$$x^* = \frac{d}{a(\alpha - dh)} \tag{28}$$

and

$$y^* = \left(\frac{\alpha r}{a^3 K(\alpha - dh)^3}\right)(d - Aa(\alpha - dh))\,(Ka(\alpha - dh) - d) \tag{29}$$

At the boundary equilibria $(0,0)$, the jacobian matrix takes the form

$$J\Big|_{(0,0)} = \begin{pmatrix} -ra & 0 \\ 0 & -d \end{pmatrix}$$

with eigenvalues $\lambda_1 = -rd$ and $\lambda_2 = -d < 0$. Hence $(0,0)$ is locally asymptotically stable. At the boundary equilibrium point $(A,0)$, the jacobian matrix takes the form

$$J\Big|_{(A,0)} = \begin{pmatrix} rA\left(1-\frac{A}{K}\right) & -\frac{aA}{1+ahA} \\ 0 & \frac{\alpha aA}{1+ahA} - d \end{pmatrix}$$

with eigenvalues $\lambda_1 = rA\left(1-\frac{A}{K}\right) > 0$ and $\lambda_2 = \frac{\alpha aA}{1+ahA} - d$. So $(A,0)$ is unstable if $\frac{\alpha aA}{1+ahA} > d$ and a saddle if $\frac{\alpha aA}{1+ahA} < d$. The jacobian matrix at $(K,0)$ is of the form

$$J\Big|_{(K,0)} = \begin{pmatrix} -r(K-A) & -\frac{aK}{1+ahK} \\ 0 & \frac{\alpha aK}{1+ahK} - d \end{pmatrix}$$

with eigenvalues $\lambda_1 = -r(K-A) < 0$ (since $K > A$) and $\lambda_2 = \frac{\alpha a K}{1+ahK} - d$. So $(K, 0)$ is locally asymptotically stable if $\frac{\alpha a K}{1+ahK} < d$. At the interior equilibria (x^*, y^*), the jacobian matrix takes the form,

$$J\Big|_{(x^\star, y^\star)} = \begin{pmatrix} g(x^*, y^*) & -\frac{ax^\star}{1+ahx^\star} \\ \frac{\alpha a y^\star}{(1+ahx^\star)^2} & \frac{\alpha a x^\star}{1+ahx^\star} - d \end{pmatrix}$$

where

$$g(x^*, y^*) = r(x^* - A)\left(1 - \frac{x^*}{K}\right) + rx^*\left(1 - \frac{x^*}{K}\right) - \mathfrak{r}Kx^*(x^* - A) - \frac{ay^*}{(1+ahx^*)^2} \quad (30)$$

Now for interior equilibrium $\frac{\alpha a x^\star}{1+ahx^\star} - d = 0$. The eigenvalues are given by the equation, $\lambda^2 - \lambda g(x^*, y^*) + \frac{\alpha a^2 x^\star y^\star}{(1+ahx^\star)^3}$. The sufficient condition for stability is, $g(x^*, y^*) < 0$ and $\frac{\alpha a^2 x^\star y^\star}{(1+ahx^\star)^3} > 0$. But $\frac{\alpha a^2 x^\star y^\star}{(1+ahx^\star)^3}$ is always greater than 0. So the sufficient condition reduces to $g(x^*, y^*) < 0$. where g is given in (30).

To study the quasi-stationary distribution of the population size, we have considered the birth-death process with birth and death rates are defined as,

$$b(x) = \frac{r(A+K)}{K^2}x^2\left(1 - \frac{x}{A+K}\right) \text{ and} \quad (31)$$

$$d(x) = \frac{rA}{K}x \quad (32)$$

We have also shown the effect of different relevant parameters associated with the model.

7 Result and Discussion

In this paper we develop the method to find the probability of reaching the extinction equilibrium $(0, 0)$ before reaching to any other coexisting states of both of the population size. This probability denotes the probability of simultaneous extinction when the size of the coexisting population is very high. To validate the theoretical aspect we consider the prey-predator dynamical system where the growth rate of prey population follows θ-logistic and Allee mechanism and evaluate the simultaneous extinction probability of prey and predator. The method we used here can also be used to other dynamical system such as SIS model.

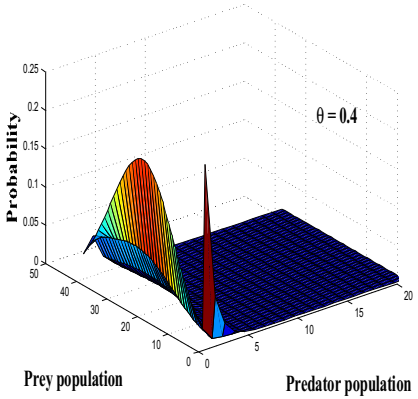
θ = 0.4
Probability
0.25
0.2
0.15
0.1
0.05
0
50
40
30
20
10
0
0
5
10
15
20
Prey population
Predator population

(a)

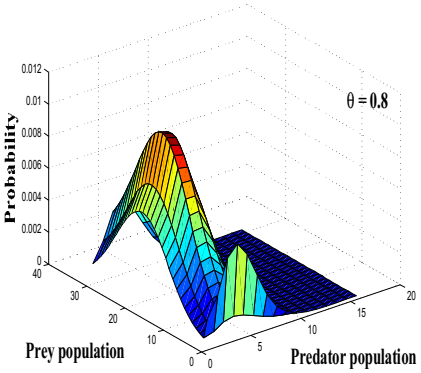
θ = 0.8
Probability
0.012
0.01
0.008
0.006
0.004
0.002
0
40
30
20
10
0
0
5
10
15
20
Prey population
Predator population

(b)

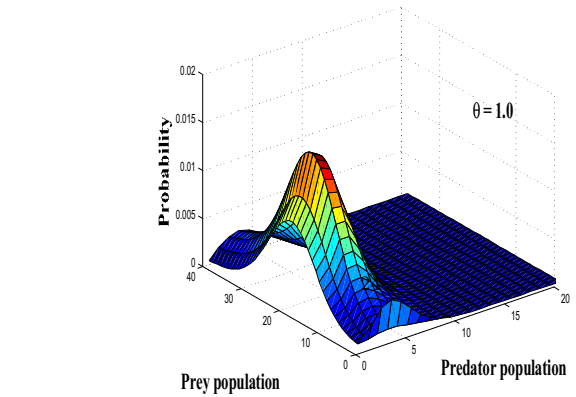

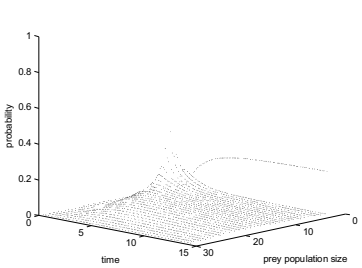

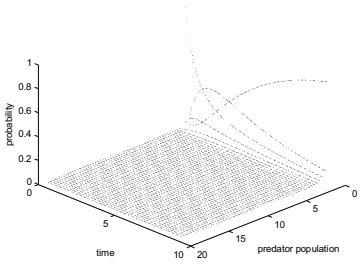

(a) The marginal probability distribution of prey. (b) The marginal probability distribution of predator.

Figure 4: The parameters are $\alpha = 0.5$, $r = 1$, $\theta = 0.8$, $K = 20$,$d = 0.8$,$a = 0.1$, $H = 0.3$.

References

[1] A. S. Ackleh, L. J.S. Allen, and J. Carter. Establishing a beachhead: A stochastic population model with an Allee effect applied to species invasion. *Theoretical Population Biology*, 71:290–300, 2007.

[2] A. S. Ackleh, L.J.S. Allen, and J. carter. Establishing a beachhead: A stochastic population model with an Allee effect applied to species invasion. *Theoretical Population Biology*, 71:290–300, 2007.

[3] E. J. Allen. Stochastic differential equations and persistence time for two interacting populations. *Dynamics of Continuous, Discrete and Impulsive Systems*, 5:271–281, 1999.

[4] L. J. S. Allen and E. J. Allen. A comparison of three different stochastic population models with regard to persistence time. *Theoritical Population Biology*, 64:439–449, 2003.

[5] L. J.S. Allen and V. A. Bokil. Stochastic Models for Competing Species With a Shared Psathogen. *Mathematical Biosciences and Engineering*, 9(3):461–485, July 2012.

[6] F. J. Ayala, M. E. Gilpin, and J. G. Ehrenfeld. *Theoretical Population Biology*, 4:331–356, 1973.

[7] N. T. J. Bailey. *Element of Stochastic Processes with applications to the natural sciences*. Wiley, New York, 1964.

[8] M. S. Bartlett, J. C. Gower, and P. H. Leslie. A comparison of theoretical and empirical results for some stochastic population models. *Biometrica*, 47:1–11, 1960.

[9] A. R. Bhowmick, B. Saha, S. Ray, J. Chattopadhyay, and S. Bhattacharya. Cooperation in species: Interplay of population regulation andextinction through global population dynamics database. *Ecological Modelling*, 312:150–165, 2015.

[10] F. Courchamp, L. Berce, and J. Gascoigne. *Allee effects in ecology and conservation*. Oxford Univ. Press, Oxford, UK., 2008.

[11] B. Dennis. Allee effects in stochastic populations. *Oikos.*, 96:389–401, 2002.

[12] C. W. Fowler. Density dependence as related to life history strategy. *Ecology*, 62:602–610, 1981.

[13] R.P. Freckleton, D.M.S. Matos, M.L.A. Bovi, and A.R. Watkinson. Predicting the impacts of harvesting using structured population models: the importance of density-dependence and timing of harvest for a tropical palm tree. *Journal of Applied Ecology*, 40:846–858, 2003.

[14] J. M. Fryxell, A. Mosser, A. R. E. Sinclair, and C. Packer. Group formation stabilizes predatorprey dynamics. *Nature*, 449:1041–1043, 2007.

[15] G. F. Gause. The struggle for existence. 1934.

[16] M. E. Gilpin and M. E. Soule. *Conservation Biology- The Science of Scarcity and Biodiversity*, chapter Minimum viable populations: processes of species extinction, pages 19–34. Sinauer Associates, Michigan, 1986.

[17] M.E. Gilpin and F.J. Ayala. Global models of growth and competition. *Proceedings of the National Academy of Sciences of the USA*, 70:3590–3593, 1973.

[18] C.S. Holling. Some characteristics of simple types of predation and parasitism. *Canadian Entomologist*, 91:385–398, 1959.

[19] K. Johst, A. Berryman, and M. Lima. From individual interactions to population dynamics: individual resource partitioning simulation exposes the causes of nonlinear intra-specific competition. *Population Ecology*, 50:79–90, 2008.

[20] S. Karlin and H. M. Taylor. *A second course in stochastic process*. Academic Press, New York., 1981.

[21] M.J. Keeling. Multiplicative moments and measures of persistence in ecology. *Journal of Theoretical Biology*, 205:269–281, 2000.

[22] I. Krishnarajah, A. Cook, G. Marion, and G. Gibson. Novel moment closure approximations in stochastic epidemics. *Bulletin of Mathematical Biology*, 67:855–873, 2005.

[23] R. Lande. Extinctiont Thresholds in Demographic Models of Territorial Populations. *The American Naturalist*, 130:624–635, 1987.

[24] R. Lande. Risks of Population Extinction from Demographic and Environmental Stochasticity and Random Catastrophes. *The American Naturalist*, 142(6):911–927, 1993.

[25] R. Lande. Risks of population extinction from demographic and environmental stochasticity and random catastrophes. *The American Naturalist*, 142:911–927, 2004.

[26] R. Lande, S. Engen, and B-E. Sæther. *Stochastic Population Dynamics in Ecology and Conservation*. Oxford University Press, Oxford, 2003.

[27] A. J. Lotka. *Elements of Physical Biology Baltimore*. 1926.

[28] J. H. Matis and T. R. Kiffe. On Approximating the Moments of the Equilibrium Distribution of a Stochastic Logistic Model. *Biometrics*, 52:980–991, 1996.

[29] J. H. Matis and T. R. Kiffe. Effects of Immigration on Some Stochastic Logistic Models: A Cumulant Truncation Analysis. *Theoretical Population Biology*, 56:139–161, 1999.

[30] J. H. Matis, T. R. Kiffe, and P. R. Parthasarathy. On the cumulants of population size for the stochastic power law logistic model. *Theoretical Population Biology*, 53:16–29, 1998.

[31] R. M. May. Stability in Randomly Fluctuating Versus Deterministic Environments. *The American Naturalist*, 107(957):621–650, 1973.

[32] D.R. McCullough. Density dependence and life-history strategies of ungulates. *Journal of-Mammalogy*, 80:1130–1146, 1999.

[33] I. Nåsell. Extinction and quasi-stationarity in the Verhulst logistic model. *Journal of Theoretical Biology*, 211:11–27, 2001.

[34] I. Nåsell. Moment closure and the stochastic logistic model. *Theoretical Population Biology*, 63:159–168, 2003.

[35] R. M. Nisbet and W. C. S. Gurney. Modelling Fluctuating Population. *The Blackburn Press.*, 1982.

[36] N. Owen-Smith. Demographic determination of the shape of density dependence for three african ungulate populations. *Ecological Monographs*, 76:93–109, 2006.

[37] G. M. Palamara, G. W. Delius, M. J. Smith, and O. L. Petchey. Predation effects on mean time to extinction under demographic stochasticity. *Journal of Theoretical Biology*, 80:1–10, 2013.

[38] P. R. Parthasarathy. The effect of super infection on the distribution of infectious period–a continued fraction approximation. *J. Math. Appl. in Med and Biol.*, 1996.

[39] E. Renshaw. *Modelling Biological Populations in Space and Time*. Cambridge, 1991.

[40] E. Renshaw. *Modelling Biological Populations in Space and Time*. Cambridge University Press, Cambridge., 1993.

[41] E. Renshaw. Saddlepoint approximations for stochastic processes with truncated cumulant generating functions. *IMA J ournal of Mathematics Applied in Medicine & Biology*, 15:41–52, 1998.

[42] E. Renshaw. *Stochastic Population Processes: Analysis, Approximations, Simulations*. Oxord University Press, New York, 2011.

[43] M. Rosenzweig. The Paradox of Enrichment. *Science*, 171:385387, 1971.

[44] B. Saha, A. R. Bhowmick, J. Chattopadhyay, and S. Bhattacharya. On the evidence of an Allee effect in Herring populations and consequences for population survival: A model-based study. *Ecological Modelling*, 250:72–80, 2013.

[45] R. M. Sibly, D. Barker, M. C. Denham, J. Hone, and M. Pagel. On the regulation of populations of mammals, birds, fish, and insects. *Science*, 309:607–610, 2005.

[46] W.R. Thomas, M.J. Pomerantz, and M.E. Gilpin. Chaos, asymmetric growth and group selection for dynamical stability. *Ecology*, 61:1313–1320, 1980.

[47] P Turchin. *Complex Population Dynamics: A Theoretical/empirical Synthesis*. Number 35 in Monograph in Population Biology. Princeton University Press, Princeton, 2003.

[48] V Volterra. Lecons sur la thorie mathmatique de la lutte pour la vie, gauthier-villars, paris. 1931.

[49] S. Wolfram. *A System for Doing Mathematics by Computer*. Addison–Wesley, Redwood City, CA, 1991.

Effect of Reinforcement and Heterogeneity on the Propagation of SH-waves

Anup Saha*and Santimoy Kundu

Department of Applied Mathematics, Indian School of Mines, Dhanbad-826004, India

August 26, 2016

Abstract

This paper aims to study the propagation of SH-waves in a fibre-reinforced medium over a heterogeneous orthotropic half-space under initial stress. The lower half-space is caused by consideration of exponential variation in initial stress, rigidity and shear moduli. The closed form of dispersion equation has been obtained for SH-waves in terms of Whittaker's function which is further expanded asymptotically, retaining the terms upto second degree. As a special case when the layer and the half-space both are homogeneous our computed equation coincides with the standard equation of Love wave. Numerical results analyzing the dispersion equation are discussed and presented by number of graphs. This study shows that the reinforcement as well as heterogeneity, initial stress parameters have remarkable effect on the propagation of SH-waves.

Keywords: SH-waves, initial stress, heterogeneity, fibre-reinforced medium, orthotropic, phase velocity.

1 Introduction

When an earthquake occurs, the shockwaves of released energy which shake the Earth and temporarily turn soft deposits are called seismic waves. These are waves of energy that travel at different speeds when they pass through different types of material and move similarly to other types of waves, like sound waves, light waves and water waves. These waves contain vital information about the internal structure of the Earth. Because the speed of seismic waves depends on the material properties, one can use the travel-time of seismic waves to map change

*sahaanup1989@gmail.com (Corresponding Author) and kundu_santi@yahoo.co.in

in density with depth, and show that the Earth is composed of several layers. There are two basic types of seismic waves body waves and surface waves. Surface waves are similar in nature to water waves and travel just under the Earth's surface.

Since our planet is a spherical body having finite dimension and the elastic waves generated must receive the effect of the boundaries. Naturally, this concept leads us to study surface waves. The study of surface waves in elastic media is very important due to their devastating damage capabilities during earthquake and for homogeneous, non-homogeneous and layered media it has been central interest to theoretical seismologists in recent time. One type of surface waves is Love wave that may be available in non-homogeneous Earth. Love waves are transverse waves that vibrate the ground in the horizontal direction perpendicular to the direction that the waves are travelling. Quite a good amount of information about the propagation of seismic waves is contained in the well-known book by Ewing et al. (1957). A large number of papers have been published in different journals after publishing this book. Chattopadhyay et al. (2011) investigated the propagation of torsional surface waves in an inhomogeneous layer over an inhomogeneous half-space. Georgiadis et al. (2000) showed the existence of torsional surface waves in a gradient-elastic half space. Dey et al. (2004) presented a study of Love wave propagation in an elastic layer with void pores. Love-type surface waves in homogeneous micropolar elastic media was studied by Midya (2004). Davini et al. (2008) studied the propagation of torsional waves in a thin rectangular domain using asymptotic approach. Gupta et al. (2012) pointed that in a homogeneous layer over a heterogeneous half-space torsional waves do exist. Ghorai and Tiwary (2014) found that in-homogeneity of rigidity and density of the medium influences the velocity of torsional surface wave. Sethi et al. (2012) made an attempt to investigate the effect of viscoelastic material on the phase velocity of torsional wave. Manna et al. (2013) discussed Love wave propagation in a piezoelectric layer lying over an inhomogeneous elastic half-space. The commendable works by Islam et al. (2014), Abd-Alla et al. (2013), Chattopadhyay et al. (2013) in the study of seismic waves may be cited.

The study of wave propagation in fibre-reinforced medium plays an important role in geomechanics and civil engineering. The characteristic property of a fibre-reinforced material is that its components, i.e., concrete and steel act as a single anisotropic unit as long as they remain in elastic condition, i.e., the components are bound together so that there are no relative displacement between them. There are some hard and soft rocks inside the Earth that show reinforced property. There are also artificial fibre-reinforced composites used to minimize the damage due to earthquake. Many papers have been publishes on the propagation of seismic waves in fibre-reinforced medium. Pradhan et al. (2003) considered the influence of anisotropy on the Love waves in self-reinforced layer lying over an elastic non-homogeneous half-space. The effects of reinforcement, gravity and porosity on the propagation of Love waves were discussed by

Chattaraj and Samal (2013). Dhua et al. (2013) observed that the presence of reinforcement in the layer increases the phase velocity of tosrional wave significantly. Kundu et al. (2014) investigated Love waves in a fibre-reinforced layered medium lying over an initially stressed orthotropic half-space. Vishwakarma (2014) showed the effect of reinforced and viscoelastic parameters on torsional wave propagation.

The earth is considered as an initially stressed body as layered structured. These initial stresses exist due to various reasons viz., temperature, atmospheric pressure, gravity variation, slow process of creep etc. The presence of initial stress has remarkable effect on the phase velocity of surface wave. Gupta et al. (2013) discussed the propagation of torsional surface waves in an inhomogeneous layer over an initially stressed inhomogeneous half-space. Kepceler (2010) examined and found the existence of torsional wave dispersion relations in a pre-stressed bi-material compounded cylinder with an imperfect interface. Ahmed and Abo-Dahab (2010) showed the existence of Love waves in an orthotropic Granular layer under initial stress overlying a semi-infinite Granular medium. Abd-Alla and Ahmed (1999) investigated Love waves in a non-homogeneous orthotropic elastic layer under changeable initial stress. Sethi et al. (2011) studied the effect of non-homogeneity of the orthotropic media as well as the changeable initial stress on the dispersion equation of Love waves. References can be made to Kundu et al. (2014), Ozturk and Akbarov (2009), Chattaraj et al. (2011) for their excellent contributions in investigating seismic waves in various mediums under various circumstances.

So far it has been found that the propagation of SH-waves in a fibre-reinforced layer over a heterogeneous orthotropic half-space has remained un-attempted. So in the present paper, the effects of reinforcement, initial stress and heterogeneity parameter are shown on the propagation of SH-waves. The crust region of our planet is composed of various heterogeneous layers with different geological parameters. For the present study the heterogeneity in the lower half-space is caused by exponential variation in initial stress, density and shear moduli. The dispersion equation of SH-waves under these conditions has been derived. The study reveals that the reinforcement as well as heterogeneity, initial stress have remarkable effect on the propagation of SH-waves. The graphical representation has shown the relation between dimensionless phase velocity and wave number.

2 Formulation of the problem

We consider the positive z-axis vertically downwards and the x-axis along the direction of wave propagation. Let H be the thickness of the fibre-reinforced layer lying over a heterogeneous orthotropic half-space. The free surface of the reinforced layer is assumed to be traction free. The heterogeneity in the half-space is considered in initial stress, density and shear moduli. The

following variations for the half-space are taken into account:

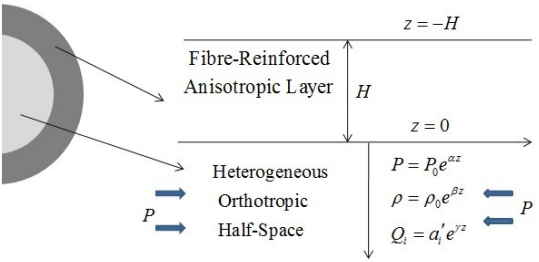

Figure 1: Geometry of the problem

$$\left.\begin{aligned} P &= P_0 e^{\alpha z}, \\ \rho &= \rho_0 e^{\beta z}, \\ Q_i &= a_i' e^{\gamma z}, \end{aligned}\right\} \tag{2.1}$$

where P is initial stress, ρ is density, Q_i are shear moduli, α, β, γ are constants having dimension that is inverse of length.

3 Solution for fibre-reinforced layer

The constitutive equation for a transversely isotropic linear elastic material with preferred direction $\vec{a}$ (Spencer, 1972) is

$$\begin{aligned} \sigma_{ij} \quad = \quad & \lambda e_{kk}\delta_{ij} + 2\mu_T e_{ij} + \alpha(a_k a_m e_{km}\delta_{ij} + a_i a_j e_{kk}) + \\ & 2(\mu_L - \mu_T)(a_i a_k e_{kj} + a_j a_k e_{ki}) + \beta(a_k a_m e_{km} a_i a_j) \end{aligned} \tag{3.1}$$

where σ_{ij} are components of stress; e_{ij} are the infinitesimal strain components; δ_{ij} is Kronecker delta; $a_i = (a_1, a_2, a_3)$ are the direction cosines of $\vec{a}$ with respect to Cartesian coordinate system such that $a_1^2 + a_2^2 + a_3^2 = 1$; μ_T and μ_L are transverse and longitudinal elastic shear modulus respectively; λ is elastic parameter; $\alpha, \beta, \mu_L - \mu_T$ are reinforced anisotropic elastic parameters; u_i are the components of displacement vector. We assume the direction of fibre along x and z-axis, i.e., $\vec{a} = \vec{a}(a_1, 0, a_3)$.

Using the conventional SH-wave conditions $u_1 = u_3 = 0, u_2 = v(x, z, t)$ in equation (3.1), we get the non-zero stress components as

$$\sigma_{12} = \mu_T \left[P\frac{\partial v}{\partial x} + R\frac{\partial v}{\partial z} \right], \sigma_{23} = \mu_T \left[Q\frac{\partial v}{\partial z} + R\frac{\partial v}{\partial x} \right] \tag{3.2}$$

where

$$\left.\begin{array}{l} P = 1 + (\frac{\mu_L}{\mu_T} - 1)a_1^2, \\ Q = 1 + (\frac{\mu_L}{\mu_T} - 1)a_3^2, \\ R = (\frac{\mu_L}{\mu_T} - 1)a_1 a_3. \end{array}\right\} \tag{3.3}$$

The equation of motion for SH-waves in a fibre reinforced layer is

$$\frac{\partial \sigma_{12}}{\partial x} + \frac{\partial \sigma_{22}}{\partial y} + \frac{\partial \sigma_{23}}{\partial z} = \rho \frac{\partial^2 v}{\partial t^2}. \tag{3.4}$$

With the help of (3.2) and (3.3), the equation of motion (3.4), takes the form

$$P\frac{\partial^2 v}{\partial x^2} + Q\frac{\partial^2 v}{\partial z^2} + 2R\frac{\partial^2 v}{\partial x \partial z} = \frac{\rho}{\mu_T}\frac{\partial^2 v}{\partial t^2}. \tag{3.5}$$

For the wave changing harmonically, we assume

$$v = V(z)e^{ik(x-ct)}, \tag{3.6}$$

where k is wave number, $\omega(= kc)$=circular frequency, c is the speed of simple harmonic waves. On substituting (3.6) into (3.5), one gets

$$Q\frac{d^2V}{dz^2} + 2Rik\frac{dV}{dz} + k^2\left(\frac{c^2}{c_0^2} - P\right)V = 0, \tag{3.7}$$

where $c_0 = \sqrt{\frac{\mu_T}{\rho}}$ is shear wave velocity in the reinforced layer.
The solution of (3.7) may be taken as

$$V(z) = D_1 e^{-ik\zeta_1 z} + D_2 e^{-ik\zeta_2 z},$$

where

$$\zeta_1 = \frac{R + \sqrt{R^2 + Q\left(\frac{c^2}{c_0^2} - P\right)}}{Q}, \quad \zeta_2 = \frac{R - \sqrt{R^2 + Q\left(\frac{c^2}{c_0^2} - P\right)}}{Q} \tag{3.8}$$

Thus the solution for the upper reinforced layer is

$$v = v_0(say) = \left(D_1 e^{-ik\zeta_1 z} + D_2 e^{-ik\zeta_2 z}\right)e^{ik(x-ct)}. \tag{3.9}$$

4 Solution for Orthotropic Half-Space

The equations of motion without body force under initial stress ($\tau_{11} = -P$) are given by

$$\left.\begin{array}{l} \frac{\partial \tau_{11}}{\partial x} + \frac{\partial \tau_{12}}{\partial y} + \frac{\partial \tau_{13}}{\partial z} - P(\frac{\partial \omega_z}{\partial y} - \frac{\partial \omega_y}{\partial z}) = \rho \frac{\partial^2 u}{\partial t^2}, \\ \frac{\partial \tau_{12}}{\partial x} + \frac{\partial \tau_{22}}{\partial y} + \frac{\partial \tau_{23}}{\partial z} - P(\frac{\partial \omega_z}{\partial x}) = \rho \frac{\partial^2 v}{\partial t^2}, \\ \frac{\partial \tau_{13}}{\partial x} + \frac{\partial \tau_{23}}{\partial y} + \frac{\partial \tau_{33}}{\partial z} - P(\frac{\partial \omega_y}{\partial x}) = \rho \frac{\partial^2 w}{\partial t^2}, \end{array}\right\} \tag{4.1}$$

where τ_{ij} are the incremental stress components; u, v, w are the components of displacement vector ; $\omega_x,\ \omega_y,\ \omega_z$ are the components of rotational vector given by

$$\omega_x = \frac{1}{2}\left(\frac{\partial w}{\partial y} - \frac{\partial v}{\partial z}\right),\ \omega_y = \frac{1}{2}\left(\frac{\partial u}{\partial z} - \frac{\partial w}{\partial x}\right),\ \omega_z = \frac{1}{2}\left(\frac{\partial v}{\partial x} - \frac{\partial u}{\partial y}\right). \tag{4.2}$$

The stress-strain relations are

$$\left.\begin{aligned} \tau_{11} &= \beta_{11}e_{xx} + \beta_{12}e_{yy} + \beta_{13}e_{zz}, \\ \tau_{22} &= \beta_{21}e_{xx} + \beta_{22}e_{yy} + \beta_{23}e_{zz}, \\ \tau_{33} &= \beta_{31}e_{xx} + \beta_{32}e_{yy} + \beta_{33}e_{zz}, \\ \tau_{23} &= 2Q_1e_{yz}, \tau_{31} = 2Q_2e_{zx}, \tau_{12} = 2Q_3e_{xy}. \end{aligned}\right\} \tag{4.3}$$

In above β_{ij} are the incremental normal elastic coefficients and Q_i are the shear moduli. Now the strain-displacement relations are given by

$$e_{xy} = \frac{1}{2}\left(\frac{\partial u}{\partial y} + \frac{\partial v}{\partial x}\right),\ e_{yz} = \frac{1}{2}\left(\frac{\partial v}{\partial z} + \frac{\partial w}{\partial y}\right),\ e_{zx} = \frac{1}{2}\left(\frac{\partial u}{\partial z} + \frac{\partial w}{\partial x}\right). \tag{4.4}$$

For the propagation of SH-waves along x-direction having the displacement of particles along y-direction, we have

$$u = 0, w = 0, v = v(x, z, t). \tag{4.5}$$

Using the equations (4.2)-(4.5),the dynamical equation of motion which is not automatically satisfied is

$$Q_1\frac{\partial^2 v}{\partial z^2} + \left(Q_3 - \frac{P}{2}\right)\frac{\partial^2 v}{\partial x^2} + \frac{dQ_1}{dz}\frac{\partial v}{\partial z} = \rho\frac{\partial^2 v}{\partial t^2} \tag{4.6}$$

We assume the harmonic solution of equation (4.6) as

$$v = V(z)e^{ik(x-ct)} \tag{4.7}$$

where $V(z)$ satisfies the following equation

$$Q_1\frac{d^2V}{dz^2} + \frac{dQ_1}{dz}\frac{dV}{dz} + k^2\left(\rho c^2 + \frac{P}{2} - Q_3\right)V = 0. \tag{4.8}$$

In above equation, k is the angular wave number and $w(= kc)$ is angular frequency. Substituting $V = \frac{V_1}{\sqrt{Q_1}}$, above equation reduces to

$$\frac{d^2V_1}{dz^2} + \left[\frac{1}{4Q_1^2}\left(\frac{dQ_1}{dz}\right)^2 - \frac{1}{2Q_1}\frac{d^2Q_1}{dz^2} + k^2\left(\frac{\rho c^2}{Q_1} + \frac{P}{2Q_1} - \frac{Q_3}{Q_1}\right)\right]V_1 = 0. \tag{4.9}$$

Using equation (2.1), equation (4.9) gives

$$\frac{d^2V_1}{dz^2} + k^2\left[\frac{d_1 + d_2 z}{1+\gamma z} - \frac{\gamma^2}{4k^2} - \frac{a_3'}{a_1'}\right]V_1 = 0, \tag{4.10}$$

where

$$\begin{aligned} d_1 &= \frac{c^2}{c_1^2} + \frac{P_0}{2a_1'}, \\ d_2 &= \beta\frac{c^2}{c_1^2} + \alpha\frac{P_0}{2a_1'}, \\ c_1 &= \sqrt{\frac{a_1'}{\rho_0}} = \text{Characteristic velocity of transverse waves for lower heterogeneous orthotropic half-space.} \end{aligned}$$

Using dimensionless parameters $\eta = \frac{2\gamma_1 k(1+\gamma z)}{\gamma}$ and $\gamma_1 = \sqrt{\frac{a_3'}{a_1'} + \frac{\gamma^2}{4k^2} - \frac{d_2}{\gamma}}$ in equation (4.10), one gets

$$\frac{d^2V_1}{d\eta^2} + \left[-\frac{1}{4} + \frac{R}{\eta}\right]V_1 = 0, \tag{4.11}$$

where $R = \frac{k(d_1\gamma - d_2)}{2\gamma_1\gamma^2}$.
Solution of (4.11) satisfying the condition $V(z) \to 0$ as $z \to \infty$, i.e., $V_1(\eta) \to 0$ as $\eta \to \infty$ may be taken as

$$V_1 = A_3 W_{R,\frac{1}{2}}(\eta),$$

where A_3 is arbitrary constant and $W_{R,\frac{1}{2}}(\eta)$ is Whittaker function (Whittaker and Watson, 1990).
Hence the solution of half-space may be written as

$$v = v_1(say) = \frac{D_3 W_{R,\frac{1}{2}}(\eta}{e^{\frac{\gamma z}{2}}} e^{ik(x-ct)}. \tag{4.12}$$

where $D_3 = \frac{A_3}{\sqrt{a_i'}}$.

5 Boundary conditions

The appropriate boundary conditions are as follows:

(i) Stress of layer vanishes at $z = -H$, i.e.,

$$\sigma_{23} = 0. \tag{5.1}$$

(ii) Displacement and stress components are continuous at $z = 0$, i.e.,

$$v_0 = v_1 \tag{5.2}$$

$$\text{and } \sigma_{23} = \tau_{23} \tag{5.3}$$

Using the above boundary conditions in equations (3.9) and (4.12), we obtained the following three equations

$$D_1(R-Q\zeta_1)e^{ik\zeta_1 H} + D_2(R-Q\zeta_2)e^{ik\zeta_2 H} = 0, \tag{5.4}$$

$$D_1 + D_2 - D_3 W_{R,\frac{1}{2}}\left[\frac{2\gamma_1 k}{\gamma}(1+\gamma z)\right]_{z=0} = 0, \tag{5.5}$$

$$D_1(R-Q\zeta_1)ik + D_2(R-Q\zeta_2)ik - D_3\frac{a_1'}{\mu_T}\left\{\frac{\partial}{\partial z}\left[\frac{W_{R,\frac{1}{2}}\left\{\frac{2\gamma_1 k(1+\gamma z)}{\gamma}\right\}}{e^{\frac{\gamma z}{2}}}\right]\right\}_{z=0} = 0. \tag{5.6}$$

Eliminating D_1, D_2 and D_3 from equations (5.4)-(5.6) and expanding the Whittaker function upto linear terms, the dispersion equation for SH-waves in fibre reinforced medium is obtained as

$$\tan\left[\frac{kH}{Q}\sqrt{R^2+Q\left(\frac{c^2}{c_0^2}-P\right)}\right] = \frac{a_1'}{\mu_T}\frac{\gamma_1 - \frac{\gamma}{2k} - \frac{2\gamma_1 A}{1+\frac{2\gamma_1 kA}{\gamma}}}{\sqrt{R^2+Q\left(\frac{c^2}{c_0^2}-P\right)}} \tag{5.7}$$

where $A = \frac{1-R}{2}$.
Equation (5.7) gives the dispersion equation of SH-waves in a fibre-reinforced layer over a heterogeneous orthotropic half-space.

6 Particular Cases

Case I: If $a_1 = 1,\ a_2 = a_3 = 0$, then $P \to \frac{\mu_L}{\mu_T}$, $Q \to 1$ and $R \to 0$, the equation (5.7) reduces to

$$\tan\left[kH\sqrt{\frac{c^2}{c_0^2}-\frac{\mu_L}{\mu_T}}\right] = \frac{a_1'}{\mu_T}\frac{\gamma_1 - \frac{\gamma}{2k} - \frac{2\gamma_1 A}{1+\frac{2\gamma_1 kA}{\gamma}}}{\sqrt{\frac{c^2}{c_0^2}-\frac{\mu_L}{\mu_T}}}$$

This is the dispersion equation of SH-waves in the presence of heterogeneous orthotropic half-space with initial stress .

Case II: If $\mu_L = \mu_T = \mu_0$, i.e., the upper layer is isotropic with rigidity μ_0, then by equation (5.7) we get

$$\tan\left[kH\sqrt{\frac{c^2}{c_0^2}-1}\right] = \frac{a_1'}{\mu_0}\frac{\gamma_1 - \frac{\gamma}{2k} - \frac{2\gamma_1 A}{1+\frac{2\gamma_1 kA}{\gamma}}}{\sqrt{\frac{c^2}{c_0^2}-1}},$$

which is the dispersion equation of SH-waves in an isotropic homogeneous layer lying over a heterogeneous orthotropic half-space under initial stress.

Case III: When the half-space is homogeneous, i.e., $\alpha \to 0$, $\beta \to 0$ and $\gamma \to 0$, the dispersion equation (5.7) becomes

$$\tan\left[\frac{kH}{Q}\sqrt{R^2+Q\left(\frac{c^2}{c_0^2}-P\right)}\right]=\frac{a_1'}{\mu_T}\frac{\sqrt{\frac{a_3'}{a_1'}-\frac{c^2}{c_1^2}-\frac{P_0}{2a_1'}}}{\sqrt{R^2+Q\left(\frac{c^2}{c_0^2}-P\right)}}$$

Case IV: In this case, the half-space is isotropic, i.e., $a_1' = a_3' = \mu_1$, homogeneous and free from initial compression, then the dispersive equation (5.7) takes the form

$$\tan\left[\frac{kH}{Q}\sqrt{R^2+Q\left(\frac{c^2}{c_0^2}-P\right)}\right]=\frac{a_1'}{\mu_1}\frac{\sqrt{1-\frac{c^2}{c_1^2}}}{\sqrt{R^2+Q\left(\frac{c^2}{c_0^2}-P\right)}}$$

which is the dispersion equation in a fibre-reinforced layer over an isotropic homogeneous half-space without initial stress.

Case V: If $\mu_L = \mu_T = \mu_0$, i.e., the upper layer is isotropic with rigidity μ_0 and the lower half-space is homogeneous, isotropic, i.e., $a_1' = a_3' = \mu_1$ and free from initial stress, equation (5.7) reduces to

$$\tan\left[kH\sqrt{\frac{c^2}{c_0^2}-1}\right]=\frac{\mu_1}{\mu_0}\frac{\sqrt{1-\frac{c^2}{c_1^2}}}{\sqrt{\frac{c^2}{c_0^2}-1}},$$

This is the well known Love wave equation (Love, 1927) in a homogeneous isotropic layer over a homogeneous isotropic half-space.

7 Numerical results and discussion

For numerical discussion we used the following relevant parameters in fibre-reinforced layer and orthotropic half-space.

(i) For fibre-rein-forced layer (Hool and Kinne, 1924)
$\mu_L = 5.66 \times 10^9 N/m^2$, $\mu_T = 2.46 \times 10^9 N/m^2$, $\rho = 7800 kg/m^3$

(ii) For the orthotropic half-space (Gubbins, 1990)
$a_1' = 5.82 \times 10^{10} N/m^2$, $a_3' = 3.99 \times 10^{10} N/m^2$, $\rho = 4500 kg/m^3$

To show the effect of different heterogeneity parameters, initial stress and reinforcement on nature of wave motion we have plotted dimensionless phase velocity $\frac{c}{c_0}$ against dimensionless wave number kH on the propagation of SH-waves in fibre-reinforced medium. The numerical calculations of phase velocities have been computed from equation (5.7) for different values of these parameters. The variations are shown in Figures 2 to 8. In all these we have noticed that the phase velocity decreases with the increase in dimensionless wave number.

Figure 2 gives the dispersion curves of SH-waves as function of dimensionless wave number in fibre-reinforced medium over a heterogeneous orthotropic half-space. Dispersion curves are plotted for different values of heterogeneity parameter $\frac{\alpha}{k}$ associated with initial stress. The value of $\frac{\alpha}{k}$ for curve no.1, no.2, no.3 and no.4 has been taken as 0.1, 0.2, 0.3 and 0.4 respectively. From these curves it can be realized that phase velocity increases with the decrease of $\frac{\alpha}{k}$. The curves becomes closer to each other when the value of $\frac{\alpha}{k}$ decreases. So the heterogeneity parameter $\frac{\alpha}{k}$ has much dominance at large values.

Figure 3 manifests the effect of heterogeneity parameter $\frac{\beta}{k}$ associated with density on the phase velocity of SH-waves. In this figure the value of $\frac{\beta}{k}$ has been taken as 0.2, 0.4, 0.6 and 0.8 for curve no.1, no.2, no.3 and no.4 respectively. From this figure it has been observed that the increasing value of heterogeneity parameter decreases the phase velocity for a particular frequency. Also the curves are little far apart from each other at higher phase velocity, i.e., the heterogeneity parameter $\frac{\beta}{k}$ has much dominant effect at higher phase velocity and lower wave number.

Figure 4 represents the effect of heterogeneity parameter $\frac{\gamma}{k}$ associated with shear moduli on the phase velocity of SH-waves. The value of $\frac{\gamma}{k}$ for curve no.1, no.2, no.3 and no.4 has been considered as 0.05, 0.10, 0.15 and 0.20 respectively. These curves show that the phase velocity of SH-waves decreases with the increase of $\frac{\gamma}{k}$. Also it has negligible effect for the higher magnitude.

Figure 5 gives a variation of velocity of SH-waves for the variation of compressive initial stress $\frac{P_0}{2a_1'}$ of the half-space in the presence of reinforced parameters. For curve no.1, no.2, no.3 and no.4, the value of $\frac{P_0}{2a_1'}$ has been taken as 0.2, 0.4, 0.6 and 0.8 respectively. It is observed that the phase velocity of SH-waves increases with an increase in the compressive initial stress. It has also been noticed that dominant effect on phase velocity is visible at higher magnitude of $\frac{P_0}{2a_1'}$.

In Figure 6, an attempt has been made to study the effect of initial stress parameter in the half-space when the reinforced parameters are neglected in the upper layer, i.e., $a_1 = a_3 = 0$. The value of initial stress parameter $\frac{P_0}{2a_1'}$ for curve no.1, no.2, no.3 and no.4, has been taken as 0.2, 0.4, 0.6 and 0.8 respectively. The curves of this figure also show that the phase velocity of SH-waves increases with the increase of initial stress parameter $\frac{P_0}{2a_1'}$ in the absence of reinforcement of the upper layer. Here also, the initial stress parameter has much dominance at large values.

Figure 7 gives the dispersion curves for different values of reinforced parameters in the presence of initial stress of the half-space. The values of a_1^2 and a_3^2 for curve no.1, no.2, no.3 and no.4 have been taken as 0.25, 0.30, 0.35, 0.40 and 0.75, 0.70, 0.65, 0.60 respectively. The figure shows that the effect of reinforcement is very prominent on the propagation of SH-waves. The phase velocity increases with the decrease of a_1^2 and increase of a_3^2 at a particular frequency.

In Figure 8, the effect of reinforced parameters a_1^2 and a_3^2 in the absence of initial stress of the half-space on SH-wave propagation has been shown. For curve no.1, no.2, no.3 and no.4, the values of a_1^2 and a_3^2 have been taken as 0.25, 0.30, 0.35, 0.40 and 0.75, 0.70, 0.65, 0.60 respectively. It shows that such parameters have remarkable effect on SH-wave propagation. This figure confirms that the phase velocity increases with the decrease of a_1^2 and increase of a_3^2 at a particular wave number.

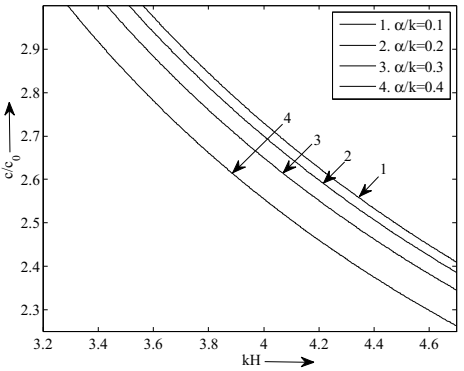

Figure 2: Dimensionless phase velocity as function of dimensionless wave number of SH-waves for different values of $\frac{\alpha}{k}$ and for $\frac{\beta}{k} = 0.1$, $\frac{\gamma}{k} = 0.6$, $a_1^2 = 0.4$, $a_3^2 = 0.6$, $\frac{P_0}{2a_1'} = 0.6$.

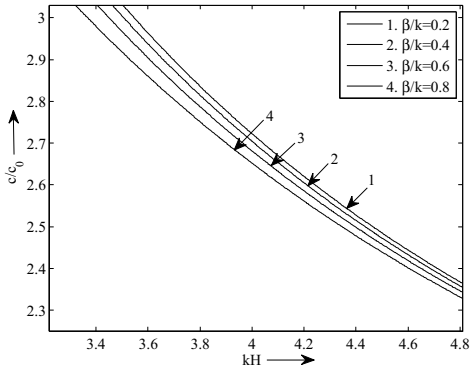

Figure 3: Dimensionless phase velocity as function of dimensionless wave number of SH-waves for different values of $\frac{\beta}{k}$ and for $\frac{\alpha}{k} = 0.1$, $\frac{\gamma}{k} = 0.6$, $a_1^2 = 0.4$, $a_3^2 = 0.6$, $\frac{P_0}{2a_1'} = 0.6$.

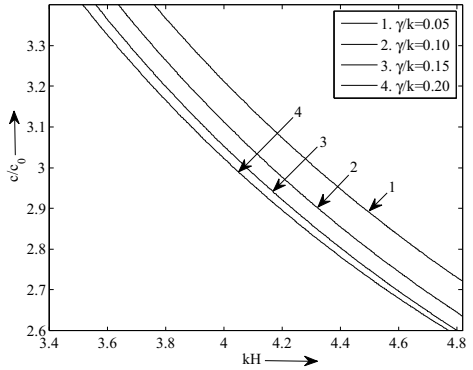

Figure 4: Dimensionless phase velocity as function of dimensionless wave number of SH-waves for different values of $\frac{\gamma}{k}$ and for $\frac{\alpha}{k} = 0.1$, $\frac{\beta}{k} = 0.6$, $a_1^2 = 0.4$, $a_3^2 = 0.6$, $\frac{P_0}{2a_1'} = 0.6$.

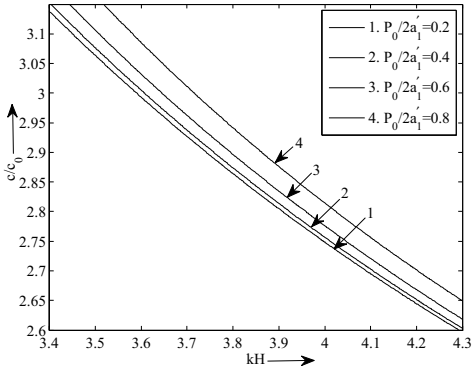

Figure 5: Dimensionless phase velocity as function of dimensionless wave number of SH-waves for different values of $\frac{P_0}{2a_1'}$ and for $\frac{\alpha}{k} = 0.1$, $\frac{\beta}{k} = 0.1$, $\frac{\gamma}{k} = 0.4$ $a_1^2 = 0.4$, $a_3^2 = 0.6$.

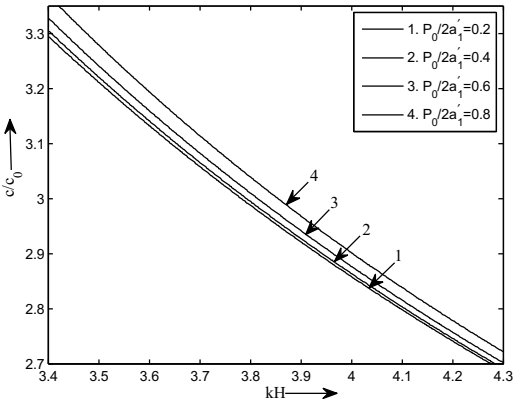

Figure 6: Dimensionless phase velocity as function of dimensionless wave number of SH-waves for different values of $\frac{P_0}{2a_1'}$ and for $\frac{\alpha}{k} = 0.1$, $\frac{\beta}{k} = 0.1$, $\frac{\gamma}{k} = 0.4$ $a_1 = a_3 = 0$.

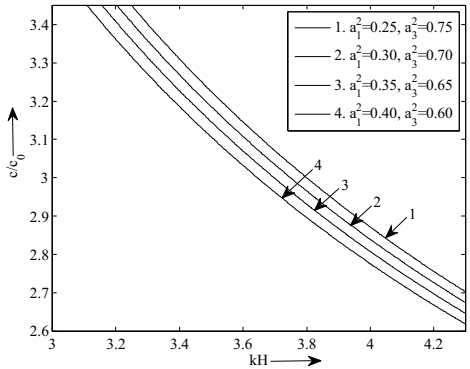

Figure 7: Dimensionless phase velocity as function of dimensionless wave number of SH-waves for different values of a_1^2 and a_3^2 and for $\frac{\alpha}{k} = 0.1$, $\frac{\beta}{k} = 0.1$, $\frac{\gamma}{k} = 0.4$, $\frac{P_0}{2a_1'} = 0.6$.

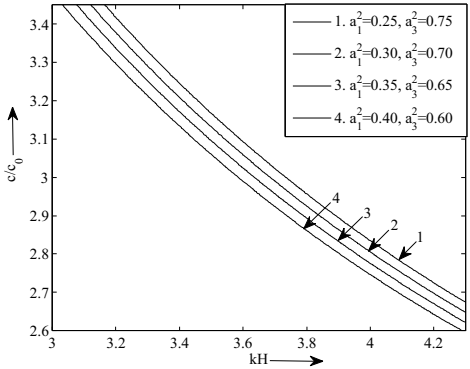

Figure 8: Dimensionless phase velocity as function of dimensionless wave number of SH-waves for different values of a_1^2 and a_3^2 and for $\frac{\alpha}{k} = 0.1$, $\frac{\beta}{k} = 0.1$, $\frac{\gamma}{k} = 0.4$, $\frac{P_0}{2a_1'} = 0$.

8 Conclusions

An analytic approach is used to investigate the propagation of SH-waves in a fibre-reinforced medium over a heterogeneous orthotropic half-space under initial stress. The method of separation of variables is applied to find the displacements in the media and generalized dispersion relation. Some special cases of interest have been deducted from the dispersion equation. When the reinforcement of the upper layer and the initial stress, orthotropy, heterogeneity in the half-space are neglected, the dispersion equation obtained is in agreement with the standard equation of SH-waves. For graphical representation, MATLAB software has been used to generalize the results. From the above discussions we may conclude that

(i) Dimensionless phase velocity $\frac{c}{c_0}$ of SH-waves increases with the decreases of non-dimensional wave number kH in all the figures.

(ii) An increase in heterogeneity associated with initial stress, density and shear moduli decreases the phase velocity of SH-waves.

(iii) The effect of initial stress on the phase velocity of SH-waves is significant. In the presence or absence of reinforcement of the layer, the phase velocity of SH-waves increases when the initial stress parameter increases.

(iv) The reinforced parameters have also pronounced influence on the propagation of SH-waves. The phase velocity of SH-waves increases with the decrease of a_1^2 and increase of a_3^2.

There are some hard and soft rocks inside the Earth which show reinforced property and the reinforced materials are basic construction materials, so the wave propagation in reinforced medium plays an important role in civil engineering.

Acknowledgements

The authors convey their sincere thanks to Indian School of Mines, Dhanbad-826004, India, for providing JRF to Mr. Anup Saha and also facilitating us with the best facilities.

References

[1] Abd-Alla, A.M. and Ahmed, S.M., 1999, Propagation of Love waves in a non-homogeneous orthotropic elastic layer under initial stress overlying semi-infinite medium, *Applied Mathematics and Computation*, **106(2-3)**, 265-275.

[2] Abd-Alla, A.M., Nofal, T.A., Abo-Dahab, S.M. and Al-Mullise, A., 2013, Surface waves propagation in fibre-reinforced anisotropic elastic media subjected to gravity field, *Int. J. Phys. Sci.*, **8(14)**, 574-584.

[3] Ahmed, S.M. and Abo-Dahab, S.M., 2010, Propagation of Love waves in an orthotropic Granular layer under initial stress overlying a semi-infinite Granular medium, *J. Vib. Control*, **16(12)**, 1845-1858.

[4] Chattaraj, R. and Samal, S.K., 2013, Love waves in the fibre-reinforced layer over a gravitating porous half-space, *Acta Geophysica*, **61(5)**, 1170-1183.

[5] Chattaraj, R., Samal, S.K. and Mahanty, N.C., 2011, Propagation of torsional surface wave in anisotropic poroelastic medium under initial stress, *Wave Motion*, **48(2)**, 184-195.

[6] Chattopadhyay, A., Gupta, S., Kumari, P. and Sharma, V.K., 2011, Propagation of torsional waves in an inhomogeneous layer over an inhomogeneous half-space, *Meccanica*, **46(4)**, 671-680.

[7] Chattopadhyay, A., Gupta, S., Kumari, P. and Sharma, V.K., 2013, Torsional wave propagation in non-homogeneous layer between two non-homogeneous half-spaces, *Int. J. Numer. Anal. Methods. Geomech.*, **37(10)**, 1280-1291.

[8] Davini, C., Paroni, R. and Puntle, E., 2008, An asymptotic approach to the torsional problem in thin rectangular domains, *Meccanica*, **43(4)**, 429-435.

[9] Dey, S., Gupta, S. and Gupta, A.K., 2004, Propagation of Love waves in an elastic layer with void pores, *Sadhana*, **29(4)**, 355-363.

[10] Dhua, S., Singh, A.K. and Chattopadhyay, A., 2013, Propagation of torsional wave in a composite layer overlying an anisotropic heterogeneous half-space under initial stress, *J. Vib. Control*, Doi: 10.1177/1077546313505124.

[11] Ewing, W.M., Jardetzky, W.S. and Press, F., 1957, *Elastic waves in layered media*, New York, McGraw-Hill,

[12] Georgiadis, H.G., Vardoulakis, I. and Lykotrafitis, G., 2000, Torsional surface waves in a gradient-elastic half space, *Wave Motion*, **31(4)**, 333-348.

[13] Ghorai, A.P. and Tiwary, R., 2014, Mathematical modeling and analysis of torsional surface waves in a transverse isotropic elastic solid semi-infinite medium with varying rigidity and density under a rigid layer, *Appl. Math*, **5**, 877-885.

[14] Gubbins, D., 1990, *Seismology and plate tectonics*, Cambridge: Cambridge University Press,

[15] Gupta, S., Chattopadhyay, A. and Kundu, S., 2012, Torsional wave in a homogeneous layer over a heterogeneous half-space-A Mathematical Model, *J. Math. Model.Appl*, **1(5)**, 59-66.

[16] Gupta, S., Kundu, S. and Vishwakarma, S.K., 2013, Propagation of torsional surface waves in an inhomogeneous layer over an initially stressed inhomogeneous half-space, *J. Vib. Control*, Doi: 10.1177/1077546313493818

[17] Hool, G.A. and Kinne, W.S., 1924, *Reinforced concrete and masonry structure*, New York: McGraw-Hill.

[18] Islam, Z.M., Jia, P. and Lim. C.W., 2014, Torsional wave propagation and vibration of circular nanostructures based on nonlocal elasticity theory, *Int. J. Appl. Mech*, **06(02)**, Doi:10.1142/S17588255114500112.

[19] Kepceler, T., 2010, Torsional wave dispersion relations in a pre-stressed bi-material compounded cylinder with an imperfect interface, *Appl. Math. Model*, **34(12)**, 4058-4073.

[20] Kundu, S., Gupta, S. and Manna, S., 2014, Propagation of G-type seismic waves in heterogeneous layer lying over an initially stressed heterogeneous half-space, *Appl. Math. Comput*, **234**, 1-12.

[21] Kundu, S., Gupta, S. and Manna, S., 2014, Propagation of Love wave in fibre-reinforced medium lying over an initially stressed orthotropic half-space, *Int. J. Numer. Anal. Methods. Geomech*, **38(11)**, 1172-1182.

[22] Love, A.E.H., 1927, *The mathematical theory of elasticity*, Cambridge: Cambridge University Press,

[23] Manna, S., Kundu, S. and Gupta, S., 2013, Love wave propagation in a piezoelectric layer overlying in an inhomogeneous elastic half-space, *J. Vib. Control*, Doi: 10.1177/1077546313513626.

[24] Midya, G. K., (2004), On Love-type surface waves in homogeneous micropolar elastic media, *Int. J. Eng. Sci*, **42(11-12)**, 1275-1288.

[25] Ozturk, A. and Akbarov, S.D., 2009, Torsional wave propagation in a pre-stressed circular cylinder embedded in a pre-stressed elastic medium, *Appl. Math. Model*, **33(9)**, 3636-3649.

[26] Pradhan, A., Samal, S.K. and Mahanty, N.C., 2003, Influence of anisotropy on the Love waves in a self-reinforced medium, *Tamkang J. Sci. Eng*, **6(3)**, 173-178.

[27] Sethi, M., Gupta, K.C., Kakar, R. and Gupta, M.P., 2011, Propagation of Love waves in a non-homogeneous orthotropic layer under compression 'P' overlying semi-infinite non-homogeneous medium, *Int. J. Appl. Math. Mech*, **7(10)**, 97-110.

[28] Sethi, M., Gupta, K.C. and Rani, M., 2012, Propagation of torsional surface waves in a non-homogeneous crustal layer over a viscoelastic mantle, *Mathematica Aeterna*, **2(10)**, 879-900.

[29] Spencer, A.J.M., 1972, *Deformation of fibre-reinforced material*, Oxford University Press, London.

[30] Vishwakarma, S.K., 2014, Tosional wave propagation in a self-reinforced medium sandwiched between a rigid layer and viscoelastic half-space under gravity, *Appl.Math.comput*, **242**, 1-9.

[31] Whittaker, E.T. and Watson, G.N., 1990, *A course in modern analysis*, Cambridge: Cambridge University Press.

VALEDICTORY ADDRESS

A.B.Raha

Let me begin by thanking the Organizers of the 2-day Seminar,and in particular, Bhargav maharaj, the Vice-Principal of The Ramakrishna Mission Vidyamandira, for inviting me to deliver the Valedictory address. I have been in a real predicament doubting my competence for this task. Being a practitioner in Pure Mathematics I am now required to sketch a brief idea of application of modern mathematics. The situation is akin to one when a classical musician is asked to sing popular film songs. Let me strive to do as much justice as possible to this occasion.

Let me start my talk by quoting a famous saying of Paul Richard Halmos : The only way to learn mathematics is to do mathematics.

In his famous as well as sensational monograph " A Mathematician's Apology " Godfrey Harold Hardy(more popularly G.H.Hardy),the British mathematical icon of the 20^{th} century, is full of praise for Pure Mathematics for its own sake,its sheer beauty and its being divorced of application. According to him Applied mathematics which is useful in construction of bridges or in warfare is "Intolerably dull" and thus worthless. He writes "A mathematician, like a painter or a poet ,is a maker of patterns. If his patterns are more permanent than theirs, it

is because they are made with ideas… The mathematician's patterns , like the painter's or poet's, must be beautiful; the ideas, like the colours or the words, must fit together in a harmonious way. Beauty is the first test; there is no permanent place in the world for ugly."

German mathematician Jacobi shared a similar sentiment when he expressed " It is true that Fourier has the opinion that the principal object of mathematics is the public utility and the explanation of natural phenomena; but a scientist like him ought to know that the unique object of science is the honour of the human spirit and on this basis a question of the theory of numbers is worth as much as a question about planetary system."

Exactly an opposite view is held by the mathematician Cedric Villani, the director of the Institute of Henri Poincare and a recipient of Fields Medal in 2010 who recently visited India. According to him Hardy's was a "monstrous way of Thinking".One should not underestimate Applied Mathematics or application of mathematics. Some of Hardy's work in pure mathematics later turned out to be very useful in Genetics (e.g., Hardy-Weinberg Law) and several other, apparently non-mathematical, branches. Hardy's favourite Number Theory yielded extremely useful and non-trivial applications to this date. Because of all these aspects Prof.Villani refuses to distinguish between Pure

and Applied mathematics. He, indeed, feels that Applied mathematics together with application of Pure Mathematics have added further glamour to Pure Mathematics. Another strong and appropriate view in favour of application of mathematics by a famous Polish mathematician S.M.Ulam who played a very important role in the Hydrogen Bomb project of U.S.A. asserts " It seems to me the impact and role of the electronic computer will significantly affect pure mathematics also, just as it has already done so in the mathematical sciences , principally physics, astronomy and chemistry".

In order to highlight the application of Pure mathematics let me present the following two tell-tale views as last two in the present list: Alexey Sosinsky in 1991 writes " the notion of a 'group', viewed only 30 years ago as the epitome of sophistication, is today one of the mathematical concepts most widely used in physics, chemistry, biochemistry and mathematics itself."

A Mathematical Physicist echoes " All modern theories of nuclear and electromagnetic interactions are based on Group theory".

Turning towards Pure Mathematics let me first present an "Old wine in a new bottle" as an application of modern method to prove an old classical Theorem. Here

is a smart cryptique proof of the celebrated result of Euclid: **The set of prime numbers is infinite**.

" If the set **P** of primes is finite let M = $\prod_p p$. Then

$0 < \prod_p \left(\sin \frac{\pi}{p}\right) = \prod_p \sin\left(\frac{(1+2M)\pi}{p}\right) = 0$. **A contradiction** ! "

Note that M is divisible by each prime p. Hence $\sin\left(\frac{(1+2M)\pi}{p}\right) = \sin\left(\frac{2M\pi}{p} + \frac{\pi}{p}\right) = \sin\frac{\pi}{p}$. As 1+2M > M > p for every prime p $\in$ **P** , 2M+1 is a composite number and consequently divisible by some prime $p_0 \in$ **P.** Then the term on the R.H.S involving p_0 is 0.

I conclude my talk with the following problem in Topology. It is a well-known theorem of Alexandroff and Hausdorff (1929) that every compact metric space is a continuous image of the Cantor Ternary set. Now question arises : which topological spaces are continuous images of the Cantor set? Clearly such a space must be compact and has cardinality $\leq$ c= the cardinality of the continuum. In the case of Hausdorff spaces it can be shown that a continuous image of the Cantor set has to be compact and metrizable. Hence the problem remains in the case of non-Hausdorff spaces : what are the non-Hausdorff spaces that are continuous images of the Cantor set ?

As an illustration it can be shown that **R** with **cofinite topology** is a non-Hausdorff space which is a continuous image of the Cantor set.

With these words I stop. I don't know whether I could do justice to what has been expected of me. In any case let me thank the audience for the patient hearing paid to me.
